



Universiteit  
Leiden  
The Netherlands

## DNA repair and gene targeting in plant end-joining mutants

Jia, Q.

### Citation

Jia, Q. (2011, April 21). *DNA repair and gene targeting in plant end-joining mutants*. Retrieved from <https://hdl.handle.net/1887/17582>

Version: Corrected Publisher's Version

License: [Licence agreement concerning inclusion of doctoral thesis in the Institutional Repository of the University of Leiden](#)

Downloaded from: <https://hdl.handle.net/1887/17582>

**Note:** To cite this publication please use the final published version (if applicable).

# DNA Repair and Gene Targeting in Plant End-joining Mutants

Qi Jia

贾琪

To my dear Mum and Dad

献给我最亲爱的妈妈和爸爸

# DNA Repair and Gene Targeting in Plant End-joining Mutants

PROEFSCHRIFT

ter verkrijging van  
de graad van Doctor aan de Universiteit Leiden,  
op gezag van Rector Magnificus prof.mr.P.F. van de Heijden,  
volgens besluit van het College voor Promoties  
te verdedigen op donderdag 21 april 2011  
klokke 11:15 uur

door

Qi Jia

贾琪

Geboren te Wuhu (China)

in 1981

# Promotiecommissie

Promotor: Prof. Dr. P.J.J. Hooykaas

Co-promoter: Dr. B.S. de Pater

Overige leden: Dr. E. van der Graaff  
(Karl-Franzens-Universität Graz, Austria)

Prof. Dr. J. Memelink

Prof. Dr. H.P. Spaink

Prof. Dr. R. Verpoorte

Cover design: Kunzhi Jia & Qi Jia

Printed: Wöhrmann Print Service, Zutphen, the Netherlands

ISBN: 978-90-8570-744-8

# Contents

Chapter 1	7
General introduction: DNA repair and gene targeting	
Chapter 2	41
Characterization of <i>Arabidopsis thaliana</i> NHEJ mutants	
Chapter 3	69
Poly(ADP-ribose) polymerase facilitating back-up non-homologous end joining via micro-homologous sequences in plants	
Chapter 4	91
AtKu and AtParp are involved in distinct NHEJ pathways	
Chapter 5	111
Characterization of a plant specific DNA ligase AtLig6	
Summary	129
Samenvatting	133
Curriculum vitae	137
Acknowledgement	139

# **Chapter 1**

## General introduction: DNA repair and gene targeting

Qi Jia, B.Sylvia de Pater and Paul J.J. Hooykaas

1. Introduction	9
2. DNA Damage Checkpoints	10
3. Homologous Recombination (HR)	12
4. Non-Homologous End Joining (NHEJ)	16
4.1 Classical Non-Homologous End Joining (C-NHEJ)	18
4.1.1 Detecting and tethering DSB ends	18
4.1.2 Processing DSB ends	19
4.1.3 Ligating DSB ends	20
4.2 Backup Non-Homologous End Joining (B-NHEJ): Microhomology-Mediated End Joining (MMEJ)	21
5. Regulation of DSB repair pathways	23
6. Gene Targeting (GT)	24
6.1 Facilitating the HR pathway	25
6.2 Introducing DSBs in the target	27
7. Outline of the thesis	28

## 1. Introduction

The genome is subject to various assaults by both exogenous environmental factors (e.g. ionizing radiation, chemicals and reactive oxygen species) and endogenous cellular events (e.g. transposition, meiotic double strand break formation). These assaults cause a wide range of genetic damage, such as base lesions, DNA single-strand breaks (SSBs) and DNA double-strand breaks (DSBs). Among these DNA lesions, DSBs are particularly detrimental, because both strands are damaged and it is, therefore, impossible to reconstitute the missing information from a complementary strand. Defects in the repair of DSBs may cause chromosomal aberrations and genomic instability, which can promote mutation, accelerate aging and induce cell death. Even a single unrepaired DSB may induce cell death (1).

In order to maintain genomic integrity and stability, organisms have evolved multiple DNA repair mechanisms. Cellular responses to DNA damage activate cell-cycle checkpoints, which can stop the cell cycle and provide time for the cell to repair the damage before division (2). Base lesions and SSBs can be detected and removed by nucleotide excision repair (NER), mismatch repair or base excision repair (BER) (3). The most harmful damage, DSBs, can be repaired by two types of pathways: homologous recombination (HR) and non-homologous end joining (NHEJ).

HR utilizes sequence homology to align and join the DNA ends of the break. It employs a homologous stretch of DNA on a sister chromatid as a template. The HR pathway mediates an accurate form of repair. On the other hand, NHEJ is a straightforward pathway that can rejoin the two ends independently of significant homology. It is an error-prone process with insertion or deletion of nucleotides as a result. HR is only operative during the S/G2 phases of the cell cycle when sister chromatids are present. By contrast NHEJ can function



in all phases of the cell cycle, but is mainly used in the G1 phase when HR is suppressed. HR and NHEJ operate in both competitive and collaborative manners, depending on the repair context and specific attributes of the broken DNA. HR is the predominant DSB repair mechanism in prokaryotes and lower eukaryotes. NHEJ seems the main DSB repair pathway in multicellular eukaryotes (e.g. mammals and plants). Most of the major factors involved in NHEJ were initially identified in mammals. Genome sequencing has led to the discovery of homologous NHEJ factors in other eukaryotes and prokaryotes. It indicates that NHEJ has been conserved during evolution (4).

In this chapter, I shall review first how the cell responds to DNA DSBs and repairs those breaks. Then the main regulatory mechanisms that affect the choice of DNA repair pathway throughout the cell cycle are discussed, and how they affect gene targeting is addressed. Finally I will give an outline of the thesis.

## 2. DNA Damage Checkpoints

DNA damage checkpoints are the cellular surveillance systems, which prevent damaged DNA from being converted into heritable mutations in order to maintain the genomic stability. The presence of DNA damage leads to the initiation of signal transduction cascades (Figure 1), which leads to chromatin remodeling, transcriptional responses, cell cycle arrest, DNA repair or in some cases apoptosis (5). Cell cycle arrest is necessary to provide the cell with enough time to repair the DNA lesions. Chromatin remodeling and transcriptional responses facilitate DNA repair, and increase the resistance to further damage.

The checkpoints are initiated by the transient recruitment of the MRE11/RAD50/NBS1 (MRN) complex in mammals and plants (6) or the equivalent MRE11/RAD50/Xrs2 (MRX) complex in yeast (7;8), to DSB sites, followed by the activation of phosphoinositide-3-kinase-related kinases (PIKKs). This group of proteins comprises the ataxia-telangiectasia mutated (ATM in mammals and plants; Tel1 in yeast), the ATM and Rad3 related (ATR in mammals and plants; Mec1 in yeast) and the catalytic subunit of DNA protein kinase (DNA-PKcs, which is lacking in yeast). In general, ATM and DNA-PKcs respond mainly to DSBs, whereas ATR is activated by single-stranded DNA (ssDNA) and stalled replication forks (9). These kinases are activated and recruited to DNA lesions by direct interactions with specific factors: NBS1/Xrs2 (for ATM/Tel1), ATR-interacting protein (ATRIP)/Ddc2 in yeast (for ATR/Mec1) and Ku80 (for DNA-PK) (10). Then these checkpoint kinases transmit and amplify the checkpoint signal by different phosphorylation events to different downstream effectors that are essential for the DNA-damage response and DNA repair, including phosphorylation of H2AX ( $\gamma$ H2AX), mediator of DNA damage checkpoint 1 (MDC1), tumor protein 53 binding protein 1 (TP53BP1) and breast cancer 1 (BRCA1).

In general, there are two possibilities for the following steps (Figure 1). In the first possibility, ATM phosphorylates the histone H2AX ( $\gamma$ H2AX) which forms foci covering many megabases of chromatin surrounding the DSBs within seconds of DNA damage (11).

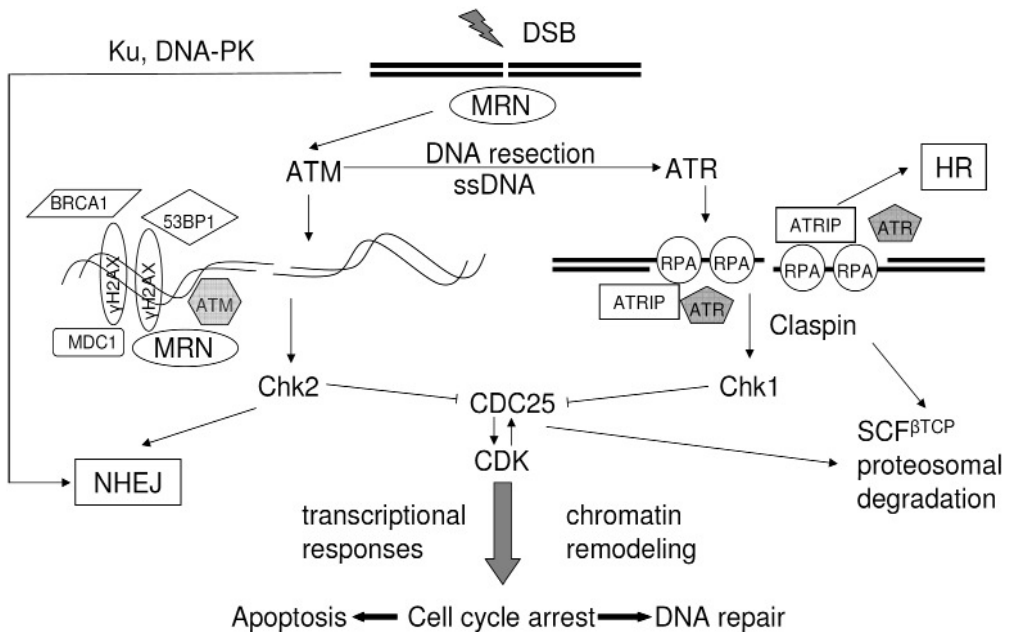


**Figure 1.** Responses to DNA Double Strand Breaks and checkpoint activation.

Ku and MRN complexes bind to DSBs and activate the PIKKs: DNA-PKcs and ATM respectively. The DNA-PK complex promotes NHEJ repair of DSBs which take place throughout the cell cycle. The MRN complex allows the activation of the checkpoint, mediated by ATM. ATM phosphorylates H2AX, which serves as a docking platform for MDC1, 53BP1, BRCA1, MRN and ATM itself. Active, phosphorylated ATM monomers are increased at the site of damage and activate the downstream signaling kinase Chk2. During S and G2 phases, DSBs are resected to ssDNA which is coated by RPA. The RPA coated ssDNA recruits the ATR-ATRIP complex to DNA lesions. With the help of Claspin mediator protein, ATR phosphorylates Chk1. Claspin maintains stable with the presence of Chk1 and can be degraded via SCF<sup>βTCP</sup> proteasome. Both activated Chk2 and Chk1 phosphorylate CDC25, marking it for proteasomal degradation by SCF<sup>βTCP</sup> ubiquitin ligase. This regulates the activity of CDK, which controls cell cycle arrest and facilitates one of the following steps: apoptosis or DNA repair. Chk2 and Chk1 can also facilitate other processes such as damage induced transcription and chromatin remodeling. In general, the ATM pathway promotes NHEJ repair, while the ATR pathway facilitates HR repair.

Alternatively,  $\gamma$ H2AX associates with the DSB-flanking chromatin regions, serving as a docking platform for MDC1, 53BP1, BRCA1, the MRN complex, and indeed ATM itself (12). The increased ATM phosphorylates and activates checkpoint kinase 2 (Chk2), or RAD53 in *Saccharomyces cerevisiae*, which induces the phosphorylation of CDC25A, marking it for proteasomal degradation by SCF<sup>βTCP</sup> ubiquitin ligase. This blocks the activation of the cyclin-dependent kinases (CDKs) and leads to cell cycle arrest. The G1-S cell phase is thus arrested to avoid the replication of damaged DNA. Recent research showed that Chk2 also appears to have a conserved function in the control of mitotic progression following DNA damage after the G2/M transition (13). CDKs orchestrate control of the cell cycle. The activation of CDKs is also regulated by the mitosis-inhibiting kinase Wee1. In the G1 phase, this ATM signaling pathway facilitates NHEJ. In the G2 phase, initial

activation of ATM is followed by activation by the ATR signaling pathway and repair by HR (14). In this case, the DSB is resected, leading to formation of ssDNA which is coated and stabilized by the replication protein A (RPA), and which recruits the ATR-ATRIP complex. ATR phosphorylates the Chk1 with the help of the Claspin mediator protein (12). Activated Chk1 phosphorylates CDC25A. This will cause S and G2 arrest. p53, a key player in DNA-damage checkpoints is also activated by Chk1 and Chk2.

To sum up, the checkpoint generates a broad spectrum of responses to DNA damage, leading to cell cycle arrest and DNA repair in animals. Although checkpoint activation is not essential for DSB repair, it modulates how the damage is repaired and whether HR or NHEJ is used for repair (15).

In plants, there is no functional CDC25 homolog identified yet. Mitosis-inhibiting kinase Wee1 activates DNA damage checkpoints in an ATM/ATR-dependent manner (16). Also many other genes, needed for checkpoints in mammals, have not been identified in plants yet (such as Chk1, Chk2, PLK, p53, Claspin, 53BP1, ATRIP and MDC1). Two kinds of CDKs have been identified in plants: CDKA and CDKB. They can control the cell cycle directly. These checkpoint genes are not essential for normal growth in plants, whereas they are essential in mammals (17).

### 3. Homologous Recombination (HR)

HR is a mechanism which uses DNA homology to direct DNA repair. It occurs in all life forms. In eukaryotes, HR is carried out by the Radiation sensitive 52 (Rad52) epistasis group of proteins, which were initially identified in *Saccharomyces cerevisiae* from the genetic analysis of ionizing radiation (IR) hypersensitive mutants (18). The Rad52 epistasis group is composed of Rad50, Rad51, Rad52, Rad54, Rad55, Rad57, Rad59 and the MRX complex. Most of those proteins are well preserved among eukaryotes. Orthologs have been identified in mammals and plants (Table1), except for Rad55/57 and Rad59, which are functionally replaced by five Rad51 paralogs (19). All HR events are initiated by 5'-3' resection at the DSB end, which is facilitated by the MRX/MRN complex. The MRX/MRN complex plays a critical role in the early DSB response. It has 3'-5' exonuclease, single-strand endonuclease, and DNA unwinding activities and is involved in the 5'-3' resection of DSB ends to produce 3' single-strand overhangs. Sae2 in *S. cerevisiae* and CtIP in mammals are involved together with the MRX/MRN complex in the processing of DSB ends. Sae2 exhibits endonuclease activity on ssDNA and DNA strand transition and cooperates with MRX to cleave DNA hairpin structures. After this initial processing of the DSB resection, it is taken over by the exonuclease (Exo1) and the Sgs1 helicase (20). This may lead to a several-kbp-long region of single stranded DNA (ssDNA). Mammals and plants have orthologues of those proteins, suggesting a general mechanism for DSB end processing in eukaryotes.

Once 3'-ssDNA overhangs are generated, they are coated by RPA. RPA directly interacts with Rad52 in yeast, which recruits Rad51 to load on single-strand DNA by displacing

**Table 1.** HR factors in yeast, mammals and plants.

<i>Saccharomyces cerevisiae</i>	<i>Homo sapiens</i>	<i>Arabidopsis thaliana</i>	Locus in <i>Arabidopsis</i> and ref.	Function
Rad50	Rad50	AtRad50	At2G31970 (169-171)	DNA binding, DNA-dependent ATPase, complex with Mre11 and Xrs2/Nbs1, DSB ends processing, DNA-damage checkpoints
Mre11	Mre11	AtMre11	At5G54260 (169;172;173)	3'-5' exonuclease, complex with Rad50 and Xrs2/Nbs1, DSB end processing, DNA-damage checkpoints
Xrs2	Nbs1	AtNbs1	At3G02680 (6)	DNA binding, complex with Rad50 and Xrs2/Nbs1, DSB end processing, DNA-damage checkpoints
Sae2	CtIP	AtCom1/ AtGr1	At3G52115 (174)	Endonuclease, DNA strand transition
Rad51	Rad51	AtRad51	At5G20850 (175-177)	RecA homologue, strand invasion
Dmc1	Dmc1	AtDmc1	At3G22880 (178;179)	Rad51 homologue
Rad52	Rad52	AtRad52 (22)		ssDNA binding and annealing, recombination mediator, interacts with Rad51 and RPA
Rad54	Rad54	AtRad54	At3G19210 (180)	ATP binding, DNA binding, helicase activity, recombination mediator
Rad55-Rad57	-	-		ssDNA binding, recombination mediator
Rad59	-	-		single-strand annealing

<i>Saccharomyces cerevisiae</i>	<i>Homo sapiens</i>	<i>Arabidopsis thaliana</i>	Locus in <i>Arabidopsis</i> and ref.	Function
-	Rad51B	AtRad51B	At2G28560 (181;182)	ssDNA binding, recombination mediator
-	Rad51C	AtRad51C	At2G45280 (181;183;184)	
-	Rad51D	AtRad51D	At1G07745 (181;185)	
-	Xrcc2	AtXrcc2	At5G64520 (181)	
-	Xrcc3	AtXrcc3	At5G57450 (186)	
	Brca1	AtBrca1	At4G21070 (187;188)	checkpoint mediator, recombination mediator
-	Brca2	AtBrca2-1, AtBrca2-2	At4G00020 (178;179)	recombination mediator
Exo1	Exo1	At1G18090?	At1G18090?	exonuclease
Sgs1	BLM	AtRecQ4A	At1G10930 (189)	ATP binding, RecQ helicases

RPA. RAD51 is present in mammals. But RAD52 is not identified in mammals, BRCA2 fulfills the role of yeast Rad52 (19;21). Recently the orthologs of Rad52 were also identified in plants (22). Several possible homology directed repair subpathways have been postulated on the basis of the outcome of the recombination reaction: classical double-strand break repair (DSBR), synthesis-dependent strand-annealing (SDSA), single-strand annealing (SSA) and break-induced replication (BIR) (Figure 2) (23). DSBR was initially described to explain gene conversion and crossover events during meiosis (24). SDSA is based on mitotic DSB repair data in model organisms (25) and is thought to be the predominant mechanism to repair two-ended DSBs by HR. SSA may be utilized to repair a two-ended DSB, when a repeat sequence is present adjacent to the DSB. BIR has been described in yeast and may be used for one-ended DSBs to restart collapsed replication forks and elongate uncapped telomeres (26). In plants, there is evidence for the existence of SDSA, DSBR and SSA (27).

After 3'-end resection and Rad51 coating of the ssDNA, the nucleoprotein filament may invade into a homologous double stranded DNA (dsDNA) sequence and form a heteroduplex DNA intermediate which is called D-loop. This process occurs in the case of repair by the SDSA or classical DSBR subpathways (Figure 2). The "X" shaped structure formed at the border between the hetero- and homoduplex of a D-loop is called a Holliday Junction (HJ) (28). DNA is synthesized from the 3' end of the ssDNA beyond the original break site by D-loop migration to restore the missing sequence information. In the case of SDSA, the newly synthesized end of the invading strand is released by sliding the HJ toward

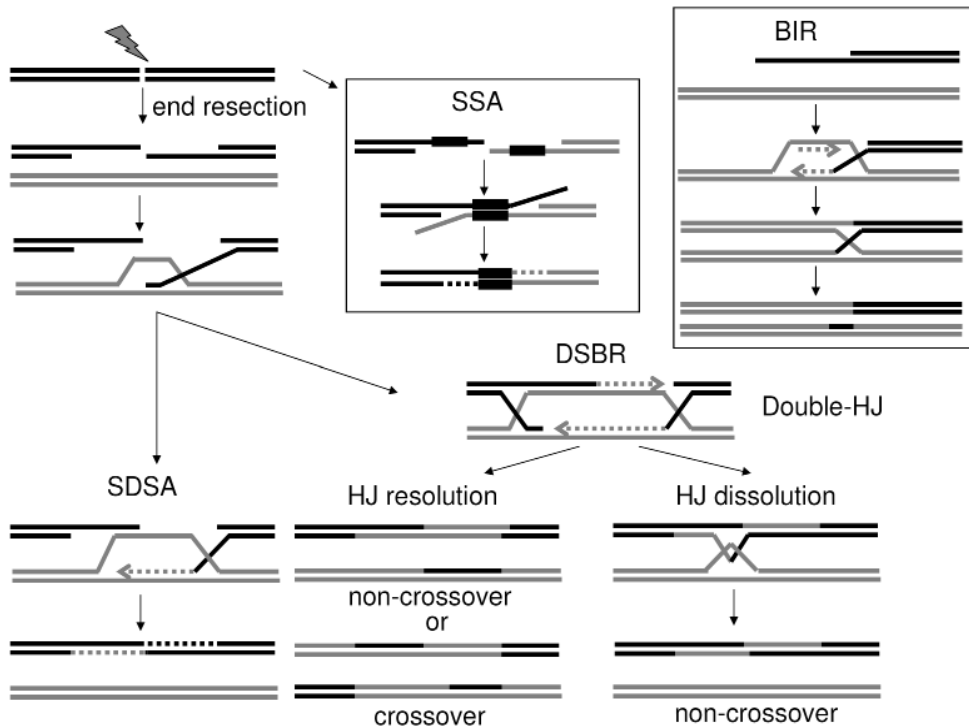


**Figure 2.** Models for DSBs repair via HR.

DSBs can be repaired by several HR pathways, including SDSA, DSBR, SSA and BIR. SDSA, DSBR and SSA are supposed to repair two-end DSBs. In those pathways, repair is initiated by end resection to provide 3' ssDNA overhangs. In the SDSA and DSBR pathways, the 3' ssDNA overhang invades into a strand with a homologous sequence by forming a D-loop, followed by DNA synthesis. In the SDSA pathway, the newly synthesized DNA forms a migrating replication bubble and is released from the template to anneal to the ssDNA on the other break end. The next step is gap-filling DNA synthesis and ligation. This will result in gene conversion. In the DSBR pathway, the other DSB end is also captured to form a double-HJ intermediate. The double-HJ structure can be resolved or dissolved in a non-crossover or crossover mode. DSBR can lead to gene conservation and crossover events. In the SSA pathway, the complementary DNA repeats (black boxes) serve to anneal the DSB ends and the noncomplementary overhangs are removed, followed by gap-filling and ligation. SSA produces a deletion between two sequence repeats. BIR is utilised to repair one-end DSBs. The single DSB end invades into a homologous strand, initiates a unidirectional DNA synthesis and replicates the entire homologous template arm. A single HJ is formed and is cleaved to repair the break with a duplication of the chromosome arm used as a template. BIR might result in a large-scale loss of heterozygosity, or a high mutation rate by template switching.

the 3' end. The displaced end can then anneal with the second resected DSB end. After removing flaps and filling-in gaps, the remaining nicks are ligated to complete this pathway. In the case of classical DSBR, both DNA ends invade a homologous chromosome to copy genetic information into the donor chromosome. The DNA joint molecule harbors two HJs that may be resolved to create a crossover or a non-crossover product. Whereas classical DSBR is used in meiosis for recombination between the two homologous chromosomes,

SDSA is used in somatic cells to restore DNA damage using the sister chromatid for repair.

In the case of SSA, the resected ends anneal to each other, which is possible when repeats are present near the DSB site (Figure 2). The protruding single-strand tails are removed by nucleases. Then gaps and nicks are filled in by DNA synthesis and ligation. SSA leads to permanent deletions, so it is error-associated.

For BIR, the DSB end is nucleolytically processed to a single-stranded tail that invades a homologous DNA sequence, followed by DNA synthesis to replicate the chromosome template (Figure 2). Unlike SDSA, for BIR a homologous sequence in a non-homologous chromosome is utilized as a template to initiate repair, and thus BIR can result in a non-reciprocal translocation.

#### 4. Non-Homologous End Joining (NHEJ)

The basic NHEJ event is the direct joining of DSB ends, which are juxtaposed through end bridging, end-processed and ligated. NHEJ is a potentially less accurate mechanism for DSB repair, compared with HR. DNA end bridging occurs via protein-protein interactions between DNA end binding proteins, which bind directly to the DNA ends immediately after the breaking.

Most factors involved in the NHEJ pathway were initially identified in mammalian systems, such as the Ku heterodimer, DNA-dependent protein kinase catalytic subunit (DNA-PKcs), DNA ligase IV (Lig4), XRCC4, XLF/Cernunnos (Table 2). The classical NHEJ (C-NHEJ) pathway utilizes Ku, DNA-PKcs, Lig4, XRCC4 and XLF/Cernunnos as central components; therefore it is also called DNA-PK-dependent NHEJ (D-NHEJ). C-NHEJ repairs rapidly a large proportion of DSBs. Recent findings show there are also one or several distinct alternative pathways, so-called backup NHEJ (B-NHEJ) pathways, which repair DSBs more slowly in the absence of the C-NHEJ factors. B-NHEJ pathways are Ku-independent, but utilize instead poly(ADP-ribose) polymerase (Parp) and DNA ligase III (Lig3) in mammalian cells. The most commonly discussed form of B-NHEJ is the microhomology-mediated end joining (MMEJ), which is mediated by a stretch of microhomologous base pairing of about 5 to 25 base pairs (bps).

There are two possibilities for the ligation of the juxtaposed DSB ends in NHEJ (Figure 3). Firstly, the ends can be ligated precisely. But the majority of DSBs generated by exposure to DNA damaging agents does not have ligatable termini and must be processed prior to ligation. In most cases, this will eventually produce deletions or insertions at the restored break site. Secondly, micro-homologous repeats surrounding the DSB ends may be aligned to repair the break by microhomology-mediated end joining (MMEJ). The mechanism is similar to SSA, but the homologous sequence used for MMEJ is only 5 to 25 bps, which is much shorter than the homology required for SSA. MMEJ will delete one of the repeats and the sequence between the repeats.

**Table 2.** NHEJ factors in yeast, mammals and plants.

<i>Saccharomyces cerevisiae</i>	<i>Homo sapiens</i>	<i>Arabidopsis thaliana</i>	Locus in Arabidopsis and ref.	Function
Ku70	Ku70	AtKu70	At1G16970 (151;190;191)	DSB end binding, protection and juxtaposition
Ku80	Ku80	AtKu80	At1G48050 (153;191)	
-	DNA-PKcs	-		protein kinase
Snm1/Pso	Artemis	AtSnm1?	At3G26680 (59;192)	DNA end processing, 5'-3' exonuclease, endonuclease
Pol4	Pol $\chi$ family	Pol $\lambda$	At1G10520 (60)	DNA end processing, filling in DNA gap
Tpp1?	PNK	-		DNA end processing, 3'-DNA phosphatase, 5'-DNA kinase
Tdp1	Tdp1	At5G15170	At5G15170 (193)	DNA end processing, 3'-DNA phosphatase
Dnl4	DNA ligase IV	AtLig4	At5G57160 (150;152)	ATP-dependent DNA ligase
Lif1	XRCC4	AtXRCC4	At3G23100 (152)	Complex with Lig4, DNA binding
Nej1	XLF/ Cernunnos	-		Lig4/XRCC4 binding
-	Parp1	AtParp1 (ZAP)	At2G31320 (194-196)	DNA binding, NAD+ADP-ribosyltransferase activity
-	Parp2	AtParp2 (APP)	At4G02390 (99;194-196)	DNA binding, NAD+ADP-ribosyltransferase activity
-	DNA ligase III	-		ATP-dependent DNA ligase
	XRCC1	AtXRCC1	At1G80420 (197)	Complex with Lig3
		AtLig6	At1G66730 (101)	ATP-dependent DNA ligase



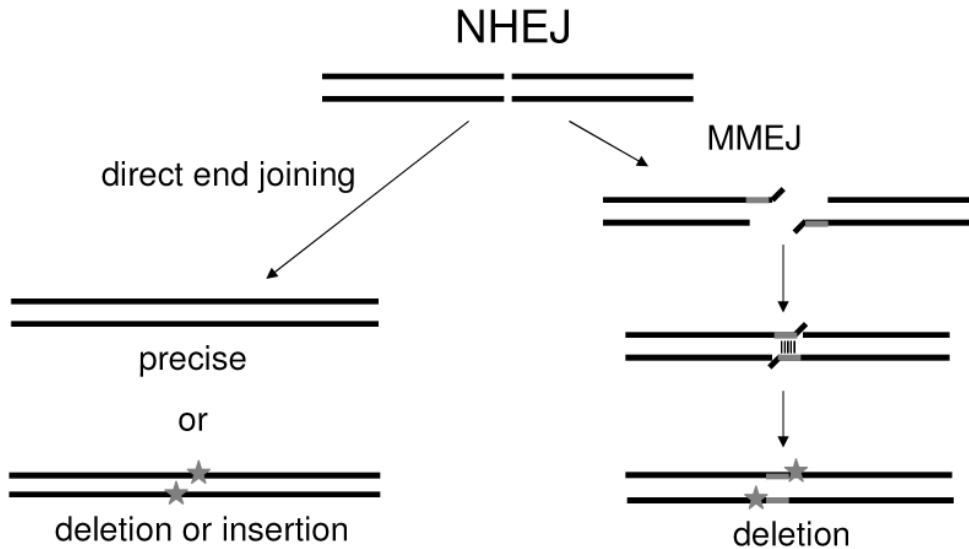


**Figure 3.** Ligation models of the juxtaposed DSB ends in NHEJ.

There are different ways for DSB ends to join: direct end joining or MMEJ. DSB ends can be joined precisely if the two ends are ligatable. But in most cases, the damaged ends are not ligatable, and they need end processing before ligation. This may induce deletions or insertions. For MMEJ, the ends are also processed to ssDNA, followed by strand annealing promoted by a short stretch of homologous sequence. Any non-paired flaps are removed and the ends are ligated. This will produce deletions.

#### 4.1 Classical Non-Homologous End Joining (C-NHEJ)

##### 4.1.1 Detecting and tethering DSB ends

It is generally assumed that NHEJ is initiated by the binding of a heterodimeric complex (Ku) to both DNA ends at the DSB site. The Ku heterodimer is composed of a 70kDa and 80kDa subunit, termed Ku70 and Ku80 respectively (29). Ku can bind various types of DNA ends (hairpins, blunt ends and 5' or 3' overhangs) in a sequence independent fashion with a high affinity *in vitro* (29;30). It associates with the DSB ends immediately after the generation of the break (31). The redox conditions can regulate the DNA-Ku binding by changing the structure of Ku, but it is still unclear how this happens (32). The Ku70 and Ku80 heterodimer forms a ring structure that slides over the DSB ends in an ATP independent manner (29). Ku stabilizes the DNA ends to facilitate NHEJ repair and protects DSB ends from DNA 5'-end resection which is a prerequisite for HR repair (23). Ku also recruits other NHEJ factors (such as DNA-PKcs, Lig4/XRCC4/XLF) to DSB ends and serves as a scaffold for the assembly of the NHEJ synapse (33).

In mammals, the DNA-Ku complex recruits DNA-PKcs, a ~465kDa member of the PIKKs, to form the active DNA-PK holoenzyme. DNA-PKcs is a nuclear protein serine/threonine kinase. The flexible arm of the Ku80 C-terminal region extends from the DNA-binding core to recruit and retain DNA-PKcs at DSBs (34). Crystallography studies revealed that DNA-PKcs forms a large open-ring cradle to promote the DSB repair (35). Electron

microscopy studies suggested that DNA-PKcs functions as a DNA-end bridging factor to tether the broken ends for rejoining (36). Two DNA-PKcs molecules interact across the DSB with the Ku dimer in a synaptic complex (37). This interaction stimulates the kinase activity of DNA-PKcs (38). The active DNA-PK catalyzes autophosphorylation and phosphorylation of other downstream NHEJ proteins. DNA-Pkcs phosphorylation appears to be important for DNA repair. Upon autophosphorylation DNA-PKcs is released from the DNA ends by changing the conformation (34). This conformation change would make the DNA ends accessible for the processing enzymes and ligases (39). This suggested that DNA-PKcs might regulate NHEJ by phosphorylation.

In yeast and fungi, no homologues of DNA-PKcs have been identified. Biochemical evidence shows that the MRX complex takes the role of end bridging in the yeast NHEJ instead of DNA-PKcs (40). Rad50 contains a high-affinity DNA-binding domain and a split ATPase domain. A functional ATPase is formed when two Rad50 proteins associate. Rad50 may be able to bridge the DNA ends together (41). Mre11 interacts with yKu80 and Xrs2 interacts with the Lif1 cofactor of the Lig4 ligase (8). It seems that MRX enables formation of a stable NHEJ complex (23). MRX is the only protein complex that participates in both NHEJ and HR DSB-repair pathways in yeast (23) and thus, might regulate repair pathway utilization.

#### 4.1.2 Processing DSB ends

DSBs may have various ends. In case of incompatible ends, DSB ends processing is required to remove non-ligatable end groups and other lesions prior to ligation. Processing may consist of resection by nucleases, filling DNA gaps by polymerases or addition of 5' phosphate groups by polynucleotide kinase (PNK) (39). Several accessory enzymes have been implicated in this process, including Artemis, Mre11, DNA polymerase Pol  $\chi$  family members and PNK, as mentioned above.

In mammals, Artemis, a key end-processing enzyme, may be recruited to DSBs by interacting with DNA-PKcs (42). The activity of Artemis can be regulated via phosphorylation by DNA-Pkcs and ATM, suggesting that Artemis may participate in multiple aspects of the DNA damage response (14;42). Artemis is a 5'-3' exonuclease and also possesses an endonuclease activity in a DNA-PKcs-dependent manner to remove both 5' and 3' overhangs for NHEJ repair and cleave the DNA hairpins during V(D)J recombination (38). The nucleolytic processing of DNA ends might create small gaps that must be filled in by DNA polymerase Pol  $\chi$  prior to DNA joining during NHEJ. The mammalian Pol  $\chi$  family includes DNA polymerases  $\beta$  (Pol  $\beta$ ), Pol  $\mu$ , Pol  $\lambda$  and terminal deoxynucleotidyl transferase (TdT) (43). TdT is a unique template-independent polymerase, which can add random nucleotides during V(D)J recombination. Pol  $\mu$  is template-dependent, and Pol  $\beta$  and Pol  $\lambda$  can synthesize in both template-independent and template-dependent manner (44). If DNA ends contain non-ligatable 5' hydroxyls and 3' phosphates, the mammalian PNK can modify those groups to facilitate the ligation (45). PNK possesses both 3'-DNA phosphatase

and 5'-DNA kinase activities and interacts with XRCC4 during NHEJ (23).

In yeast, the MRX complex is suggested to have the same function as the mammalian DNA-PKcs/Artemis complex (4). Mre11 is a nuclease and can remove hairpins and 3'-ssDNA overhangs at the ss/ds DNA junction. So Mre11 may be involved in end processing in NHEJ (7). Pol4 is the only Pol  $\chi$  polymerase which acts in gap filling without strict dependence on the template during NHEJ in yeast (46;47). The yeast homologue of mammalian PNK, 3'-phosphatase-1 (Tpp1), lacks 5' kinase activity (48). Recent reports showed that 3' nucleosidase activity of tyrosyl-DNA-phosphodiesterase 1 (Tdp1) regulates the processing of DNA ends by generating a 3' phosphate and restricts the ability of polymerases from acting at DNA ends (49).

#### 4.1.3 Ligating DSB ends

After the proper processing of DNA ends, NHEJ is completed by the final ligation step. This rejoining step is carried out by the complex of DNA ligase IV (Lig4) and XRCC4. A third essential component for the NHEJ ligation step is XRCC4-like factor (XLF, also named Cernunnos), which stimulates the activity of Lig4 and is required for NHEJ and V(D)J recombination (50;51).

Lig4 contains an ATP utilizing catalytic domain in the N-terminal region and two C-terminal BRCT domains. The two BRCT domains of Lig4 and the linker region between them interact with XRCC4 to form a stable complex (39;52). The BRCT motifs may also be involved in the interaction with the Ku complex (53). XRCC4 stabilizes Lig4 and stimulates its activity (38). The globular N-terminal head of XRCC4 interacts with the DNA helix (54). Like Ku proteins, XRCC4 acts as a scaffold to recruit other NHEJ factors, including the processing enzyme PNK. The Lig4/XRCC4 complex not only facilitates the ligation step but may also stimulate the DNA end processing. Lig4 has a high degree of substrate flexibility in the presence of XRCC4 and XLF. The complex can ligate both blunt ends and compatible overhangs. It can also ligate across gaps and incompatible ends with short overhangs (44). XLF has a similar structure as XRCC4, with which it interacts. The crystal structure of XLF reveals that it has an N-terminal globular coiled-coil head and a C-terminal stalk, which is suitable for the head-to-head interactions in a 2:2:1 XRCC4:XLF:Lig4 complex (55). XLF can enhance Lig4/XRCC4 ligation activity by promoting its re-adenylation, but XLF is dispensable for the stability of Lig4/XRCC4 complex suggesting that XLF is not essential for all DSB rejoining (56). Both XRCC4 and XLF are phosphorylated by ATM and DNA-PK, though phosphorylation seems to be not required for NHEJ (57;58).

Homologs of Lig4/XRCC4 have been identified in mammals, yeast and plants, suggesting that the mechanism by which the ligation step occurs is universal in eukaryotes. The counterpart of XLF has also been found in yeast and is named Nej1. But so far no XLF homolog has been identified in plants.

In plants, no affirmative homologues of DNA-Pkcs have been identified until now. This

suggests that Ku of plants may have more general functions in NHEJ pathway than that of mammals, and it could be that Ku or MRN bridge the two DNA ends together. The processing of DSB ends in NHEJ is largely unknown in plants. Plants contain an Artemis homologous protein known as Pso2p/Snm1p. However, due to the low similarity of amino acid sequence between Artemis and Pso2p/Snm1p, they may have different functions in DNA repair (59). DNA ends may be processed by the MRN complex to make them suitable substrates for DNA ligase in plants as that in yeast. The only member of the Pol  $\chi$  family identified in plants is DNA Pol  $\lambda$ . It has a close similarity to mammalian Pol  $\beta$  and is supposed to function as a DNA repair enzyme in meristematic and meiotic tissues (60).

#### **4.2 Backup Non-Homologous End Joining (B-NHEJ): Microhomology-Mediated End Joining (MMEJ)**

Nowadays more and more evidence show that the majority of DSBs can be rejoined with slow kinetics in the absence of C-NHEJ core factors, such as DNA-PKcs, Ku70/Ku80 and Lig4/XRCC4, suggesting the existence of one or multiple alternative or backup pathways of NHEJ (61;62). The alternative pathways were well demonstrated in C-NHEJ deficient cells or in wild-type cells after the treatment with inhibitors against C-NHEJ factors (63-66). Compared to the extremely fast and efficient C-NHEJ, the alternative pathways are quite slow and error-prone (67). Defects in C-NHEJ are implicated in chromosomal translocation and gene instability (68-70). Many studies utilizing *in vitro* plasmid based end joining assays also have provided evidence for the existence of B-NHEJ (62;71;72). End joining is observed in the extracts of DNA-Pkcs deficient cells and in Ku-depleted extracts. Anti-Ku antibodies inhibit DNA end joining strongly only in the presence of DNA-PKcs, and Ku is also essential for the inhibition of DNA end joining by the DNA-PKcs inhibitor wortmannin (62). It suggests that Ku, cooperating with DNA-PKcs, directs joining of broken ends to C-NHEJ, at the same time suppressing B-NHEJ. The repair events via B-NHEJ preferentially use short stretches of homology (5-25bps) (65;73;74), and therefore this type of repair has also been called microhomology-mediated end joining (MMEJ). It seems that MMEJ is the dominant pathway among the B-NHEJ pathways. MMEJ induces small deletions and causes gene instabilities (75). Several proteins have been identified as participating in B-NHEJ in mammals: histone H1, poly(ADP-ribose) polymerase-1 (Parp1), DNA Ligase III (Lig3) and XRCC1 (76;77).

Histone H1 is a major structural component of chromatin with functions in DNA repair. Protein fractionation and *in vitro* end-joining assays showed that histone H1 enhances DNA-end joining strongly by activating Lig3 and Parp1, suggesting it is a putative B-NHEJ factor (78). Histone H1 has been shown to inhibit HR (79) and C-NHEJ (80). It binds to naked DNA and may juxtapose to form end to end polymers (81), and thus histone H1 may be an alignment factor operating in B-NHEJ (78).

Poly(ADP-ribose)polymerases (Parps) catalyze the covalent attachment of poly(ADP-ribose) units on amino acid residues of itself and other acceptor proteins using NAD<sup>+</sup> as

a substrate in order to modulate various cellular processes by poly(ADP)ribosylation (82). Among the 17 members of the Parp family, Parp1 and its close homologue Parp2 are activated in response to DNA damage (83). Parp1 has a high binding affinity for DNA SSBs and DSBs by its two zinc finger motifs. Binding to DNA leads to Parp1 automodification and subsequent release from DNA to allow the access of other repair proteins (76). There is plenty of evidence that Parp1 is implicated in SSB repair and base excision repair (BER) and thus prevents formation of DSBs during replication (83;84). Parp1 is probably also involved in B-NHEJ. The synapsis activity of Parp1 and the ligation activity of Lig3/XRCC1 were established via a two-step DNA *in vitro* pull down assay with nuclear extracts and recombinant proteins (85). In absence of DNA-PK or Lig4/XRCC4, DSB end joining activity was observed, which was dependent on Parp1 and Lig3/XRCC1. Recent reports also show that Parp1 facilitates B-NHEJ using microhomology (86). Parp1 binds to DNA ends in direct competition with Ku to regulate the utilization of C-NHEJ and B-NHEJ pathways (87). Parp1 is supposed to be a sensor of DNA breaks and may help to form the end synapsis. Parp2 may have a similar function as Parp1 (88). Parp2 has a higher affinity for gaps or flaps than SSBs, indicating that Parp2 is involved in later steps of the repair process (88). Parp1 regulates the activity of Pol  $\beta$  in long patch BER (89) and interacts with Mre11 for end processing in the restart of replication forks (90), suggesting that Pol  $\beta$  and MRN may also function in end processing during B-NHEJ.

Unlike other DNA ligases, Lig3 appears to be unique to vertebrates. Lig3 is recruited to SSBs by preferentially interacting with automodified Parp1 (91). Thus Lig3 is considered to be involved in SSB repair and BER (92;93). Lig3 is also found to play a major role in end joining by using extract fractionation of Hela cells (94). DNA end joining activity can be reduced by knocking down Lig3 in Lig4-deficient mouse embryo fibroblasts (94). This indicates that Lig3 has a potential role in B-NHEJ pathway. XRCC1 interacts with Lig3 and is required to stabilize Lig3 (95). XRCC1 interacts with several other BER and SSB repair factors as well, such as Parp1 and Pol  $\beta$  (92), suggesting that XRCC1 may act as a scaffold for the protein assembly (96).

MMEJ has also been found in yeast which is repressed by Ku70 (97), suggesting that there may be similar backup NHEJ pathway in yeast. Specific B-NHEJ proteins have not been identified in yeast as yet. Although Parp activity is absent in yeast, human Parp1 expression in *Saccharomyces cerevisiae* leads to the inhibition of growth due to its effects on ribosome biogenesis (98). Other proteins may replace the function of Parp in yeast.

Like in mammals, there may be backup pathways of NHEJ in plants. Homologues of Parp1 and Parp2 have been identified in plants. One is the classical Zn-finger-containing polymerase (ZAP) and the other is APP/NAP, which is structurally different from the classical Parp and is lacking the N-terminal Zn-finger domain (99). APP/NAP is a DNA-dependent poly(ADP-ribose) polymerase and the expression of APP/NAP is induced by deficiency of Lig1 (99). Microarray data also showed that APP/NAP displayed transcriptional induction in the presence of bleomycin and in the *Atku80* mutant (100). All these observations

point to the implication of APP/NAP in DNA repair. Though no homologues of Lig3 has been identified in plants, a novel ATP-dependent DNA ligase, named Lig6, is found uniquely in plants. Bonatto *et. al.* (101) found that Lig6 has a high homology with Lig1 and is hypothesized to function in BER and B-NHEJ. Recently the work of Waterworth *et. al.* (102) showed that the *Atlig6* mutant was hypersensitive to X-ray and delayed in seed germination.

## 5. Regulation of DSB repair pathways

As discussed above, eukaryotes have two primary pathways to repair DSBs: HR and NHEJ. Both of them play an important role in maintaining genome stability and preventing the consequent disorders, such as the loss of genetic information, chromosomal translocations, cell death and diseases like cancer. How do cells modulate the respective usage of those pathways? Since different pathways generate distinct products, it is an important and compelling question. Also when the control mechanisms are well studied, ways to regulate them may be found, and used for instance to increase the usage of HR, which will facilitate gene targeting. These control factors may also become helpful as biomarkers for cancer detection and as targets for cancer therapy.

Different organisms prefer different pathways to repair DSB. Yeast tends to use HR, whereas higher eukaryotes like plants and mammals mainly use NHEJ in somatic cells. This is based on the observation that NHEJ-deficient yeast is not sensitive to IR unless HR is also deficient. In contrast, NHEJ-deficient mammals and plants are hypersensitive to IR whether HR is operative or not (23;103). Higher eukaryotes have larger and more complex genomes and enormous amounts of repetitive DNA, which may be the reason that NHEJ is preferred in order to prevent mistakes leading to translocation. The choice between the different forms of DSB repair also depends on the cell type, phase of the cell cycle and developmental stages of the organism. HR is more efficient in diploid than in haploid yeast due to template availability and the absence of Nej1, which is involved in NHEJ (104). Though most higher eukaryotes predominately utilize NHEJ in somatic cells, Chicken B cells (DT-40) possess a highly efficient HR machinery (105). Mouse embryonic stem (ES) cells are more prone to HR, than primary cells (106). HR is the predominant mode of DSB repair during early neural development, and NHEJ takes over the function at the later stage (107). DSB repair mechanisms are developmentally regulated in plants. Rad51 activity drops and Ku70 activity increases after germination, therefore, the rate of HR decreases with plant age in *Arabidopsis* (108).

It is well documented that NHEJ is active in all phases of the cell cycle, whereas HR is mainly restricted to the S and G2 phases of the cell cycle and directed to the utilization of the new sister chromatid as a template (104). This means that the cell cycle stage could be a decisive factor for the selection of the DSB repair pathway when a DSB is generated. Cell cycle progression is primarily controlled by cyclin-dependent kinases (CDKs) (109).



In yeast, Cdc28/Cln (Cdk1/cyclin B) is activated in the *S/G2* phases and is suppressed in *G1* phase. In the *S/G2* phases, active CDK facilitates the DNA resection of DNA ends, which is the initiation step of HR. DSB ends are resected in 5'-3' direction to generate ssDNA, which can anneal with a homologous sequence to effect HR, or if homology is not available, MMEJ. It was shown that CDKs phosphorylate Sae2 (budding yeast)/Ctp1 (fission yeast) and the mammalian orthologue CtIP to promote DSB resection and HR cooperatively with MRX/MRN in the *S/G2* phases (110-112). The endonuclease activity of Sae2 for DSB resection is also regulated by the Cdc28/Cdk1-mediated phosphorylation in a cell-cycle dependent manner (112). Yun et al. (111) reported that CtIP is required for both HR in the *S/G2* phases and MMEJ in *G1* in the DT40 cell line. In mammals, CtIP is also found to regulate DSB resection by interaction with MRN and BRCA1 in the *S/G2* phases (113). Phosphorylated CtIP recruits BRCA1 to DNA damage sites and increases the level of ssDNA (111). In the late *M/G1* phases, CDK phosphorylates BRCA2, resulting in disassociation of the Rad51-BRCA2 complex, and in blocking HR (114).

During the cell cycle, the components of different DSB repair pathways seem to compete for the selection of DSB repair pathway. Ku is always the first factor recruited to DNA ends due to its high affinity for DNA ends. Ku protects the ends from resection and interferes with HR during the whole cell cycle. HR factors may also interact with the Ku-bound ends. Indirect evidence showed that in the *S/G2* phase, HR factors, such as CtIP1 and BRCA1, are highly activated by phosphorylation, which facilitates HR over NHEJ. In the *G1* phase, the Ku complex recruits the Lig4 complex to stabilize Ku and ligate the DNA ends via NHEJ. Biochemical evidence has shown that Parp physically interacts with Ku and decreases the affinity of Ku to DSBs so as to favor HR (106;115). Studies with DT40 cells implicate that Parp1 and the post-replicative repair protein Rad18 independently promote HR and suppress NHEJ (116;117). Parp1 also competes for DNA ends with Ku to enhance B-NHEJ in *G2* (87;118). Recent results from studies with human somatic cells indicate that Ku suppresses other DSB repair pathways (HR and B-NHEJ), suggesting that Ku could be a critical regulator of DSB repair choice (74).

In summary, there is a crosstalk between all the DSB repair pathways. The cell cycle progression could be the key regulator for the switch between NHEJ and HR. The regulation involves among others the availability of repair templates, the activity of CDKs, DNA end resection and protein competition. HR and NHEJ work in a competitive and cooperative manner to maintain the genome stability.

## 6. Gene Targeting (GT)

Gene targeting (GT) is a technique by which endogenous genes in the genome are modified using HR with a transgene. It has broad applications. It is a powerful tool for studying gene function by the inactivation or modification of specific genes, and it is also a potential means for gene therapy and biotechnological improvement of crop plants. The implementation

of HR-based GT relies not only on the design of the sequence homology between the exogenous transforming DNA molecule (the donor) and the chromosomal DNA (the target), but also on the DNA-repair system used by the target cell. Efficient GT has been achieved in yeast, fungi and some cell lines, such as mouse embryonic stem cells, chicken DT40 cells, and human Nalm-6 pre-B cells (119;120). However, GT is inefficient in plants, and most other animal and human cell lines. How to improve the frequency of GT events in these organisms is a big issue and challenge.

There are several strategies to select and detect gene targeting events, one of which, the positive/negative selection (P/NS) scheme, proved to be very successful. In the P/NS strategy, the targeting construct contains a positive selectable marker placed in between homologous regions and a negative selectable marker gene placed outside the homology (121). It enriches for gene targeting events by selection for the positive selection marker and against the negative selection marker, thus reducing transformants in which the transgene had integrated by non-homologous recombination. The Herpes simplex virus thymidine kinase gene (HSV-TK) and the diphtheria toxin A-chain gene (DT-A) have been commonly used as negative selection markers in mammals (121;122). Also in plants several negative selection marker genes have been tested (123-125) and the results depended on the species and the developmental stage.

Based on the mechanism of GT, there are two general ways to increase the frequency of GT events. The first one is to genetically modify the organisms in order to facilitate the HR pathway by either increasing the HR components or reversely by blocking the NHEJ pathway. The second is to introduce specific DNA breaks in the target sequence so as to increase the chance of recombination at the target locus. Sufficient homology between the targeting vector and the target locus obviously is also important. In murine embryonic cells, a dramatic increase in the targeting frequency can be observed by an increase of homology in a range between 2 and 10kb (126). If the area of homologous DNA is reduced to below 1kb in length, gene targeting is strongly diminished (127). The need for homology is saturated by ~14kb (126).

### **6.1 Facilitating the HR pathway**

Several reports showed that elevation of the expression of exogenous HR components, such as Rad51, Rad52 and Rad54, can enhance gene targeting frequencies (128-131). Previous reports also showed that HR could be enhanced by expression of bacterial RecA provided with a nuclear localization signal in mammals and plants (132;133). Enhanced gene targeting was also observed by overexpression of Rad51 in murine embryonic stem cells (128). In the yeast *Saccharomyces cerevisiae*, yRad52 and yRad51 are required for the targeted integration of *Agrobacterium* T-DNA via HR (134). Di Primio *et al.* (129) expressed the yRad52 in human cells and this increased the frequency of gene targeting by 37 fold. They proposed that yRad52 has a greater affinity for ssDNA to promote strand exchange than hsRad52, suggesting that the yeast protein could be used as a tool to enhance gene targeting. Recently



Kalvala et al. (130) followed up on this finding by delivering yRad52 directly into the human cells by the fusion of yRad52 to the arginine-rich domain of the HIV TAT protein (tat11), which is known to permeate cell membranes. The recombinant yRAD52tat11 still maintained the ability to bind ssDNA and promote intrachromosomal recombination after entering the nuclei of the cells. By using this approach, a 50-fold increase of gene targeting was observed. This approach of expression of yeast HR proteins to improve gene targeting was also utilized in plants. Shaked *et al.* (131) expressed the yRad54 in Arabidopsis plants and gene targeting was analyzed using a high-throughput assay based on visual screening of GFP in seeds. An increased frequency of gene targeting by 27 fold on average was found. yRad54, a member of the Swi2/Snf2 family of ATP-dependent chromatin remodeling factors, promotes strand invasion in HR. Disruption of the *Rad54* gene reduced gene targeting and increased radiation sensitivity in various species (135;136). Thus Rad54-like activity may be a limiting factor in gene targeting. All of these observations indicated that elevated expression of the factors involved in HR could be potentially useful to increase gene targeting. Whether it can be utilized in other organisms like livestock or crop plants, is still unknown.

Since random DNA integration in yeast can be suppressed by a deficiency in NHEJ (137), the number of gene targeting events may be increased after disruption of NHEJ. So far, this has been well manifested in lower eukaryotes, such as yeast and several species of filamentous fungi (134;137-145). Unlike the yeast *Saccharomyces cerevisiae*, other yeasts and fungi preferably use NHEJ over HR for DNA integration, leading to a low efficiency of gene targeting. This can be dramatically improved to 80%-90% after the abolishment of the NHEJ system, compared to less than 10% in the wild-type background (137;138;140-142;145). Like in fungi, NHEJ is also the predominant DNA repair pathway in plants and animals. A similar approach was used to improve gene targeting in plants and animals. Since the NHEJ components have important functions in early mammalian development, viable NHEJ mutants are hard to obtain and most research has therefore been done only with cell lines. In human somatic HCT116 cells with the Ku70<sup>+/-</sup> genotype, the frequency of gene targeting was increased by 5-10 fold compared to that in wild-type cells, and the result was affirmed by using RNA interference (RNAi) or short-hairpinned RNA (shRNA) strategies to deplete Ku70 in the cells of wild-type background (146). The GT frequency was further increased by 30 fold in the Ku70<sup>+/-</sup> cells of combined with the RNAi of Ku70. Recently, a 33-fold increase in gene targeting was also observed using the RNAi treatment of Ku70 and XRCC4 in human somatic HCT116 cells (147). The targeted integration was enhanced by Lig4 knock-out in chicken DT40 cells, but not in human Nalm-6 cell lines indicating that the impact of NHEJ factors on gene targeting varies between cell types (148). In murine embryonic stem cells, the gene targeting frequencies were increased by 3 fold in *parp1* knockout cells, but not in *ku80* or *DNA-PKcs* knockout cells, suggesting that Ku80 and DNA-PKcs would also be involved in HR or that a B-NHEJ is activated (149). Few reports described similar experiments in plants until now. Unlike mammals, most of

the NHEJ mutants in plants have no obvious phenotype under normal growth conditions (150-154), which gives us more chances to study the effects of these NHEJ factors on gene targeting. Tanaka et al. (155) claimed highly efficient gene targeting in an Arabidopsis *Atlig4* mutant by introducing double strand DNA fragments to plant cells with a particle gun. However, this result is probably the result of PCR artefacts.

## 6.2 Introducing DSBs in the target

Targeted recombination will be enhanced by the introduction of genomic DSBs at the target site. This has been demonstrated in a wide range of animal and plant species (156). Meganucleases, which can generate DSBs at a specific large recognition site in the genome, are preferably used for this purpose. Meganucleases are sequence specific endonucleases with long recognition sequences (12-45 bp), including not only the natural homing nucleases, such as HO and I-SceI, but also the artificial endonucleases such as Zinc Finger Nucleases (ZFNs).

HO of budding yeast can induce HR by creating a DSB at the MAT locus to switch the mating type (157). I-SceI, encoded by a mitochondrial intron of *Saccharomyces cerevisiae*, can help to convert intronless alleles into alleles with an intron (158). Though gene targeting can be increased considerably by the use of the natural homing endonucleases (156;159;160), its application is so far limited to artificial target homing endonucleases recognition sites that are present in the target sites. Recently, however, a combinatorial approach was reported to redesign homing endonucleases to match with target sites that are naturally present in the genome (161).

Artificial ZFNs do not need the pre-insertion of recognizing sites into the target genome, making them useful as a novel genomic tool. ZFNs consist of the nonspecific DNA cleavage domain of the *FokI* enzyme and a specific DNA binding domain composed of several engineered Cys<sub>2</sub>-His<sub>2</sub> zinc fingers. The cleavage activity of the *FokI* domain requires dimerization. The DSB can be generated in a spacer sequence (5-7bp) between the two ZFN monomers binding sites when they bind together in a tail to tail configuration. Since one single ZF recognizes 3 bases of DNA sequence, a heterodimer of two ZFN, each containing 3 to 6 ZFs, could recognize 18bp to 36bp target site, which is enough to define a unique sequence in most organisms statistically. ZFNs have been successfully used for GT experiments in a lot of organisms, such as *Drosophila*, *Xenopus*, *Caenorhabditis elegans*, zebrafish, human cell lines, Arabidopsis, tobacco and maize. The increase of GT frequencies vary from 10 to 10000 among different organisms and cell types (162-165). The activity and the expression level of ZFNs in the target cells also influence the GT efficiency. There are still some problems that need to be solved with this strategy. One issue is about the specificity and the toxicity of the ZFN (166-168). If ZFNs are not extremely specific and can cut the genome at off-target sites, they will cause instability of the genome and be toxic. The safety of ZFNs needs to be improved by optimizing the design of the ZFNs' structure or regulating the expression level and duration of the presence of ZFNs in the target cells.

## 7. Outline of the thesis

Non-homologous end joining (NHEJ) is the predominant pathway for the repair of DNA double strand breaks in higher eukaryotes, such as plants and mammals. This pathway has been well characterized in yeast and mammals, but in plants no detailed analysis has been described. In mammals, it includes the classical NHEJ (C-NHEJ), which is dependent on Ku proteins, and the backup NHEJ (B-NHEJ), which is dependent on the Ku proteins and is much less characterized (61-63;94). In plants, the major components of the C-NHEJ have been identified (19). The NHEJ pathway is used for random integration of T-DNA in yeast. Inactivation of NHEJ in yeast and fungi prevented integration by non-homologous end joining (134;145). As a consequence, T-DNA integration could only occur by homologous recombination (HR; gene targeting). The first objective of this project was to investigate the NHEJ pathway in plants and to find out whether the B-NHEJ pathway exists in plants using *Arabidopsis thaliana* as a model. The second objective was to analyze whether gene targeting frequencies increased in the absence of NHEJ as had been found in yeast and fungi (134;137;145).

Several NHEJ single mutants were ordered from the Salk collection for our research, such as *Atku70*, *Atku80*, *Atlig4*, *Atmre11*, *Atparp1*, *Atparp2* and *Atlig6*. They were functionally characterized in this thesis. Some double and triple mutants were also obtained by crossing the single mutants. In **chapter 2**, the T-DNA insertion single mutants (*Atku70*, *Atku80*, *Atlig4*), which are deficient in the main components of C-NHEJ, are described. Together with *Atku70* (Ws) and *Atmre11* (Ws), which had been characterized by our lab previously, they were all tested for the frequency of T-DNA integration and gene targeting.

As it was reported that Parp1 and Parp2 not only are involved in SSB DNA repair, but also in the B-NHEJ pathway in mammals (83;85;87), the orthologs of Parp proteins have been identified in plants as well (99), DNA repair in *Atparp1* and *Atparp2* mutants was studied in **chapter 3** and **chapter 4**. **Chapter 3** describes the characterization of the *Atparp1* and *Atparp2* mutants. The results show that also in plants the AtParp proteins play an important role in SSB repair and that they are also involved in B-NHEJ using areas of micro-homology. **Chapter 4** focuses on how exactly the DNA ends join in the NHEJ mutants, which were deficient in C-NHEJ, B-NHEJ or both. To this end, the *Atp1p2* double mutant and the *Atp1p2k80* triple mutant were obtained by crossing. The results are in accord with **chapter 3** showing that AtParp proteins facilitate MMEJ, and also suggest that AtKu plays a role in DNA end protection and thus prevents MMEJ and HR. Unexpectedly, the *Atp1p2k80* triple mutant still has the ability of end joining indicating that there must exist even a third pathway for end joining besides C-NHEJ and B-NHEJ.

DNA ligase 3 (Lig 3) has been reported to ligate the DNA ends for DNA repair in the B-NHEJ pathway in mammals (94). Since no ortholog of Lig3 was found in plants, a plant specific DNA ligase 6 (Lig6) was postulated to function in B-NHEJ. **Chapter 5** presents the

study on the two *Atlig6* mutants showing that *Atlig4lig6* double mutants still ligate DNA ends and integrate T-DNA. The *in silico* analysis of DNA ligases in plants revealed another possible candidate, which is possibly involved in B-NHEJ.

### Reference List

1. Rich, T., Allen, R.L. and Wyllie, A.H. (2000) Defying death after DNA damage. *Nature*, **407**, 777-783.
2. Su, T.T. (2006) Cellular responses to DNA damage: one signal, multiple choices. *Annu. Rev. Genet.*, **40**, 187-208.
3. Nagy, Z. and Soutoglou, E. (2009) DNA repair: easy to visualize, difficult to elucidate. *Trends Cell Biol.*, **19**, 617-629.
4. Hefferin, M.L. and Tomkinson, A.E. (2005) Mechanism of DNA double-strand break repair by non-homologous end joining. *DNA Repair (Amst)*, **4**, 639-648.
5. Clemenson, C. and Marsolier-Kergoat, M.C. (2009) DNA damage checkpoint inactivation: adaptation and recovery. *DNA Repair (Amst)*, **8**, 1101-1109.
6. Waterworth, W.M., Altun, C., Armstrong, S.J., Roberts, N., Dean, P.J., Young, K., Weil, C.F., Bray, C.M. and West, C.E. (2007) NBS1 is involved in DNA repair and plays a synergistic role with ATM in mediating meiotic homologous recombination in plants. *Plant J.*, **52**, 41-52.
7. Zhang, X. and Paull, T.T. (2005) The Mre11/Rad50/Xrs2 complex and non-homologous end-joining of incompatible ends in *S. cerevisiae*. *DNA Repair (Amst)*, **4**, 1281-1294.
8. Matsuzaki, K., Shinohara, A. and Shinohara, M. (2008) Forkhead-associated domain of yeast Xrs2, a homolog of human Nbs1, promotes nonhomologous end joining through interaction with a ligase IV partner protein, Lif1. *Genetics*, **179**, 213-225.
9. Branzei, D. and Foiani, M. (2008) Regulation of DNA repair throughout the cell cycle. *Nat. Rev. Mol. Cell Biol.*, **9**, 297-308.
10. Falck, J., Coates, J. and Jackson, S.P. (2005) Conserved modes of recruitment of ATM, ATR and DNA-PKcs to sites of DNA damage. *Nature*, **434**, 605-611.
11. Nakamura, A.J., Rao, V.A., Pommier, Y. and Bonner, W.M. (2010) The complexity of phosphorylated H2AX foci formation and DNA repair assembly at DNA double-strand breaks. *Cell Cycle*, **9**, 389-397.
12. Bartek, J. and Lukas, J. (2007) DNA damage checkpoints: from initiation to recovery or adaptation. *Curr. Opin. Cell Biol.*, **19**, 238-245.
13. Varmark, H., Kwak, S. and Theurkauf, W.E. (2010) A role for Chk2 in DNA damage induced mitotic delays in human colorectal cancer cells. *Cell Cycle*, **9**, 312-320.
14. Beucher, A., Birraux, J., Tchouandong, L., Barton, O., Shibata, A., Conrad, S., Goodarzi, A.A., Krempler, A., Jeggo, P.A. and Lobrich, M. (2009) ATM and Artemis promote homologous recombination of radiation-induced DNA double-strand breaks in G2. *EMBO J.*, **28**, 3413-3427.
15. O'Driscoll, M. and Jeggo, P.A. (2006) The role of double-strand break repair - insights from human genetics. *Nat. Rev. Genet.*, **7**, 45-54.
16. De Schutter, K., Joubes, J., Cools, T., Verkest, A., Corellou, F., Babychuk, E., Van Der Schueren, E., Beeckman, T., Kushnir, S., Inze, D. *et al.* (2007) Arabidopsis WEE1 kinase controls cell cycle arrest in response to activation of the DNA integrity checkpoint. *Plant Cell*, **19**, 211-225.
17. Cools, T. and De Veylder, L. (2009) DNA stress checkpoint control and plant development. *Curr. Opin. Plant Biol.*, **12**, 23-28.
18. Symington, L.S. (2002) Role of RAD52 epistasis group genes in homologous recombination and double-strand break repair. *Microbiol. Mol. Biol. Rev.*, **66**, 630-70.

19. Bleuyard, J.Y., Gallego, M.E. and White, C.I. (2006) Recent advances in understanding of the DNA double-strand break repair machinery of plants. *DNA Repair (Amst)*, **5**, 1-12.
20. Mimitou, E.P. and Symington, L.S. (2008) Sae2, Exo1 and Sgs1 collaborate in DNA double-strand break processing. *Nature*, **455**, 770-774.
21. Lisby, M. and Rothstein, R. (2009) Choreography of recombination proteins during the DNA damage response. *DNA Repair (Amst)*, **8**, 1068-1076.
22. Samach, A., Melamed-essudo, C., Avivi-ragolski, N., Korchia, J., Pietrokovski, S. and Levy, A.A. Plant RAD52 Homologs: Identification and Activity. Plant DNA repair and recombination 2010. 64. 3-2-2010. Ref Type: Conference Proceeding
23. Pardo, B., Gomez-Gonzalez, B. and Aguilera, A. (2009) DNA repair in mammalian cells: DNA double-strand break repair: how to fix a broken relationship. *Cell Mol. Life Sci.*, **66**, 1039-1056.
24. Szostak, J.W., Orr-Weaver, T.L., Rothstein, R.J. and Stahl, F.W. (1983) The double-strand-break repair model for recombination. *Cell*, **33**, 25-35.
25. San, F.J., Sung, P. and Klein, H. (2008) Mechanism of eukaryotic homologous recombination. *Annu. Rev. Biochem.*, **77**, 229-257.
26. Llorente, B., Smith, C.E. and Symington, L.S. (2008) Break-induced replication: what is it and what is it for? *Cell Cycle*, **7**, 859-864.
27. Bray, C.M. and West, C.E. (2005) DNA repair mechanisms in plants: crucial sensors and effectors for the maintenance of genome integrity. *New Phytol.*, **168**, 511-528.
28. Helleday, T., Lo, J., van Gent, D.C. and Engelward, B.P. (2007) DNA double-strand break repair: from mechanistic understanding to cancer treatment. *DNA Repair (Amst)*, **6**, 923-935.
29. Walker, J.R., Corpina, R.A. and Goldberg, J. (2001) Structure of the Ku heterodimer bound to DNA and its implications for double-strand break repair. *Nature*, **412**, 607-614.
30. Smith, G.C. and Jackson, S.P. (1999) The DNA-dependent protein kinase. *Genes Dev.*, **13**, 916-934.
31. Mari, P.O., Florea, B.I., Persengiev, S.P., Verkaik, N.S., Bruggenwirth, H.T., Modesti, M., Giglia-Mari, G., Bezstarosti, K., Demmers, J.A., Luidert, T.M. *et al.* (2006) Dynamic assembly of end-joining complexes requires interaction between Ku70/80 and XRCC4. *Proc. Natl. Acad. Sci. U. S. A.*, **103**, 18597-18602.
32. Bennett, S.M., Neher, T.M., Shatilla, A. and Turchi, J.J. (2009) Molecular analysis of Ku redox regulation. *BMC. Mol. Biol.*, **10**, 86.
33. Yano, K., Morotomi-Yano, K., Adachi, N. and Akiyama, H. (2009) Molecular mechanism of protein assembly on DNA double-strand breaks in the non-homologous end-joining pathway. *J. Radiat. Res. (Tokyo)*, **50**, 97-108.
34. Hammel, M., Yu, Y., Mahaney, B.L., Cai, B., Ye, R., Phipps, B.M., Rambo, R.P., Hura, G.L., Pelikan, M., So, S. *et al.* (2010) Ku and DNA-dependent protein kinase dynamic conformations and assembly regulate DNA binding and the initial non-homologous end joining complex. *J. Biol. Chem.*, **285**, 1414-1423.
35. Sibanda, B.L., Chirgadze, D.Y. and Blundell, T.L. (2010) Crystal structure of DNA-PKcs reveals a large open-ring cradle comprised of HEAT repeats. *Nature*, **463**, 118-121.
36. Yaneva, M., Kowalewski, T. and Lieber, M.R. (1997) Interaction of DNA-dependent protein kinase with DNA and with Ku: biochemical and atomic-force microscopy studies. *EMBO J.*, **16**, 5098-5112.
37. DeFazio, L.G., Stansel, R.M., Griffith, J.D. and Chu, G. (2002) Synapsis of DNA ends by DNA-dependent protein kinase. *EMBO J.*, **21**, 3192-3200.
38. Mahaney, B.L., Meek, K. and Lees-Miller, S.P. (2009) Repair of ionizing radiation-induced DNA double-strand breaks by non-homologous end-joining. *Biochem. J.*, **417**, 639-650.
39. Weterings, E. and Chen, D.J. (2008) The endless tale of non-homologous end-joining.

- Cell Res.*, **18**, 114-124.
40. Chen,L., Trujillo,K., Ramos,W., Sung,P. and Tomkinson,A.E. (2001) Promotion of Dnl4-catalyzed DNA end-joining by the Rad50/Mre11/Xrs2 and Hdf1/Hdf2 complexes. *Mol. Cell*, **8**, 1105-1115.
  41. Riha,K., Heacock,M.L. and Shippen,D.E. (2006) The role of the nonhomologous end-joining DNA double-strand break repair pathway in telomere biology. *Annu. Rev. Genet.*, **40**, 237-277.
  42. Ma,Y., Pannicke,U., Schwarz,K. and Lieber,M.R. (2002) Hairpin opening and overhang processing by an Artemis/DNA-dependent protein kinase complex in nonhomologous end joining and V(D)J recombination. *Cell*, **108**, 781-794.
  43. Nick McElhinny,S.A. and Ramsden,D.A. (2004) Sibling rivalry: competition between Pol X family members in V(D)J recombination and general double strand break repair. *Immunol. Rev.*, **200**, 156-164.
  44. Lieber,M.R. (2008) The mechanism of human nonhomologous DNA end joining. *J. Biol. Chem.*, **283**, 1-5.
  45. Chappell,C., Hanakahi,L.A., Karimi-Busheri,F., Weinfeld,M. and West,S.C. (2002) Involvement of human polynucleotide kinase in double-strand break repair by non-homologous end joining. *EMBO J.*, **21**, 2827-2832.
  46. Daley,J.M., Palmbo,P.L., Wu,D. and Wilson,T.E. (2005) Nonhomologous end joining in yeast. *Annu. Rev. Genet.*, **39**, 431-451.
  47. Daley,J.M. and Wilson,T.E. (2008) Evidence that base stacking potential in annealed 3' overhangs determines polymerase utilization in yeast nonhomologous end joining. *DNA Repair (Amst)*, **7**, 67-76.
  48. Vance,J.R. and Wilson,T.E. (2001) Uncoupling of 3'-phosphatase and 5'-kinase functions in budding yeast. Characterization of *Saccharomyces cerevisiae* DNA 3'-phosphatase (TPP1). *J. Biol. Chem.*, **276**, 15073-15081.
  49. Bahmed,K., Nitiss,K.C. and Nitiss,J.L. (2010) Yeast Tdp1 regulates the fidelity of nonhomologous end joining. *Proc. Natl. Acad. Sci. U. S. A.*, **107**, 4057-4062.
  50. Buck,D., Malivert,L., de,C.R., Barraud,A., Fondaneche,M.C., Sanal,O., Plebani,A., Stephan,J.L., Hufnagel,M., le,D.F. *et al.* (2006) Cernunnos, a novel nonhomologous end-joining factor, is mutated in human immunodeficiency with microcephaly. *Cell*, **124**, 287-299.
  51. Ahnesorg,P., Smith,P. and Jackson,S.P. (2006) XLF interacts with the XRCC4-DNA ligase IV complex to promote DNA nonhomologous end-joining. *Cell*, **124**, 301-313.
  52. Recuero-Checa,M.A., Dore,A.S., rias-Palomo,E., Rivera-Calzada,A., Scheres,S.H., Maman,J.D., Pearl,L.H. and Llorca,O. (2009) Electron microscopy of Xrcc4 and the DNA ligase IV-Xrcc4 DNA repair complex. *DNA Repair (Amst)*, **8**, 1380-1389.
  53. Costantini,S., Woodbine,L., Andreoli,L., Jeggo,P.A. and Vindigni,A. (2007) Interaction of the Ku heterodimer with the DNA ligase IV/Xrcc4 complex and its regulation by DNA-PK. *DNA Repair (Amst)*, **6**, 712-722.
  54. Sibanda,B.L., Critchlow,S.E., Begun,J., Pei,X.Y., Jackson,S.P., Blundell,T.L. and Pellegrini,L. (2001) Crystal structure of an Xrcc4-DNA ligase IV complex. *Nat. Struct. Biol.*, **8**, 1015-1019.
  55. Li,Y., Chirgadze,D.Y., Bolanos-Garcia,V.M., Sibanda,B.L., Davies,O.R., Ahnesorg,P., Jackson,S.P. and Blundell,T.L. (2008) Crystal structure of human XLF/Cernunnos reveals unexpected differences from XRCC4 with implications for NHEJ. *EMBO J.*, **27**, 290-300.
  56. Riballo,E., Woodbine,L., Stiff,T., Walker,S.A., Goodarzi,A.A. and Jeggo,P.A. (2009) XLF-Cernunnos promotes DNA ligase IV-XRCC4 re-adenylation following ligation. *Nucleic Acids Res.*, **37**, 482-492.
  57. Yu,Y., Mahaney,B.L., Yano,K., Ye,R., Fang,S., Douglas,P., Chen,D.J. and Lees-



- Miller,S.P. (2008) DNA-PK and ATM phosphorylation sites in XLF/Cernunnos are not required for repair of DNA double strand breaks. *DNA Repair (Amst)*, **7**, 1680-1692.
58. Yu,Y., Wang,W., Ding,Q., Ye,R., Chen,D., Merkle,D., Schriemer,D., Meek,K. and Lees-Miller,S.P. (2003) DNA-PK phosphorylation sites in XRCC4 are not required for survival after radiation or for V(D)J recombination. *DNA Repair (Amst)*, **2**, 1239-1252.
  59. Bonatto,D., Brendel,M. and Henriques,J.A. (2005) *In silico* identification and analysis of new Artemis/Artemis-like sequences from fungal and metazoan species. *Protein J.*, **24**, 399-411.
  60. Uchiyama,Y., Kimura,S., Yamamoto,T., Ishibashi,T. and Sakaguchi,K. (2004) Plant DNA polymerase lambda, a DNA repair enzyme that functions in plant meristematic and meiotic tissues. *Eur. J. Biochem.*, **271**, 2799-2807.
  61. Nussenzweig,A. and Nussenzweig,M.C. (2007) A backup DNA repair pathway moves to the forefront. *Cell*, **131**, 223-225.
  62. Wang,H., Perrault,A.R., Takeda,Y., Qin,W., Wang,H. and Iliakis,G. (2003) Biochemical evidence for Ku-independent backup pathways of NHEJ. *Nucleic Acids Res.*, **31**, 5377-5388.
  63. Wachsberger,P.R., Li,W.H., Guo,M., Chen,D., Cheong,N., Ling,C.C., Li,G. and Iliakis,G. (1999) Rejoining of DNA double-strand breaks in Ku80-deficient mouse fibroblasts. *Radiat. Res.*, **151**, 398-407.
  64. DiBiase,S.J., Zeng,Z.C., Chen,R., Hyslop,T., Curran,W.J., Jr. and Iliakis,G. (2000) DNA-dependent protein kinase stimulates an independently active, nonhomologous, end-joining apparatus. *Cancer Res.*, **60**, 1245-1253.
  65. Verkaik,N.S., Esveldt-van Lange,R.E., van Heemst,D., Bruggenwirth,H.T., Hoeijmakers,J.H., Zdzienicka,M.Z. and van Gent,D.C. (2002) Different types of V(D) J recombination and end-joining defects in DNA double-strand break repair mutant mammalian cells. *Eur. J. Immunol.*, **32**, 701-709.
  66. Wang,H., Zeng,Z.C., Perrault,A.R., Cheng,X., Qin,W. and Iliakis,G. (2001) Genetic evidence for the involvement of DNA ligase IV in the DNA-PK-dependent pathway of non-homologous end joining in mammalian cells. *Nucleic Acids Res.*, **29**, 1653-1660.
  67. Kuhfittig-Kulle,S., Feldmann,E., Odersky,A., Kuliczowska,A., Goedecke,W., Eggert,A. and Pfeiffer,P. (2007) The mutagenic potential of non-homologous end joining in the absence of the NHEJ core factors Ku70/80, DNA-PKcs and XRCC4-LigIV. *Mutagenesis*, **22**, 217-233.
  68. Karanjawala,Z.E., Grawunder,U., Hsieh,C.L. and Lieber,M.R. (1999) The nonhomologous DNA end joining pathway is important for chromosome stability in primary fibroblasts. *Curr. Biol.*, **9**, 1501-1504.
  69. Ferguson,D.O., Sekiguchi,J.M., Chang,S., Frank,K.M., Gao,Y., DePinho,R.A. and Alt,F.W. (2000) The nonhomologous end-joining pathway of DNA repair is required for genomic stability and the suppression of translocations. *Proc. Natl. Acad. Sci. U. S. A.*, **97**, 6630-6633.
  70. Lieber,M.R. (2010) NHEJ and its backup pathways in chromosomal translocations. *Nat. Struct. Mol. Biol.*, **17**, 393-395.
  71. Cheong,N., Perrault,A.R., Wang,H., Wachsberger,P., Mammen,P., Jackson,I. and Iliakis,G. (1999) DNA-PK-independent rejoining of DNA double-strand breaks in human cell extracts in vitro. *Int. J. Radiat. Biol.*, **75**, 67-81.
  72. Feldmann,E., Schmiemann,V., Goedecke,W., Reichenberger,S. and Pfeiffer,P. (2000) DNA double-strand break repair in cell-free extracts from Ku80-deficient cells: implications for Ku serving as an alignment factor in non-homologous DNA end joining. *Nucleic Acids Res.*, **28**, 2585-2596.
  73. Simsek,D. and Jasin,M. (2010) Alternative end-joining is suppressed by the canonical NHEJ component Xrcc4-ligase IV during chromosomal translocation formation. *Nat.*

- Struct. Mol. Biol.*, **17**, 410-416.
74. Fattah,F., Lee,E.H., Weisensel,N., Wang,Y., Lichter,N. and Hendrickson,E.A. (2010) Ku regulates the non-homologous end joining pathway choice of DNA double-strand break repair in human somatic cells. *PLoS. Genet.*, **6**, e1000855.
  75. McVey,M. and Lee,S.E. (2008) MMEJ repair of double-strand breaks (director's cut): deleted sequences and alternative endings. *Trends Genet.*, **24**, 529-538.
  76. Iliakis,G. (2009) Backup pathways of NHEJ in cells of higher eukaryotes: cell cycle dependence. *Radiother. Oncol.*, **92**, 310-315.
  77. Liang,L., Deng,L., Nguyen,S.C., Zhao,X., Maulion,C.D., Shao,C. and Tischfield,J.A. (2008) Human DNA ligases I and III, but not ligase IV, are required for microhomology-mediated end joining of DNA double-strand breaks. *Nucleic Acids Res.*, **36**, 3297-3310.
  78. Rosidi,B., Wang,M., Wu,W., Sharma,A., Wang,H. and Iliakis,G. (2008) Histone H1 functions as a stimulatory factor in backup pathways of NHEJ. *Nucleic Acids Res.*, **36**, 1610-1623.
  79. Downs,J.A., Kosmidou,E., Morgan,A. and Jackson,S.P. (2003) Suppression of homologous recombination by the *Saccharomyces cerevisiae* linker histone. *Mol. Cell*, **11**, 1685-1692.
  80. Kysela,B., Chovanec,M. and Jeggo,P.A. (2005) Phosphorylation of linker histones by DNA-dependent protein kinase is required for DNA ligase IV-dependent ligation in the presence of histone H1. *Proc. Natl. Acad. Sci. U. S. A.*, **102**, 1877-1882.
  81. Thomas,J.O., Rees,C. and Finch,J.T. (1992) Cooperative binding of the globular domains of histones H1 and H5 to DNA. *Nucleic Acids Res.*, **20**, 187-194.
  82. Schreiber,V., Dantzer,F., Ame,J.C. and de Murcia,G. (2006) Poly(ADP-ribose): novel functions for an old molecule. *Nat. Rev. Mol. Cell Biol.*, **7**, 517-528.
  83. Woodhouse,B.C. and Dianov,G.L. (2008) Poly ADP-ribose polymerase-1: an international molecule of mystery. *DNA Repair (Amst)*, **7**, 1077-1086.
  84. Woodhouse,B.C., Dianova,I.I., Parsons,J.L. and Dianov,G.L. (2008) Poly(ADP-ribose) polymerase-1 modulates DNA repair capacity and prevents formation of DNA double strand breaks. *DNA Repair (Amst)*, **7**, 932-940.
  85. Audebert,M., Salles,B. and Calsou,P. (2004) Involvement of poly(ADP-ribose) polymerase-1 and XRCC1/DNA ligase III in an alternative route for DNA double-strand breaks rejoining. *J. Biol. Chem.*, **279**, 55117-55126.
  86. Robert,I., Dantzer,F. and Reina-San-Martin,B. (2009) Parp1 facilitates alternative NHEJ, whereas Parp2 suppresses IgH/c-myc translocations during immunoglobulin class switch recombination. *J. Exp. Med.*, **206**, 1047-1056.
  87. Wang,M., Wu,W., Wu,W., Rosidi,B., Zhang,L., Wang,H. and Iliakis,G. (2006) PARP-1 and Ku compete for repair of DNA double strand breaks by distinct NHEJ pathways. *Nucleic Acids Res.*, **34**, 6170-6182.
  88. Yelamos,J., Schreiber,V. and Dantzer,F. (2008) Toward specific functions of poly(ADP-ribose) polymerase-2. *Trends Mol. Med.*, **14**, 169-178.
  89. Sukhanova,M., Khodyreva,S. and Lavrik,O. (2010) Poly(ADP-ribose) polymerase 1 regulates activity of DNA polymerase beta in long patch base excision repair. *Mutat. Res.*, **685**, 80-89.
  90. Bryant,H.E., Petermann,E., Schultz,N., Jemth,A.S., Loseva,O., Issaeva,N., Johansson,F., Fernandez,S., McGlynn,P. and Helleday,T. (2009) PARP is activated at stalled forks to mediate Mre11-dependent replication restart and recombination. *EMBO J.*, **28**, 2601-2615.
  91. Okano,S., Lan,L., Tomkinson,A.E. and Yasui,A. (2005) Translocation of XRCC1 and DNA ligase IIIalpha from centrosomes to chromosomes in response to DNA damage in mitotic human cells. *Nucleic Acids Res.*, **33**, 422-429.
  92. Caldecott,K.W., Aoufouchi,S., Johnson,P. and Shall,S. (1996) XRCC1 polypeptide



- interacts with DNA polymerase beta and possibly poly (ADP-ribose) polymerase, and DNA ligase III is a novel molecular 'nick-sensor' in vitro. *Nucleic Acids Res.*, **24**, 4387-4394.
93. Cappelli,E., Taylor,R., Cevasco,M., Abbondandolo,A., Caldecott,K. and Frosina,G. (1997) Involvement of XRCC1 and DNA ligase III gene products in DNA base excision repair. *J. Biol. Chem.*, **272**, 23970-23975.
  94. Wang,H., Rosidi,B., Perrault,R., Wang,M., Zhang,L., Windhofer,F. and Iliakis,G. (2005) DNA ligase III as a candidate component of backup pathways of nonhomologous end joining. *Cancer Res.*, **65**, 4020-4030.
  95. Caldecott,K.W., McKeown,C.K., Tucker,J.D., Ljungquist,S. and Thompson,L.H. (1994) An interaction between the mammalian DNA repair protein XRCC1 and DNA ligase III. *Mol. Cell Biol.*, **14**, 68-76.
  96. Ellenberger,T. and Tomkinson,A.E. (2008) Eukaryotic DNA ligases: structural and functional insights. *Annu. Rev. Biochem.*, **77**, 313-338.
  97. Decottignies,A. (2007) Microhomology-mediated end joining in fission yeast is repressed by pku70 and relies on genes involved in homologous recombination. *Genetics*, **176**, 1403-1415.
  98. Tao,Z., Gao,P. and Liu,H.W. (2009) Studies of the expression of human poly(ADP-ribose) polymerase-1 in *Saccharomyces cerevisiae* and identification of PARP-1 substrates by yeast proteome microarray screening. *Biochemistry*, **48**, 11745-11754.
  99. Babiychuk,E., Cottrill,P.B., Storozhenko,S., Fuangthong,M., Chen,Y., O'Farrell,M.K., Van,M.M., Inze,D. and Kushnir,S. (1998) Higher plants possess two structurally different poly(ADP-ribose) polymerases. *Plant J.*, **15**, 635-645.
  100. West,C.E., Waterworth,W.M., Sunderland,P.A. and Bray,C.M. (2004) Arabidopsis DNA double-strand break repair pathways. *Biochem. Soc. Trans.*, **32**, 964-966.
  101. Diego Bonatto, Martin Brendel and Joao Antonio Pegas Henrique (2005) A new group of plant-specific ADP-dependent DNA ligases identified by protein phylogeny, hydrophobic cluster and 3-dimensional modelling. *Functional Plant Biology*, **32**, 161-174.
  102. Waterworth,W.M., Masnavi,G., Bhardwaj,R.M., Jiang,Q., Bray,C.M. and West,C.E. (2010) A plant DNA ligase is an important determinant of seed longevity. *Plant J.*, **63**, 848-860.
  103. Siede,W., Friedl,A.A., Dianova,I., Eckardt-Schupp,F. and Friedberg,E.C. (1996) The *Saccharomyces cerevisiae* Ku autoantigen homologue affects radiosensitivity only in the absence of homologous recombination. *Genetics*, **142**, 91-102.
  104. Shrivastav,M., De Haro,L.P. and Nickoloff,J.A. (2008) Regulation of DNA double-strand break repair pathway choice. *Cell Res.*, **18**, 134-147.
  105. Yamazoe,M., Sonoda,E., Hohegger,H. and Takeda,S. (2004) Reverse genetic studies of the DNA damage response in the chicken B lymphocyte line DT40. *DNA Repair (Amst)*, **3**, 1175-1185.
  106. Sonoda,E., Hohegger,H., Saberi,A., Taniguchi,Y. and Takeda,S. (2006) Differential usage of non-homologous end-joining and homologous recombination in double strand break repair. *DNA Repair (Amst)*, **5**, 1021-1029.
  107. Orii,K.E., Lee,Y., Kondo,N. and McKinnon,P.J. (2006) Selective utilization of nonhomologous end-joining and homologous recombination DNA repair pathways during nervous system development. *Proc. Natl. Acad. Sci. U. S. A.*, **103**, 10017-10022.
  108. Boyko,A., Zemp,F., Filkowski,J. and Kovalchuk,I. (2006) Double-strand break repair in plants is developmentally regulated. *Plant Physiol*, **141**, 488-497.
  109. Aylon,Y. and Kupiec,M. (2005) Cell cycle-dependent regulation of double-strand break repair: a role for the CDK. *Cell Cycle*, **4**, 259-261.
  110. Limbo,O., Chahwan,C., Yamada,Y., de Bruin,R.A., Wittenberg,C. and Russell,P. (2007)

- Ctp1 is a cell-cycle-regulated protein that functions with Mre11 complex to control double-strand break repair by homologous recombination. *Mol. Cell*, **28**, 134-146.
111. Yun, M.H. and Hiom, K. (2009) CtIP-BRCA1 modulates the choice of DNA double-strand-break repair pathway throughout the cell cycle. *Nature*, **459**, 460-463.
  112. Huertas, P., Cortes-Ledesma, F., Sartori, A.A., Aguilera, A. and Jackson, S.P. (2008) CDK targets Sae2 to control DNA-end resection and homologous recombination. *Nature*, **455**, 689-692.
  113. Sartori, A.A., Lukas, C., Coates, J., Mistrik, M., Fu, S., Bartek, J., Baer, R., Lukas, J. and Jackson, S.P. (2007) Human CtIP promotes DNA end resection. *Nature*, **450**, 509-514.
  114. Esashi, F., Christ, N., Gannon, J., Liu, Y., Hunt, T., Jasin, M. and West, S.C. (2005) CDK-dependent phosphorylation of BRCA2 as a regulatory mechanism for recombinational repair. *Nature*, **434**, 598-604.
  115. Galande, S. and Kohwi-Shigematsu, T. (1999) Poly(ADP-ribose) polymerase and Ku autoantigen form a complex and synergistically bind to matrix attachment sequences. *J. Biol. Chem.*, **274**, 20521-20528.
  116. Hohegger, H., Dejsuphong, D., Fukushima, T., Morrison, C., Sonoda, E., Schreiber, V., Zhao, G.Y., Saberi, A., Masutani, M., Adachi, N. *et al.* (2006) Parp-1 protects homologous recombination from interference by Ku and Ligase IV in vertebrate cells. *EMBO J.*, **25**, 1305-1314.
  117. Saberi, A., Hohegger, H., Szuts, D., Lan, L., Yasui, A., Sale, J.E., Taniguchi, Y., Murakawa, Y., Zeng, W., Yokomori, K. *et al.* (2007) RAD18 and poly(ADP-ribose) polymerase independently suppress the access of nonhomologous end joining to double-strand breaks and facilitate homologous recombination-mediated repair. *Mol. Cell Biol.*, **27**, 2562-2571.
  118. Wu, W., Wang, M., Wu, W., Singh, S.K., Mussfeldt, T. and Iliakis, G. (2008) Repair of radiation induced DNA double strand breaks by backup NHEJ is enhanced in G2. *DNA Repair (Amst)*, **7**, 329-338.
  119. Adachi, N., So, S., Iizumi, S., Nomura, Y., Murai, K., Yamakawa, C., Miyagawa, K. and Koyama, H. (2006) The human pre-B cell line Nalm-6 is highly proficient in gene targeting by homologous recombination. *DNA Cell Biol.*, **25**, 19-24.
  120. Capecchi, M.R. (2005) Gene targeting in mice: functional analysis of the mammalian genome for the twenty-first century. *Nat. Rev. Genet.*, **6**, 507-512.
  121. Mansour, S.L., Thomas, K.R. and Capecchi, M.R. (1988) Disruption of the proto-oncogene *int-2* in mouse embryo-derived stem cells: a general strategy for targeting mutations to non-selectable genes. *Nature*, **336**, 348-352.
  122. Yagi, T., Ikawa, Y., Yoshida, K., Shigetani, Y., Takeda, N., Mabuchi, I., Yamamoto, T. and Aizawa, S. (1990) Homologous recombination at *c-fyn* locus of mouse embryonic stem cells with use of diphtheria toxin A-fragment gene in negative selection. *Proc. Natl. Acad. Sci. U. S. A.*, **87**, 9918-9922.
  123. Czako, M. and Marton, L. (1994) The herpes simplex virus thymidine kinase gene as a conditional negative-selection marker gene in *Arabidopsis thaliana*. *Plant Physiol*, **104**, 1067-1071.
  124. Czako, M. and An, G. (1991) Expression of DNA coding for diphtheria toxin chain a is toxic to plant cells. *Plant Physiol*, **95**, 687-692.
  125. Terada, R., Johzuka-Hisatomi, Y., Saitoh, M., Asao, H. and Iida, S. (2007) Gene targeting by homologous recombination as a biotechnological tool for rice functional genomics. *Plant Physiol*, **144**, 846-856.
  126. Deng, C. and Capecchi, M.R. (1992) Reexamination of gene targeting frequency as a function of the extent of homology between the targeting vector and the target locus. *Mol. Cell Biol.*, **12**, 3365-3371.
  127. Thomas, K.R., Deng, C. and Capecchi, M.R. (1992) High-fidelity gene targeting in

- embryonic stem cells by using sequence replacement vectors. *Mol. Cell Biol.*, **12**, 2919-2923.
128. Dominguez-Bendala, J., Priddle, H., Clarke, A. and McWhir, J. (2003) Elevated expression of exogenous Rad51 leads to identical increases in gene-targeting frequency in murine embryonic stem (ES) cells with both functional and dysfunctional p53 genes. *Exp. Cell Res.*, **286**, 298-307.
  129. Di Primio, C., Galli, A., Cervelli, T., Zoppe, M. and Rainaldi, G. (2005) Potentiation of gene targeting in human cells by expression of *Saccharomyces cerevisiae* Rad52. *Nucleic Acids Res.*, **33**, 4639-4648.
  130. Kalvala, A., Rainaldi, G., Di Primio, C., Liverani, V., Falaschi, A. and Galli, A. (2010) Enhancement of gene targeting in human cells by intranuclear permeation of the *Saccharomyces cerevisiae* Rad52 protein. *Nucleic Acids Res.*, **38**, e149.
  131. Shaked, H., Melamed-Bessudo, C. and Levy, A.A. (2005) High-frequency gene targeting in Arabidopsis plants expressing the yeast RAD54 gene. *Proc. Natl. Acad. Sci. U. S. A.*, **102**, 12265-12269.
  132. Shcherbakova, O.G., Lanzov, V.A., Ogawa, H. and Filatov, M.V. (2000) Overexpression of bacterial RecA protein stimulates homologous recombination in somatic mammalian cells. *Mutat. Res.*, **459**, 65-71.
  133. Reiss, B., Klemm, M., Kosak, H. and Schell, J. (1996) RecA protein stimulates homologous recombination in plants. *Proc. Natl. Acad. Sci. U. S. A.*, **93**, 3094-3098.
  134. van Attikum, H. and Hooykaas, P.J. (2003) Genetic requirements for the targeted integration of *Agrobacterium* T-DNA in *Saccharomyces cerevisiae*. *Nucleic Acids Res.*, **31**, 826-832.
  135. Essers, J., Hendriks, R.W., Swagemakers, S.M., Troelstra, C., de, W.J., Bootsma, D., Hoeijmakers, J.H. and Kanaar, R. (1997) Disruption of mouse RAD54 reduces ionizing radiation resistance and homologous recombination. *Cell*, **89**, 195-204.
  136. Bezzubova, O., Silbergleit, A., Yamaguchi-Iwai, Y., Takeda, S. and Buerstedde, J.M. (1997) Reduced X-ray resistance and homologous recombination frequencies in a RAD54<sup>-/-</sup> mutant of the chicken DT40 cell line. *Cell*, **89**, 185-193.
  137. van Attikum, H., Bundock, P. and Hooykaas, P.J. (2001) Non-homologous end-joining proteins are required for *Agrobacterium* T-DNA integration. *EMBO J.*, **20**, 6550-6558.
  138. Krappmann, S., Sasse, C. and Braus, G.H. (2006) Gene targeting in *Aspergillus fumigatus* by homologous recombination is facilitated in a nonhomologous end-joining-deficient genetic background. *Eukaryot. Cell*, **5**, 212-215.
  139. Ninomiya, Y., Suzuki, K., Ishii, C. and Inoue, H. (2004) Highly efficient gene replacements in *Neurospora* strains deficient for nonhomologous end-joining. *Proc. Natl. Acad. Sci. U. S. A.*, **101**, 12248-12253.
  140. Takahashi, T., Masuda, T. and Koyama, Y. (2006) Enhanced gene targeting frequency in ku70 and ku80 disruption mutants of *Aspergillus sojae* and *Aspergillus oryzae*. *Mol. Genet. Genomics*, **275**, 460-470.
  141. Nielsen, J.B., Nielsen, M.L. and Mortensen, U.H. (2008) Transient disruption of non-homologous end-joining facilitates targeted genome manipulations in the filamentous fungus *Aspergillus nidulans*. *Fungal. Genet. Biol.*, **45**, 165-170.
  142. Villalba, F., Collemare, J., Landraud, P., Lambou, K., Brozek, V., Cirer, B., Morin, D., Bruel, C., Beffa, R. and Lebrun, M.H. (2008) Improved gene targeting in *Magnaporthe grisea* by inactivation of MgKU80 required for non-homologous end joining. *Fungal. Genet. Biol.*, **45**, 68-75.
  143. Schorsch, C., Kohler, T. and Boles, E. (2009) Knockout of the DNA ligase IV homolog gene in the sphingoid base producing yeast *Pichia ciferrii* significantly increases gene targeting efficiency. *Curr. Genet.*, **55**, 381-389.
  144. Abdel-Banat, B.M., Nonklang, S., Hoshida, H. and Akada, R. (2010) Random and targeted

- gene integrations through the control of non-homologous end joining in the yeast *Kluyveromyces marxianus*. *Yeast*, **27**, 29-39.
145. Kooistra,R., Hooykaas,P.J. and Steensma,H.Y. (2004) Efficient gene targeting in *Kluyveromyces lactis*. *Yeast*, **21**, 781-792.
  146. Fattah,F.J., Lichter,N.F., Fattah,K.R., Oh,S. and Hendrickson,E.A. (2008) Ku70, an essential gene, modulates the frequency of rAAV-mediated gene targeting in human somatic cells. *Proc. Natl. Acad. Sci. U. S. A.*, **105**, 8703-8708.
  147. Bertolini,L.R., Bertolini,M., Maga,E.A., Madden,K.R. and Murray,J.D. (2009) Increased gene targeting in Ku70 and Xrcc4 transiently deficient human somatic cells. *Mol. Biotechnol.*, **41**, 106-114.
  148. Iiizumi,S., Kurosawa,A., So,S., Ishii,Y., Chikaraishi,Y., Ishii,A., Koyama,H. and Adachi,N. (2008) Impact of non-homologous end-joining deficiency on random and targeted DNA integration: implications for gene targeting. *Nucleic Acids Res.*, **36**, 6333-6342.
  149. Dominguez-Bendala,J., Masutani,M. and McWhir,J. (2006) Down-regulation of PARP-1, but not of Ku80 or DNA-PKcs', results in higher gene targeting efficiency. *Cell Biol. Int.*, **30**, 389-393.
  150. van Attikum,H., Bundock,P., Overmeer,R.M., Lee,L.Y., Gelvin,S.B. and Hooykaas,P.J.J. (2003) The Arabidopsis AtLIG4 gene is required for the repair of DNA damage, but not for the integration of *Agrobacterium* T-DNA. *Nucleic Acids Res.*, **31**, 4247-4255.
  151. Bundock,P., van Attikum,H. and Hooykaas,P.J.J. (2002) Increased telomere length and hypersensitivity to DNA damaging agents in an Arabidopsis KU70 mutant. *Nucleic Acids Res.*, **30**, 3395-3400.
  152. West,C.E., Waterworth,W.M., Jiang,Q. and Bray,C.M. (2000) Arabidopsis DNA ligase IV is induced by gamma-irradiation and interacts with an Arabidopsis homologue of the double strand break repair protein XRCC4. *Plant J.*, **24**, 67-78.
  153. West,C.E., Waterworth,W.M., Story,G.W., Sunderland,P.A., Jiang,Q. and Bray,C.M. (2002) Disruption of the Arabidopsis AtKu80 gene demonstrates an essential role for AtKu80 protein in efficient repair of DNA double-strand breaks in vivo. *Plant J.*, **31**, 517-528.
  154. Friesner,J. and Britt,A.B. (2003) Ku80- and DNA ligase IV-deficient plants are sensitive to ionizing radiation and defective in T-DNA integration. *Plant J.*, **34**, 427-440.
  155. Tanaka,S., Ishii,C., Hatakeyama,S. and Inoue,H. (2010) High efficient gene targeting on the AGAMOUS gene in an ArabidopsisAtLIG4 mutant. *Biochem. Biophys. Res. Commun.*, **396**, 289-293.
  156. Paques,F. and Duchateau,P. (2007) Meganucleases and DNA double-strand break-induced recombination: perspectives for gene therapy. *Curr. Gene Ther.*, **7**, 49-66.
  157. Kostriken,R., Strathern,J.N., Klar,A.J., Hicks,J.B. and Heffron,F. (1983) A site-specific endonuclease essential for mating-type switching in *Saccharomyces cerevisiae*. *Cell*, **35**, 167-174.
  158. Jacquier,A. and Dujon,B. (1985) An intron-encoded protein is active in a gene conversion process that spreads an intron into a mitochondrial gene. *Cell*, **41**, 383-394.
  159. Haber,J.E. (2006) Transpositions and translocations induced by site-specific double-strand breaks in budding yeast. *DNA Repair (Amst)*, **5**, 998-1009.
  160. D'Halluin,K., Vanderstraeten,C., Stals,E., Cornelissen,M. and Ruiters,R. (2008) Homologous recombination: a basis for targeted genome optimization in crop species such as maize. *Plant Biotechnol. J.*, **6**, 93-102.
  161. Grizot,S., Epinat,J.C., Thomas,S., Duclert,A., Rolland,S., Paques,F. and Duchateau,P. (2010) Generation of redesigned homing endonucleases comprising DNA-binding domains derived from two different scaffolds. *Nucleic Acids Res.*, **38**, 2006-2018.
  162. Weinthal,D., Tovkach,A., Zeevi,V. and Tzfira,T. (2010) Genome editing in plant cells by

- zinc finger nucleases. *Trends Plant Sci.*, **15**, 308-321.
163. Cathomen, T. and Joung, J.K. (2008) Zinc-finger nucleases: the next generation emerges. *Mol. Ther.*, **16**, 1200-1207.
  164. de Pater, S., Neuteboom, L.W., Pinas, J.E., Hooykaas, P.J. and van der Zaal, B.J. (2009) ZFN-induced mutagenesis and gene-targeting in *Arabidopsis* through *Agrobacterium*-mediated floral dip transformation. *Plant Biotechnol. J.*, **7**, 821-835.
  165. Durai, S., Mani, M., Kandavelou, K., Wu, J., Porteus, M.H. and Chandrasegaran, S. (2005) Zinc finger nucleases: custom-designed molecular scissors for genome engineering of plant and mammalian cells. *Nucleic Acids Res.*, **33**, 5978-5990.
  166. Bibikova, M., Golic, M., Golic, K.G. and Carroll, D. (2002) Targeted chromosomal cleavage and mutagenesis in *Drosophila* using zinc-finger nucleases. *Genetics*, **161**, 1169-1175.
  167. Porteus, M.H. (2006) Mammalian gene targeting with designed zinc finger nucleases. *Mol. Ther.*, **13**, 438-446.
  168. Szczepek, M., Brondani, V., Buchel, J., Serrano, L., Segal, D.J. and Cathomen, T. (2007) Structure-based redesign of the dimerization interface reduces the toxicity of zinc-finger nucleases. *Nat. Biotechnol.*, **25**, 786-793.
  169. Daoudal-Cotterell, S., Gallego, M.E. and White, C.I. (2002) The plant Rad50-Mre11 protein complex. *FEBS Lett.*, **516**, 164-166.
  170. Gallego, M.E., Jeanneau, M., Granier, F., Bouchez, D., Bechtold, N. and White, C.I. (2001) Disruption of the *Arabidopsis* RAD50 gene leads to plant sterility and MMS sensitivity. *Plant J.*, **25**, 31-41.
  171. Bleuyard, J.Y., Gallego, M.E. and White, C.I. (2004) Meiotic defects in the *Arabidopsis* rad50 mutant point to conservation of the MRX complex function in early stages of meiotic recombination. *Chromosoma*, **113**, 197-203.
  172. Puizina, J., Siroky, J., Mokros, P., Schweizer, D. and Riha, K. (2004) Mre11 deficiency in *Arabidopsis* is associated with chromosomal instability in somatic cells and Spo11-dependent genome fragmentation during meiosis. *Plant Cell*, **16**, 1968-1978.
  173. Bundock, P. and Hooykaas, P.J.J. (2002) Severe developmental defects, hypersensitivity to DNA-damaging agents, and lengthened telomeres in *Arabidopsis* MRE11 mutants. *Plant Cell*, **14**, 2451-2462.
  174. Uanschou, C., Siwiec, T., Pedrosa-Harand, A., Kerzendorfer, C., Sanchez-Moran, E., Novatchkova, M., Akimcheva, S., Woglar, A., Klein, F. and Schlegelhofer, P. (2007) A novel plant gene essential for meiosis is related to the human CtIP and the yeast COM1/SAE2 gene. *EMBO J.*, **26**, 5061-5070.
  175. Doutriaux, M.P., Couteau, F., Bergounioux, C. and White, C. (1998) Isolation and characterisation of the RAD51 and DMC1 homologs from *Arabidopsis thaliana*. *Mol. Gen. Genet.*, **257**, 283-291.
  176. Markmann-Mulisch, U., Wendeler, E., Zobell, O., Schween, G., Steinbiss, H.H. and Reiss, B. (2007) Differential requirements for RAD51 in *Physcomitrella patens* and *Arabidopsis thaliana* development and DNA damage repair. *Plant Cell*, **19**, 3080-3089.
  177. Li, W., Chen, C., Markmann-Mulisch, U., Timofejeva, L., Schmelzer, E., Ma, H. and Reiss, B. (2004) The *Arabidopsis* AtRAD51 gene is dispensable for vegetative development but required for meiosis. *Proc. Natl. Acad. Sci. U. S. A.*, **101**, 10596-10601.
  178. Siaud, N., Dray, E., Gy, I., Gerard, E., Takvorian, N. and Doutriaux, M.P. (2004) Brca2 is involved in meiosis in *Arabidopsis thaliana* as suggested by its interaction with Dmcl. *EMBO J.*, **23**, 1392-1401.
  179. Dray, E., Siaud, N., Dubois, E. and Doutriaux, M.P. (2006) Interaction between *Arabidopsis* Brca2 and its partners Rad51, Dmcl, and Dss1. *Plant Physiol*, **140**, 1059-1069.
  180. Osakabe, K., Abe, K., Yoshioka, T., Osakabe, Y., Todoriki, S., Ichikawa, H., Hohn, B. and Toki, S. (2006) Isolation and characterization of the RAD54 gene from *Arabidopsis*



- thaliana*. *Plant J.*, **48**, 827-842.
181. Bleuyard, J.Y., Gallego, M.E., Savigny, F. and White, C.I. (2005) Differing requirements for the Arabidopsis Rad51 paralogs in meiosis and DNA repair. *Plant J.*, **41**, 533-545.
  182. Osakabe, K., Abe, K., Yamanouchi, H., Takyuu, T., Yoshioka, T., Ito, Y., Kato, T., Tabata, S., Kurei, S., Yoshioka, Y. *et al.* (2005) Arabidopsis Rad51B is important for double-strand DNA breaks repair in somatic cells. *Plant Mol. Biol.*, **57**, 819-833.
  183. Li, W., Yang, X., Lin, Z., Timofejeva, L., Xiao, R., Makaroff, C.A. and Ma, H. (2005) The AtRAD51C gene is required for normal meiotic chromosome synapsis and double-stranded break repair in Arabidopsis. *Plant Physiol.*, **138**, 965-976.
  184. Abe, K., Osakabe, K., Nakayama, S., Endo, M., Tagiri, A., Todoriki, S., Ichikawa, H. and Toki, S. (2005) Arabidopsis RAD51C gene is important for homologous recombination in meiosis and mitosis. *Plant Physiol.*, **139**, 896-908.
  185. Durrant, W.E., Wang, S. and Dong, X. (2007) Arabidopsis SN11 and RAD51D regulate both gene transcription and DNA recombination during the defense response. *Proc. Natl. Acad. Sci. U. S. A.*, **104**, 4223-4227.
  186. Bleuyard, J.Y. and White, C.I. (2004) The Arabidopsis homologue of Xrcc3 plays an essential role in meiosis. *EMBO J.*, **23**, 439-449.
  187. Kosarev, P., Mayer, K.F. and Hardtke, C.S. (2002) Evaluation and classification of RING-finger domains encoded by the Arabidopsis genome. *Genome Biol.*, **3**, RESEARCH0016.
  188. Block-Schmidt, A.S., Dukowic-Schulze, S., Wanieck, K., Reidt, W. and Puchta, H. (2010) BRCC36A is epistatic to BRCA1 in DNA crosslink repair and homologous recombination in *Arabidopsis thaliana*. *Nucleic Acids Res.*, **39**, 146-154.
  189. Hartung, F., Suer, S. and Puchta, H. (2007) Two closely related RecQ helicases have antagonistic roles in homologous recombination and DNA repair in *Arabidopsis thaliana*. *Proc. Natl. Acad. Sci. U. S. A.*, **104**, 18836-18841.
  190. Riha, K., Watson, J.M., Parkey, J. and Shippen, D.E. (2002) Telomere length deregulation and enhanced sensitivity to genotoxic stress in Arabidopsis mutants deficient in Ku70. *EMBO J.*, **21**, 2819-2826.
  191. Tamura, K., Adachi, Y., Chiba, K., Oguchi, K. and Takahashi, H. (2002) Identification of Ku70 and Ku80 homologues in *Arabidopsis thaliana*: evidence for a role in the repair of DNA double-strand breaks. *Plant J.*, **29**, 771-781.
  192. Molinier, J., Stamm, M.E. and Hohn, B. (2004) SNM-dependent recombinational repair of oxidatively induced DNA damage in *Arabidopsis thaliana*. *EMBO Rep.*, **5**, 994-999.
  193. Lee, S.Y., Kim, H., Hwang, H.J., Jeong, Y.M., Na, S.H., Woo, J.C. and Kim, S.G. (2010) Identification of tyrosyl-DNA phosphodiesterase as a novel DNA damage repair enzyme in Arabidopsis. *Plant Physiol.*, **154**, 1460-1469.
  194. Doucet-Chabeaud, G., Godon, C., Brutusco, C., de Murcia, G. and Kazmaier, M. (2001) Ionising radiation induces the expression of PARP-1 and PARP-2 genes in Arabidopsis. *Mol. Genet. Genomics*, **265**, 954-963.
  195. De Block, M., Verduyn, C., De Brouwer, D. and Cornelissen, M. (2005) Poly(ADP-ribose) polymerase in plants affects energy homeostasis, cell death and stress tolerance. *Plant J.*, **41**, 95-106.
  196. Vanderauwera, S., De Block, M., Van de Steene, N., van de Cotte, B., Metzlauff, M. and Van Breusegem, F. (2007) Silencing of poly(ADP-ribose) polymerase in plants alters abiotic stress signal transduction. *Proc. Natl. Acad. Sci. U. S. A.*, **104**, 15150-15155.
  197. Petrucco, S., Volpi, G., Bolchi, A., Rivetti, C. and Ottonello, S. (2002) A nick-sensing DNA 3'-repair enzyme from Arabidopsis. *J. Biol. Chem.*, **277**, 23675-23683.

## Chapter 2

# Characterization of *Arabidopsis thaliana* NHEJ mutants

Qi Jia, Paul Bundock, B. Sylvia de Pater  
and Paul J.J. Hooykaas

## Abstract

Eukaryotic organisms use two distinct pathways to repair DNA double-strand breaks (DSBs), namely non-homologous end joining (NHEJ) and homologous recombination (HR). NHEJ rather than HR is the major pathway for DSB repair in somatic cells of higher eukaryotes, and it may also be the major route whereby T-DNA integrates into the genome during *Agrobacterium*-mediated transformation. The NHEJ pathway has been well characterized in yeast and mammals. In order to study NHEJ in *Arabidopsis thaliana*, three plants lines with a T-DNA insertion in *AtKu80*, *AtKu70* or *AtLig4* genes were functionally characterized. Western blot analysis demonstrated that knockout of either *AtKu80* or *AtKu70* resulted in loss of the other protein, showing that heterodimer formation is needed for stability of the proteins. Plants homozygous for the T-DNA insertion were phenotypically indistinguishable from wild-type plants and were fertile. However, these mutants were hypersensitive to the genotoxic agent bleomycin, resulting in more DSBs as quantified in comet assays. They had lower end joining efficiency, suggesting that NHEJ is a critical pathway for DSB repair in plants. Both *Atku* mutants and a previously isolated *Atmre11* mutant were impaired in *Agrobacterium* T-DNA integration via floral dip transformation, whereas the *Atlig4* mutant was hardly affected, indicating that *AtKu80*, *AtKu70* and *AtMre11* play an important role in T-DNA integration in *Arabidopsis*, but that another ligase may substitute for *AtLig4*. The frequency of gene targeting was not increased in the *Atku80*, *Atku70* and *Atlig4* mutants, but it was increased at least 10 fold in the *Atmre11* mutant compared with the wild-type.

## Introduction

The genomic integrity of organisms is threatened by exogenous genotoxic agents, such as reactive oxygen species, ionizing radiation and chemicals, as well as by endogenous cellular processes, such as transcription and replication (1-3). The most threatening damage is the occurrence of a double-strand break (DSB) in the chromosomal DNA. To maintain genetic stability, organisms have developed two main independent pathways for DNA repair. One is the homologous recombination (HR) pathway involving extensive DNA sequence homology between the interacting molecules, and the other is the non-homologous end joining (NHEJ) pathway acting independently of significant homology. HR occurs during the late S to G2 phases of the cell cycle when the sister chromatid is in close proximity as repair template. On the other hand, NHEJ does not require a homologous chromosome and can function throughout the cell cycle (4). Generally, HR is mainly used in bacteria and lower eukaryotes, whereas NHEJ is used predominantly in higher eukaryotes (5;6). NHEJ is more error-prone than HR and often produces short deletions and insertions, whereas HR may lead to large-scale genetic rearrangements with repetitive sequence elements in large genomes. Emerging evidence suggests that the relative balance of the two pathways is tuned



to minimize the mutagenesis as a consequence of repair (7).

In response to DNA damage, the Mre11-Rad50-Xrs2 (MRX) complex in yeast and its counterpart in mammals, called Mre11-Rad50-Nbs1 (MRN), function early as a key player in the DNA damage sensing, signaling and repair mechanism of both HR and NHEJ pathways (8;9). The pathway of NHEJ in *S. cerevisiae* and mammals has been extensively characterized. In mammals, conserved proteins that are involved in NHEJ include the following: DNA-dependent protein kinase (DNA-PK), Ku70, Ku80, DNA ligase IV (Lig4), Xrcc4 and Cernunnos/XLF (10;11). Orthologs of these proteins have been identified also in yeast, fungi and plants with the exception of DNA-PKcs, which does not seem to play a role in NHEJ in these organisms. Ku is an abundant non-histone nuclear protein in human cells. However Ku is also found in the membrane and cytoplasm (12;13). Ku can shuttle from the cytoplasm to the nucleus dependent on the cell cycle status and external stimuli, like irradiation, alkylating agents and hormones such as somatostatin (14;15). Ku has an extremely high affinity to DNA ends, and thus rapidly binds to DSBs in living cells (4). DSB repair is initiated by the recognition and binding of the Ku heterodimer consisting of Ku70 and Ku80 to the exposed DNA ends. In mammals the Ku heterodimer recruits DNA-PKcs and activates its kinase activity (16-18). Once Ku is bound to the DNA ends, it can improve the binding equilibrium of the nuclease (Artemis-DNA-PKcs), the polymerases ( $\mu$  and  $\lambda$ ) and the ligase complex (XLF-XRCC4-Lig4) (19;20). In this way, Ku serves as a scaffold of the subsequent protein assembly and stabilizes their enzymatic activities at a DNA end (11). The following step is that the Lig4/XRCC4/XLF complex catalyzes the ligation and seals the joint (21), thereby restoring the genomic integrity. Lig4 has an exclusive function in NHEJ by forming a complex with XRCC4 through the BRCT domain in the C-terminus of Lig4 (22). This complex associates with Pol  $\chi$  family polymerases, Pol  $\mu$ , Pol  $\lambda$  and terminal transferase, which fill in the short gaps generated during DNA end alignment and processing (23;24). The Lig4/XRCC4 complex also has an impact on the association of Cernunnos/XLF which promotes the ligation of mismatched and noncohesive DNA ends (21;25). The NHEJ pathway is Ku-dependent and is also called classical NHEJ (C-NHEJ). Another NHEJ pathway has been identified in C-NHEJ deficient cells, which is Ku-independent, called back-up NHEJ (B-NHEJ) (26).

Integration of transgenes in lower eukaryotes depends on NHEJ and HR DNA repair pathways (27;28). Mutations in the NHEJ pathway favour the HR pathway and thereby increase the frequency of gene targeting, which is a useful technique using HR to change an endogenous gene (27-31). Gene targeting is very rare in higher eukaryotes, like animals and plants. Estimates of GT frequencies in several different plant species vary from  $10^{-4}$  to  $10^{-6}$  (32-40). Therefore, it would be an advantage if also in plants higher gene targeting frequencies could be achieved via inactivation of NHEJ.

Previous studies have reported on the identification of Arabidopsis NHEJ mutants (9;41-46). Most of these mutants were in the ecotype Wassilewskija (Ws). Those mutants display hypersensitivity to agents that induce DSBs, indicating the requirement of those

genes under genotoxic stress. Here we characterized three Columbia-0 (Col-0) Arabidopsis lines containing a T-DNA insertion in the *AtKu70*, *AtKu80* and *AtLig4* genes. The genome of the Col-0 ecotype has been sequenced completely and T-DNA insertion lines are available in most genes, including those involved in DNA repair, so that in the future we can analyze other DNA repair mutants including combinations of DNA repair pathways. Plants homozygous for the T-DNA insertions were analyzed for sensitivity to DNA damaging agents and it was shown directly that these proteins function in end joining in plants. *Agrobacterium*-mediated transformation and the frequency of gene targeting was analyzed in these NHEJ mutants and the *Atku70* and *Atmre11* mutants (ecotype Ws) previously described (9;41).

## Material and methods

### Characterization of the Arabidopsis T-DNA insertion mutants

*Atku80*, *Atku70* and *Atlig4* T-DNA insertion lines were obtained from the SALK T-DNA collection (SALK\_016627, SALK\_123114, SALK\_044027, respectively). Information about them is available at <http://signal.salk.edu/cgi-bin/tdnaexpress> (47). The T-DNA insertion site was mapped with a T-DNA Left Border (LB) specific primer LBa1 and a gene-specific primer. Pairs of gene-specific primers around the insertion site were used to determine whether the plants were homozygous or heterozygous for the T-DNA insertion, and the PCR products were sequenced. T-DNA right border (RB) specific primers (Sp205, Sp206) were used to detect the T-DNA Right Border/ vector junction. The sequences of all the primers are listed in Table 1. For Southern blot analysis, DNA was extracted from individual plants using the CTAB DNA isolation protocol (48) and digested with HindIII (*Atku70* and *Atlig4*) or PstI (*Atku80*). DNA (5µg) was ran on a 0.7% agarose gel and transferred onto positively charged Hybond-N membrane (Amersham Biosciences). The hybridization and detection procedures were done according to the DIG protocol from Roche Applied Sciences. The DIG probe was produced using the PCR DIG Labeling Mix (Roche) with specific primers SP271 and SP272 that amplified an 850-bp fragment from the T-DNA of pROK2. Characterization of the *Atku70* and *Atmre11* mutants (ecotype Ws) was described previously (9;41).

### Quantitative reverse-transcription PCR (Q-RT-PCR)

Leaves of 2-week-old wild-type (ecotype Col-0), *Atku80*, *Atku70* and *Atlig4* plants were ground under liquid N<sub>2</sub> in a Tissue-Lyser (Retch). Total RNA was extracted from the leaf powder using the RNeasy kit (Qiagen) according to the supplied protocol. Residual DNA was removed from the RNA samples with DNaseI (Ambion) in the presence of RNase inhibitor (Promega). RNA was quantified and 1 µg of RNA was used to make cDNA templates using iScript cDNA synthesis kit according to the manufacturer's instructions (Bio-Rad). Quantitative real-time PCR (Q-PCR) analyses were done using the iQ™ SYBR® Green

Supermix (Bio-Rad). Specific fragments (about 200 bp) were amplified by pairs of primers around the T-DNA insertion sites using a DNA Engine Thermal Cycler (MJ Research) equipped with a Chromo4 real-time PCR detection system (Bio-Rad). The sequences of the primers are listed in Table 1. The cycling parameters were 95°C for 3min, 40 cycles of (95°C for 1 min, 60°C for 40s), 72°C for 10 min. All sample values were normalized to the values of the house keeping gene *Roc1* (Primers Roc5.2, Roc3.3) and were presented as relative expression ratios. The value of the wild-type was set on 1.

**Table 1.** Sequences of primers used for characterization of T-DNA insertion lines and Q-PCR.

Name	Locus	Sequence
LBa1	T-DNA LB	5'-TGGTTCACGTAGTGGGCCATCG-3'
Sp111	<i>AtKu80</i>	5'-GAATTCCCATGGAACAACAAGCAGTAGCAG-3'
Sp112	<i>AtKu80</i>	5'-CTCGACTTAGCTCTCGAGCATTGAC-3'
Sp119	<i>AtKu70</i>	5'-TGGGTTCACAAGCACTACTGC-3'
Sp120	<i>AtKu70</i>	5'-GAATAGCCGGACGGAGTAAAGC-3'
Sp268	<i>AtLig4</i>	5'-ATGCTGAGGACTTGTTTAATG-3'
Sp269	<i>AtLig4</i>	5'-ACCAACATTTACCATCAAGG-3'
Sp205	T-DNA RB	5'-ATCAAGCGTATGCAGCCGCC-3'
Sp206	T-DNA RB	5'-TTTGGAAGTACAGAACCAGC-3'
Sp207	<i>AtKu80</i>	5'-GCGTCTTGGAGCAGGTCTCTTC-3'
Sp208	<i>AtKu80</i>	5'-GATGAAATCCCAGCGTTCTCG-3'
q1	<i>AtKu70</i>	5'-TCTACCACTCAGTCAACCTG-3'
q2	<i>AtKu70</i>	5'-CAATAGACAAGCCATCACAG-3'
q6	<i>AtLig4</i>	5'-GACACCAACGGCACAAG-3'
q7	<i>AtLig4</i>	5'-AAGTTCAATGTATGTCAGTCCC-3'
Roc5.2	<i>Roc1</i>	5'-GAACGGAACAGGCGGTGAGTC-3'
Roc3.3	<i>Roc1</i>	5'-CCACAGGCTTCGTCCGCTTTC-3'
Sp271	T-DNA	5'-CCCGTGTCTCTCCAAATG-3'
Sp272	T-DNA	5'-CAGGTCCCCAGATTAGCC-3'
q8	BamHI	5'-GTGACATCTCCACTGACGTAAG-3'
q9	BamHI	5'-GATGAACTTCAGGGTCAGCTTG-3'
q10	GFP	5'-CAAGCTGACCCTGAAGTTCATC-3'
q11	GFP	5'-GTTGTGGCGGATCTTGAAG-3'
Sp154	5' <i>PPO</i>	5'-GGTGGTACTTTTAAGGCAATTCAG-3'
Sp155	5' <i>PPO</i>	5'-GACAGAATTCCGGTGTTTGTAGAC-3'
Sp156	3' <i>PPO</i>	5'-GGTGAGTTAGTGGGAAGCAGTTGAC-3'
Sp157	3' <i>PPO</i>	5'-GTCCCATTCAACTATCTTGGTAAG-3'
Bar1	<i>Bar</i>	5'-AACCCACGTCATGCCAGTTCC-3'
Bar2	<i>Bar</i>	5'-CGGCGGTCTGCACCATCGTC-3'

### Western blotting

Leaves from plants grown in soil for 3 weeks were ground under liquid N<sub>2</sub> in a Tissue-Lyser (Retch). One hundred µl protein extraction buffer (50 mM Tris-HCl pH 7.5; 2 mM EDTA; 0.2 mM PMSF; 1 mM DTT; 1×Protease inhibitor cocktail Complete®, EDTA free) was added to 50 mg of tissue powder. Soluble protein was isolated by centrifugation at 4°C. The protein concentration was determined using the BIO-RAD protein assay reagent. Approximately 10 µg soluble proteins were electrophoresed on 10% SDS/PAGE (49). The fractionated products were semi-dry blotted onto BA85 nitrocellulose membrane (Whatman). Equal loading of the gels and quality of protein preparations were checked by staining extra sets of gels with Coomassie Brilliant Blue R250 (not shown). Blots were blocked for 3 hr in 5% nonfat dry milk in PBST (10 mM NaPO<sub>4</sub>, pH 7.4; 120 mM NaCl; 2.7 mM KCl; 0.05% v/v Tween 20) and incubated overnight at 4°C with peptide antibodies (1:1000) in the same buffer. Rabbit anti-Ku80 and anti-Ku70 polyclonal antibodies were raised against synthetic peptides corresponding to small domains of the proteins that exhibit sequence diversity and were affinity chromatography purified (Eurogentec). The sequences of the synthetic peptides for AtKu80 and AtKu70 were NH<sub>2</sub>-LLRDKPSGSDDEDN-+C-CONH<sub>2</sub> and NH<sub>2</sub>-ELDPDDVFRDEDEDP-+C-CONH<sub>2</sub>, respectively, with a C-terminal coupling on the added cysteine. The blots were washed 4 times with PBST and incubated for 3 h with anti-rabbit HRP antibodies (1:7500) (Promega). The blots were washed 4 times with PBST and detection was performed using LumiGLO™ chemoluminescence detection kit (Cell Signalling).

### Assays for sensitivity to bleomycin and methyl methane sulfonate (MMS)

Seeds from Col-0 wild-type and the *Atku80*, *Atku70* and *Atlig4* mutants were surface-sterilized as described (50) and were germinated on solidified ½ MS medium (invented by Murashige and Skoog, containing MS salts with macro- and micronutrients, vitamins, FeNaEDTA, myo-inositol, MES, sucrose, Daishin Agar) (51). For bleomycin and MMS sensitivity, 4-day-old seedlings were transferred to liquid ½ MS medium or liquid ½ MS medium containing 0.2 µg/ml and 0.4 µg/ml Bleocin™ antibiotic (Calbiochem), or 0.007% and 0.01% (v/v) MMS (Sigma). The seedlings were scored after 2 weeks of growth at 21 °C in a growth chamber (16 h light/8 h dark, 2500 lux at 70% humidity). After this period, fresh weight (compared with controls) was determined by weighing the seedlings in batches of 20 in triplicate.

### Comet assay

DSBs were detected by a neutral comet assay as described previously (52) with minor modifications. Plant nuclei were embedded in 1% low melting point Ultrapure™ agarose-1000 (Invitrogen) to make a mini gel on microscopic slides according to the protocol. Nuclei were subjected to lysis in high salt (2.5 M NaCl, 10 mM Tris-HCl, pH7.5, 100 mM EDTA) for 20 min at room temperature (N/N protocol). Equilibration for 3×5

min in 1×TBE buffer (90 mM Tris-borate, 2 mM EDTA, pH8.4) on ice was followed by electrophoresis at 4 °C in TBE buffer for 15min at 30V (1V/cm), 15-17mA. Dry agarose gels were stained with 15 ul ethidium bromide (5ug/ml) and immediately evaluated with a Zeiss Axioplan 2 imaging fluorescence microscope (Zeiss, Germany) using the DsRed channel (excitation at 510nm, emission at 595nm). Images of comets were captured at a 40-fold magnification by an AxioCam MRc5 digital camera (Zeiss, Germany). The comet analysis was carried out by comet scoring software CometScore™ (Tritek Corporation). The percentage of tail DNA (%tail-DNA) was used as a measure of DNA damage. The %tail-DNA was measured at 3 time points: 0 h, 2 h, 24 h for 1µg/ml bleomycin treatment and in the seedlings which had 24h recovery in ½ MS after 24h treatment. Measurements were performed for 4 independent gel replicas and approximately 100 comets analyzed for each treatment.

### Isolation of *Arabidopsis mesophyll* protoplasts

*Arabidopsis* Col-0 was either grown in a greenhouse at 21°C (16 h photoperiod) or in a culture chamber (21°C, 50% relative humidity, 16 h photoperiod). Rosette leaves (~1 g) from plants that were 3 to 5 weeks old were collected, rinsed with deionized water and briefly dried. The leaves were cut into 0.5 to 1 mm strips with a razor blade, placed into a sterile Petri dish containing 15 ml of filter-sterilized enzyme solution [1.5% (w/v) cellulose R10, 0.4% (w/v) macerozyme R10, 0.4 M mannitol, 20 mM KCl, 20 mM MES pH5.7, 10 mM CaCl<sub>2</sub>, 0.1% (w/v) BSA] and incubated 2-3 h in the dark at 28°C. Then the protoplasts were filtered through a 50 µm mesh to remove the undigested material and transferred to a round-bottom Falcon tube. The solution was centrifuged for 5 min at 600 rpm to pellet the protoplasts. The supernatant which contained broken cells was discarded. The protoplasts were gently washed twice by 15 ml cold W5 solution (154 mM NaCl, 125 mM CaCl<sub>2</sub>, 5 mM KCl, 2 mM MES pH5.7), and resuspended in cold W5 solution to a final concentration of 2×10<sup>5</sup> cells/ml and kept on ice for 30 min. Just before starting transfection, protoplasts were collected from the W5 solution by centrifugation and were resuspended to a density of 2×10<sup>5</sup> cells/ml in MMg solution (0.4 M mannitol, 15 mM MgCl<sub>2</sub>, 4mM MES pH5.7) at room temperature.

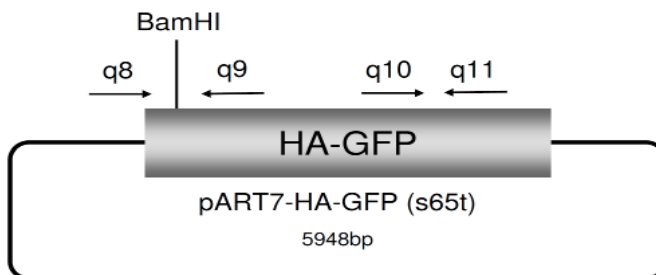


**Figure 1.** Schematic diagram of pART7-HA-GFP. The primers for Q-PCR are shown by arrows.

### End joining assay

Plasmid pART7-HA-GFP(S65T) was linearized by cleavage with BamHI (Figure 1). Fresh protoplasts prepared from leaves were transformed with either linear or circular plasmid DNA by the polyethylene glycol (PEG) transformation protocol (53). In each experiment,  $2 \times 10^4$  protoplasts were transformed with 2  $\mu\text{g}$  of plasmid. Recircularization of the linear plasmid in protoplasts by the NHEJ pathway was analyzed. DNA was extracted from protoplasts (at 0 h and 20 h) and was used to quantify rejoining by Q-PCR. The DNA extraction protocol and the cycling parameters of Q-PCR were the same as mentioned above. Two pairs of primers were used: one pair (q8+q9) was flanking the enzyme digestion site (BamHI); the other pair (q10+q11) was localized in GFP (Figure 1). When the plasmid is circular, both of them give products. When the plasmid is cleaved by BamHI, the first pair of primers will not give a product, whereas the second will still give products. The efficiency of end joining is presented by the ratio of PCR products using q8+q9 primers and q10+11 primers in comparison with the controls. The value of the wild-type was set on 1. Q-PCR was performed as three replicates and the assays were performed in triplicate.

### Root transformation

Root transformation was performed as described by Nam *et al.* (54). Sterile roots of 3-week-old wild-type and mutants grown in agar were cut into segments and inoculated with *Agrobacterium* strain AT $\Delta$ virD2 with wild-type VirD2 on a plasmid harboring a  $\beta$ -glucuronidase (GUS)-expressing binary vector (55). After 2 days co-cultivation, an excess of *Agrobacterium* cells was washed away. Some of the root segments were stained with 5-bromo-4-chloro-3-indolyl  $\beta$ -D-glucuronide (X-Gluc) to measure the transient expression. GUS activity was determined as the number of blue spots per seedling. The residual root segments were plated on callus-induction medium containing kanamycin for 3-4 weeks to test callus formation as measure for T-DNA integration (45). Stable transformation was scored as infected root segments that produced any form of callus.

### Floral dip transformation

Floral dip transformation was performed according to the procedure described by Clough and Bent (56). The *Agrobacterium* strain AGL1 (pSDM3834) (34) was used for infection. Plasmid pSDM3834 is a pCambia 1200 derivative (hpt selection marker). Seeds were harvested from the dry plants after maturation and plated on solid MA medium (57) without sucrose containing 15  $\mu\text{g}/\text{ml}$  hygromycin, 100  $\mu\text{g}/\text{ml}$  timentin (to kill *Agrobacterium* cells) and 100 mg/ml nystatin (to prevent growth of fungi). Hygromycin-resistant seedlings were scored 2 weeks after germination and transformation frequency was determined (50 seeds weigh approximately 1mg) (43).

### Gene targeting

In order to test the frequency of gene targeting in the *Atku70* mutant (ecotype Ws) (41) and

the *Atmre11* mutant (ecotype Ws) (9) which were previously characterized by our lab, floral dip transformation was performed with *Agrobacterium* strain AGL1 (pSDM1502) (original name of the plasmid is pSDM) for gene targeting using the protoporphyrinogen oxidase (*PPO*) system (32). For the three NHEJ mutants (ecotype Col-0), floral dip transformation was performed with *Agrobacterium* strain AGL1 (pSDM3900). Plasmid pSDM3900 is a pCambia 3200 derivative (phosphinothricin (ppt) selection marker). The *PPO* sequences used for gene targeting were cloned from the Col-0 ecotype and mutations were introduced to obtain resistance to the herbicide butafenacil. About 1 gram seeds were plated on solid MA medium without sucrose containing 15 µg/ml ppt, 100 µg/ml timentin and 100 µg/ml nystatin to determine the transformation frequency. The rest of the seeds were all sowed on solid MA medium without sucrose containing 50 µM butafenacil, 100 µg/ml timentin and 100 µg/ml nystatin to identify gene targeting events. The butafenacil-resistant plants were analyzed with Southern blot analysis to determine if they represented true gene targeting (TGT) events or contained extra T-DNA integration (Figure 2).

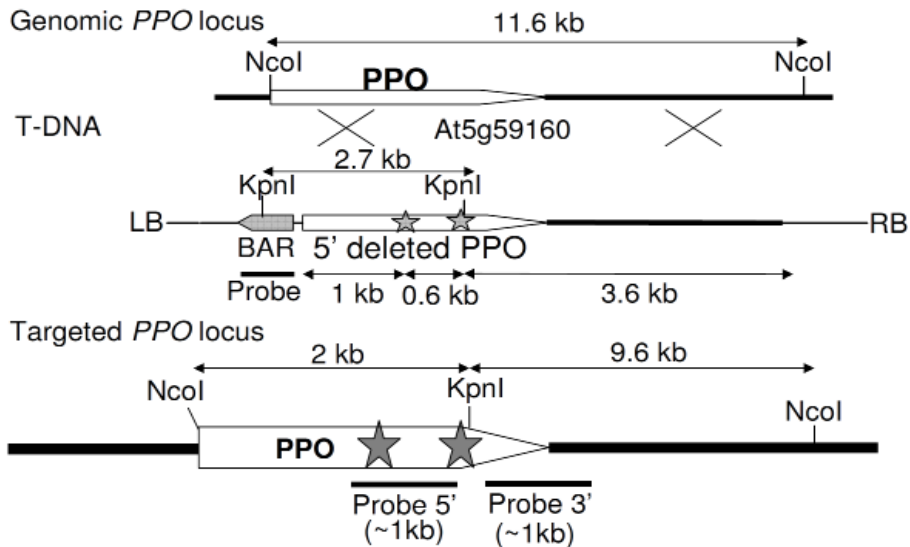


**Figure2.** The design for the targeted modification of the Arabidopsis *PPO* locus. The white box marked *PPO* represents the *PPO* coding region, and the thick black lines represent flanking plant genomic DNA. The thin lines indicate the T-DNA sequences. The two mutations conferring Butafenacil resistance are indicated as stars. The *BAR* resistance gene is linked to the truncated 5'Δ*PPO* of the T-DNA (LB for left border and RB for right border). The probes and the restriction enzyme digestion sites used for Southern blot analysis are also shown.

## Results

### Isolation and characterization of the *Atku80 Atku70* and *Atlig4* mutants

In order to study the role of *AtKu80*, *AtKu70* and *AtLig4* in *Agrobacterium* transformation and gene targeting, *Arabidopsis thaliana* (ecotype Col-0) homozygous T-DNA insertion



mutants were obtained from the Salk collection and characterized (Figure 3). When two gene-specific primers flanking the insertion site were used, PCR products were amplified for the wild-type and heterozygotes. No PCR products were obtained for homozygous mutants by using two gene-specific primers, because the PCR products in the mutant would be >10 kb in size and would not be detectable. When T-DNA-specific primer LBa1 was used in combination with one gene-specific primer, PCR products for the T-DNA-insertion mutants were amplified, whereas no PCR products were obtained for the wild-type. We identified

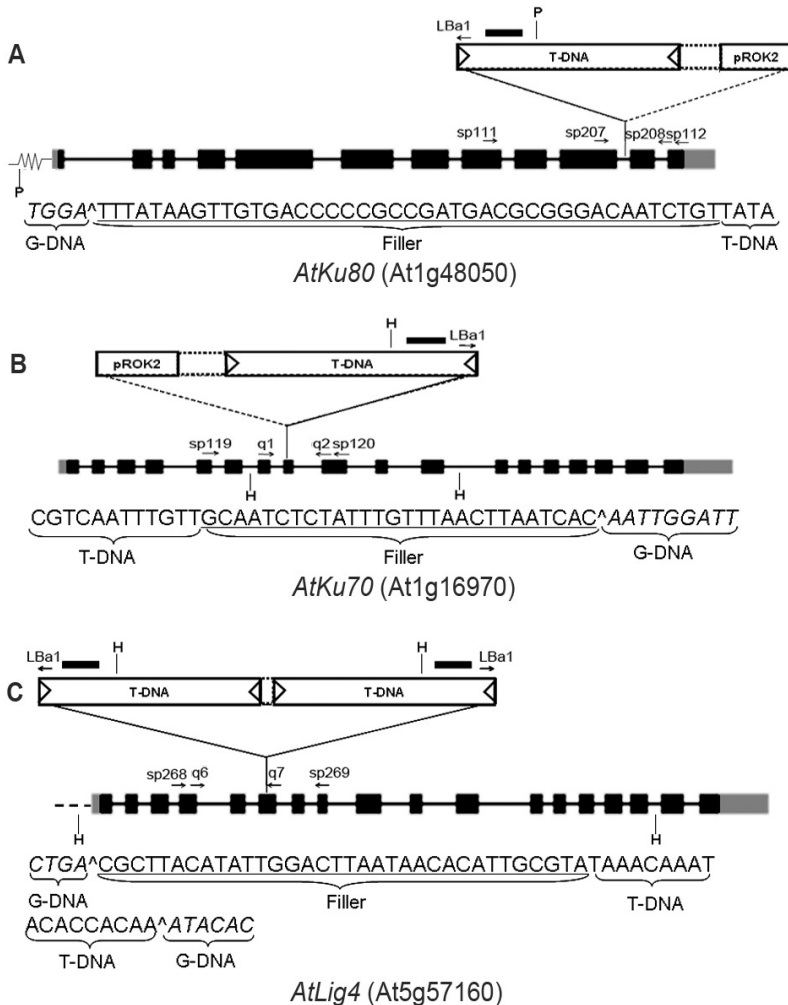


**Figure 3.** Molecular analysis of the NHEJ T-DNA insertion lines.

Genomic organization of the *AtKu80* (A), *AtKu70* (B) and *AtLig4* (C) locus. Inserted T-DNAs are indicated. Exons are shown as black boxes. 3' and 5' UTRs are shown as gray boxes. Introns are shown as lines. The primers used for genotyping and Q-RT-PCR analysis are indicated. The probe (—) and the restriction enzyme digestion sites (P for PstI, H for HindIII) used for Southern blot analysis are also indicated. Genomic DNA sequences (gDNA) flanking the T-DNA insertion are shown in italic. pROK2 denotes the vector part of this binary vector.



homozygous mutants harboring a T-DNA insertion for each of the three genes (data not shown) in the next generation. The insertion point of the T-DNA left border (LB) was mapped by sequencing of the PCR products generated by LBa1 in combination with one of the gene-specific primers. For *Atlig4*, PCR products were produced by LBa1 combined with both gene-specific primers (Sp268, Sp269), indicating the insertion of a T-DNA inverted repeat with the LB at both ends. For *Atku80* and *Atku70*, no PCR products were obtained using LBa1 or the RB primer in combination with the other gene-specific primer, but PCR products (600bp) were amplified by using primers spanning the RB/vector junction (Sp205 and Sp206). That indicated that the RB was integrated with extra vector pBin-ROK DNA. Therefore, the RB integration site could not be mapped in the *Atku80* and *Atku70* mutants.

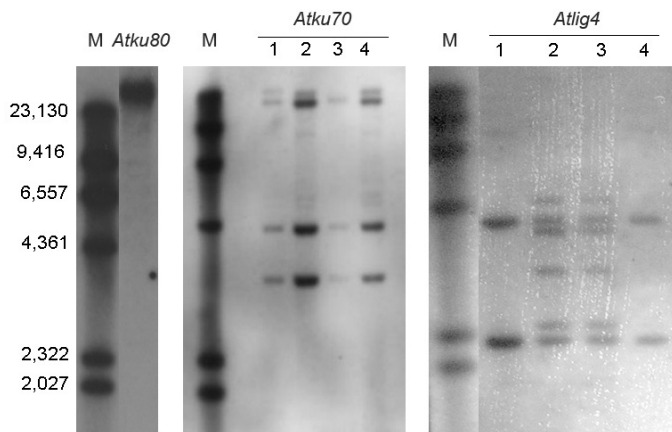


**Figure 4.** Southern blot analysis of T-DNA insertion mutants.

The genomic DNA was digested by PstI (*Atku80*) or HindIII (*Atku70* and *Atlig4*). An 850-bp amplified region of the T-DNA of pROK2, was used as probe. M:  $\lambda$ HindIII Marker. 1, 2, 3 and 4 indicate individual progeny plants of *Atku70* and *Atlig4*.

The genomic DNA was digested by the PstI (*Atku80*) or HindIII (*Atku70* and *Atlig4*) for Southern blotting (Figure 4). If there is one T-DNA inserted in the correct locus, bands with the following sizes will be detected on the blot: *Atku80*: 32 kb; *Atku70*: 3.2 kb; *Atlig4*: 2.1 kb and 3.8 kb. If T-DNAs are also present in other loci, additional bands probably with different sizes will be detected. If there are 2 or more T-DNAs inserted in one locus as direct repeat, an additional band of 4317 bp, representing a complete T-DNA, will be detected. If there are 2 or more T-DNAs inserted in one locus as indirect repeat, an additional band of 3634 bp will be detected. Sequencing results and Southern blot analysis using a pROK2 probe indicated that the T-DNAs were all inserted at the position as reported by the Salk database. A detailed characterization of the T-DNA insertions is shown in Figure 3. The *Atku80* line contained 1 T-DNA insertion. The LB end of the T-DNA in *Atku80* was integrated into intron 10, had lost 7 base pairs (bps) and had incorporated 43 bps filler DNA during integration. The *Atku70* line contained more than 2 T-DNA copies. The LB end of the T-DNA in *Atku70* was integrated into exon 8 and had 28 bps filler DNA. The

*Atlig4* line contained 2 T-DNA copies inserted as an inverted repeat. The two LB ends of the T-DNAs in *Atlig4* were integrated into exon 6, one missing 18 bps and the other missing 11 bps. The *Atlig4* gene itself had lost 25 bps. There were extra T-DNAs present in other loci in plants 2 and 3 of the *Atlig4* line, but these were absent in plants 1 and 4, which were used for further analysis (Figure 4).

We did not observe any dwarf or sterile phenotype in these *Arabidopsis* mutant lines. Also no obvious differences in growth, flowering or senescence were observed between mutants and wild-type plants. A somewhat delayed germination was the only phenotypic change exhibited by the *Atku80* mutant. This is in accordance with former reports about the phenotype of mutants with T-DNA insertions in these genes in the ecotype Wassilewskija (Ws) (41;43;46).

### Expression analysis

In order to check expression of the mutated genes, Q-RT-PCR analysis was performed for each T-DNA insertion line using primers flanking the insertion site. This resulted in a product for each gene in the wild-type, but not in the corresponding T-DNA insertion mutant (Figure 5). This indicated that in the insertion mutants no stable mRNA is produced from the mutated gene and confirms that the plants are indeed homozygous mutants. Compared with the wild-type, each mutant had a higher expression of the two other intact NHEJ genes. Thus, there could be some form of feedback regulation for the expression of these three genes.

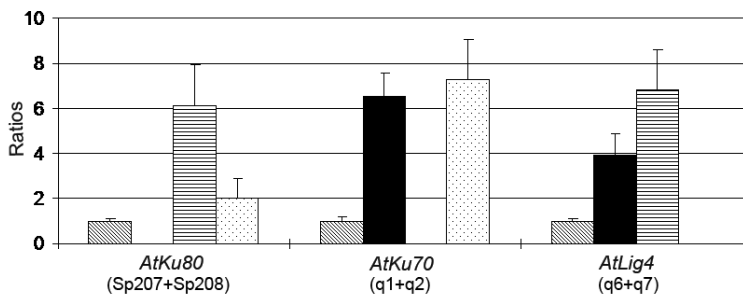


**Figure 5.** RNA expression of the NHEJ genes *AtKu80*, *AtKu70* and *AtLig4*, determined by Q-RT-PCR, in wild-type and mutant plants. All the sample values were normalized to *Roc* values and the ratios were obtained in triplicate. The values of the wild-type were set on 1. (▨ wild-type; ■ *Atku80*; ▨ *Atku70*; ▩ *Atlig4*)

Western blot analysis was performed on extracts from wild-type, *Atku80*, *Atku70* and *Atlig4* plants using polyclonal peptide antibodies raised against AtKu80 or AtKu70. An 80-kD band, the predicted size of the AtKu80, was present in the wild-type and *Atlig4* plants, but not detectable in the *Atku80* mutant with anti-Ku80 antibodies. A very weak signal was found in the *Atku70* mutant. A 70-kD band, the predicted size of the AtKu70 protein, was present in the wild-type and *Atlig4* plants, but not detectable in the *Atku70* mutant with

anti-Ku70 antibodies and the signal was very weak in the *Atku80* mutant (Figure 6). Loss of one of the Ku subunits thus resulted in a significant decrease in the amounts of the other subunit according to the western blot data. This indicated that heterodimerization of the Ku proteins is required for Ku protein stabilization in plants, as was shown before in mammals (14;58).

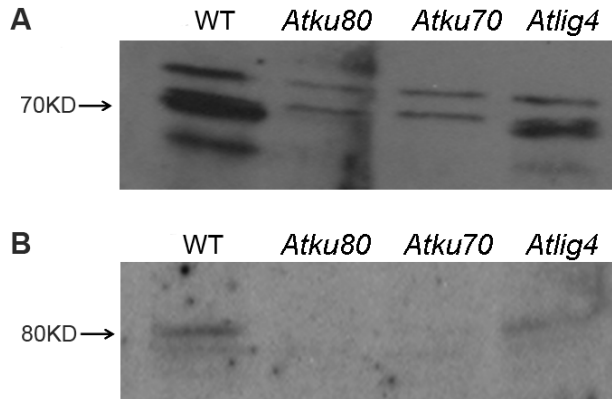


**Figure 6.** Western blot analysis of leaf protein samples from the *Atku80*, *Atku70*, *Atlig4* mutants and wild-type (Col-0) plants using anti-AtKu70 antibody (A) and anti-AtKu80 antibody (B). Detected Ku70 and Ku80 proteins are indicated with arrows. Around 10  $\mu$ g of soluble leaf protein was loaded for each plant line.

### Sensitivity to genotoxic agents

Mammalian cell lines, yeast strains and Arabidopsis mutants lacking Ku80, Ku70 or Lig4 have defects in DSB repair and are sensitive to DNA-damaging agents (10;41;43;59). We tested whether disruption of these genes in the Col-0 background also affects sensitivity of the plants to DNA-damaging agents by comparing growth of the wild-type and these NHEJ mutants during exposure to bleomycin or MMS. Bleomycin is a radiomimetic chemical that induces DNA double strand breaks (DSBs) (60). MMS is a monofunctional alkylating agent that induces *N*-alkyl lesions and DNA single strand breaks (SSBs) that can be converted into DSBs during replication (61). As expected, the *Atku80*, *Atku70* and *Atlig4* mutants turned out to be hypersensitive to bleomycin and the *Atku70* and *Atlig4* mutants seemed also somewhat more sensitive to MMS. To quantify this, the fresh weight of seedlings was determined after 2 weeks of continuous treatment. Compared with wild-type seedlings, NHEJ mutated seedlings showed growth retardation in the presence of these two genotoxic agents (Figure 7). In the presence of bleomycin, the fresh weight of *Atku80* was 2-fold less than that of the wild-type and the fresh weight of *Atku70* and *Atlig4* was about 4-fold less than that of the wild-type. The fresh weight of all seedlings was lower after growth in the presence of MMS compared to bleomycin. According to the student's T-test, the *Atku70* and *Atlig4* mutants had a significantly lower weight than the wild-type grown in the presence of MMS, but there was no significant difference between the wild-type and the *Atku80* mutant. These data corroborated that AtKu80, AtKu70 and AtLig4 are main components

of the DSB repair machinery and that the *Atku70* and *Atlig4* mutants are more sensitive to genotoxic agents than the *Atku80* mutant.

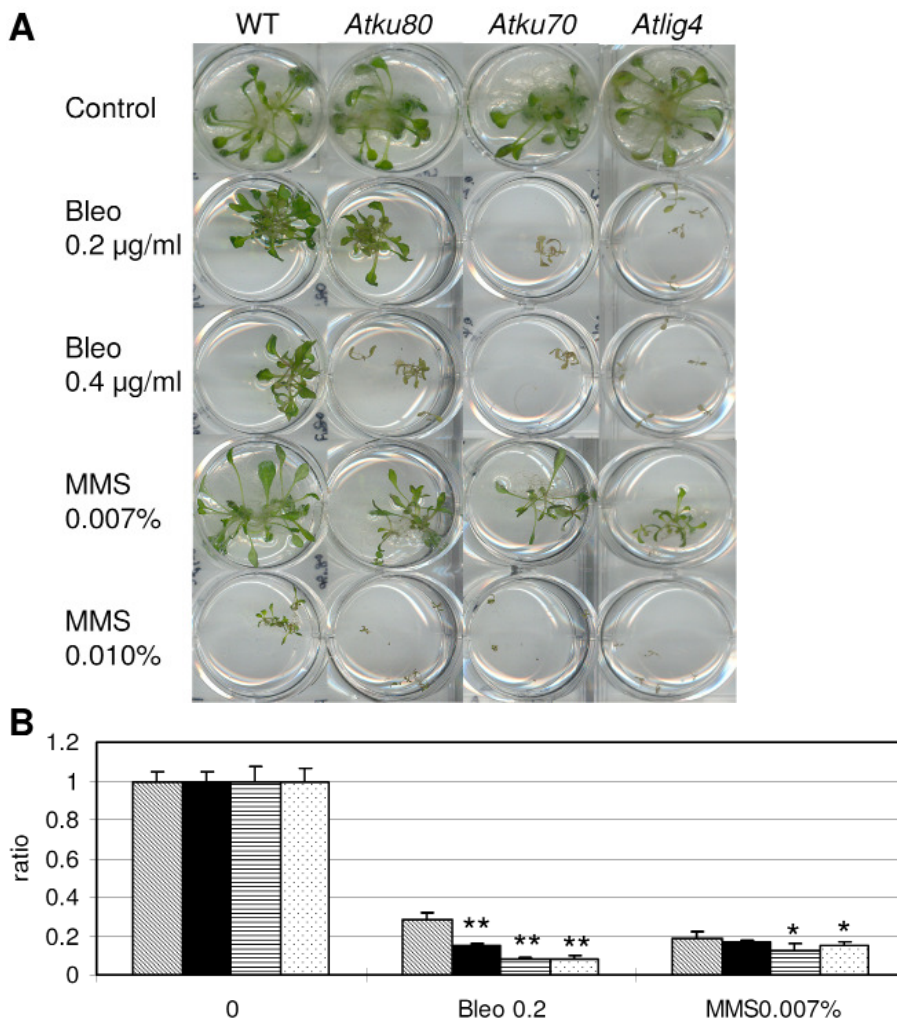


**Figure 7.** Hypersensitivity of *Atku80*, *Atku70* and *Atlig4* plants to DNA-damaging treatments. (A) Phenotypes of wild-type (Col-0) plants and *Atku80*, *Atku70* and *Atlig4* mutants to bleomycin or MMS treatment. Four-day-old seedlings were transferred to liquid  $\frac{1}{2}$  MS medium (control) or  $\frac{1}{2}$  MS medium containing different concentrations of bleomycin (Bleo) or MMS and were scored 2 weeks after germination.

(B) Fresh weight of 2-week-old wild-type plants and *Atku80*, *Atku70* and *Atlig4* mutants treated with 0.2 µg/ml bleomycin or 0.007% MMS. For each treatment 20 seedlings were weighed in triplicate. Fresh weight of the plants grown for 2 weeks without bleomycin or MMS was set at 1. Student's test: \*  $P < 0.05$ , \*\*  $P < 0.001$  (comparing mutants with the wild type of the same treatment).

(▨ wild-type; ■ *Atku80*; ▤ *Atku70*; ▩ *Atlig4*)

In order to quantify the DNA damage in these mutants, comet assays were performed. For each treatment, around 100 randomly chosen nuclei were analyzed by using CometScore™.

The percentage DNA in the tail is related to the amount of DNA damage. Scoring was done by dividing the nuclei into three groups according to percentage DNA in the tail (<5, 5-10, >10). Thereafter, for each treatment the proportion of the nuclei in each group was determined. The results showed that the genomic DNA of the *Atku80*, *Atku70* and *Atlig4* mutants was more damaged than that of the wild-type, especially after treatment with bleomycin for 24h (Figure 8). Already, after 2h treatment, more DNA damage was found in the nuclei of the *Atku80* and *Atku70* mutants, indicating that the genome of the *Atku80* and *Atku70* mutant was damaged quicker and thus that repair was slower than in the *Atlig4* mutant and the wild-type (Figure 8). Interestingly, the NHEJ mutants had less DNA damage after 24h recovery compared to the situation before recovery, though they still had more DNA damage than the wild-type, especially the *Atku70* and *Atku80* mutants (Figure 8). This showed that a slow back-up DNA repair pathway must exist for repair of DNA damage in the NHEJ mutant plants.

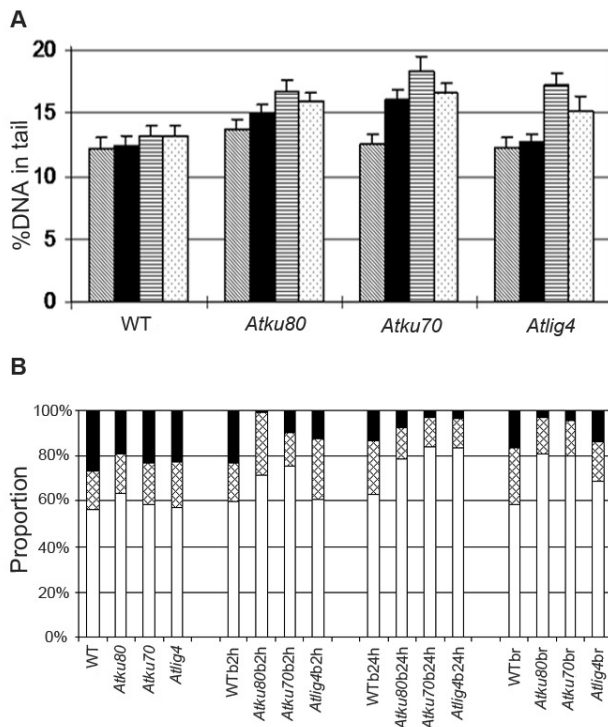


**Figure 8.** Comet assay.

(A) The fraction of DNA in comet tails (%tail-DNA) was used as a measure of DNA damage in wild-type (Col-0), *Atku80*, *Atku70* and *Atlig4* plants. For each treatment, around 100 nuclei were analyzed. The means of %tail-DNA after bleomycin treatment are shown.

(■) t=0; (■) t=2h; (▨) t=24h; (▤) 24h recovery)

(B) According to the value of %tail-DNA, nuclei were divided into three groups (■ <5; ▤ 5-10; □ >10). The proportions of these groups are shown for wild type (Col-0), *Atku80*, *Atku70* and *Atlig4* plants after: no treatment; b2h: 2h bleomycin treatment; b24h: 24h bleomycin treatment; br: 24h bleomycin treatment followed by 24h recovery.

### End joining activity

To directly test the function of *AtKu80*, *AtKu70* and *AtLig4* in end joining, we used an *in vivo* plasmid rejoining assay to quantify the capacity of the protoplasts to repair restriction enzyme generated DSBs. To this end, we transformed protoplasts from leaves with circular (control) or BamHI linearised plasmid DNA. BamHI digests the plasmid DNA in the N-terminal part of the GFP coding sequence. Rejoining of linear plasmid *in vivo* will result in GFP expression. GFP fluorescence was indeed detected in the wild-type protoplasts which were transformed with linearized plasmid. But it was difficult to quantify the difference of GFP expression between the wild-type and the mutants under the fluorescence microscope. Therefore, we analyzed the rejoining efficiency by Q-PCR, using primers around the BamHI site compared to primers in the GFP coding region. The results showed that the rejoining efficiencies were reduced by half in the *Atku80*, *Atku70* and *Atlig4* mutants compared with the wild-type (Figure 9). It proved directly that *AtKu80*, *AtKu70* and *AtLig4* are involved in NHEJ.

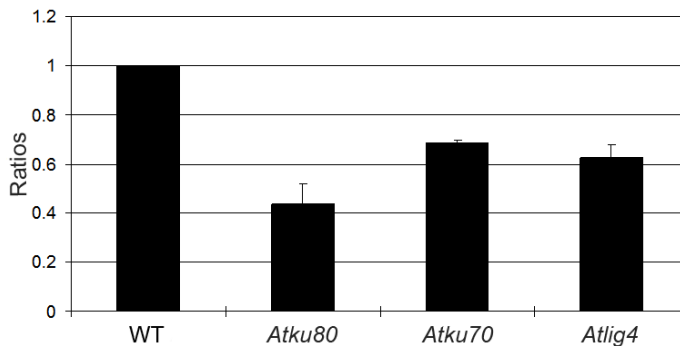


**Figure 9.** Plasmid end-joining assay.

Rejoined plasmid DNA with respect to total plasmid DNA in the wild-type Col-0 was set on 1. Values of end joining in the mutants are given relative to that of the wild-type.

### T-DNA integration

Double strand break repair forms an important mechanism for the integration of *Agrobacterium* T-DNA in the genome. In yeast non-homologous T-DNA is integrated by NHEJ (27), but the results obtained in plants so far are variable (43;45;59;62). To test whether the *AtKu70*, *AtKu80* and *AtLig4* genes are required for T-DNA integration, we compared T-DNA integration in those mutants and in wild-type plants using two different *Agrobacterium* transformation assays.

First, *in vitro* root transformation was performed as described by Nam *et al* (54), using a binary vector with both a *GUS* gene and the *nptII* gene (for Kanamycin resistance). The transient *GUS* activity was determined as the number of blue spots per root segment. T-DNA integration was scored as the percentage of infected root segments that produced any form of callus on selective callus-inducing medium. In principle, for each plant line, the transient *GUS* activity, which reflects expression of non-integrated T-DNA, should be at the same



level, whereas callus formation will be reduced in mutants affected in T-DNA integration. Our results showed no significant difference, neither in transient GUS expression nor in callus formation between the NHEJ mutants and the wild-type (data not shown).

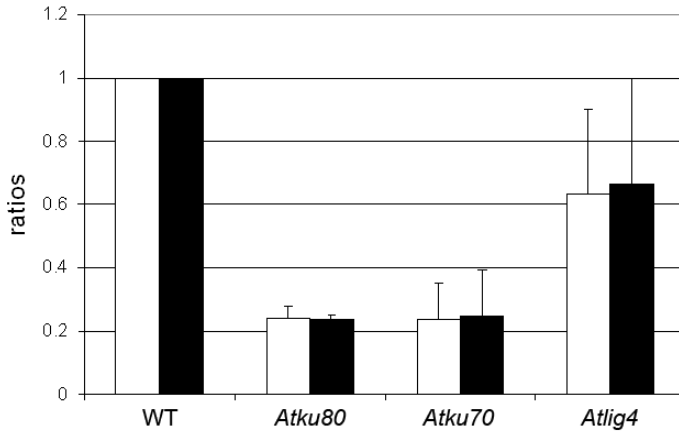


**Figure 10.** Transformation frequencies using the floral dip assay.

One gram of seeds from the wild-type (Col-0) and the NHEJ mutants obtained after floral dip transformations were selected on hygromycin (for pSDM3834) or ppt (for pSDM3900). The number of selection-marker-resistant seedlings was scored 2 weeks after germination. The transformation frequency is presented as the ratio of the percentage of selection-marker-resistant seedlings in the mutants and the wild-type. (□ pSDM3834, ■ pSDM3900)

Secondly, we transformed germline cells using the floral dip method as described by Clough and Bent (56). The transformation frequency here was determined as the number of hygromycin resistant seedlings per total number of plated seeds. In this assay, the transformation frequency of *Atku80* and *Atku70* plants turned out to be reduced significantly to 20 percent of the wild-type transformation frequency, whereas the transformation frequency of *Atlig4* plants was not significantly reduced (Figure 10). It indicated that AtKu80 and AtKu70, but not AtLig4, are required for efficient *Agrobacterium* T-DNA integration in plant germline cells.

### Gene targeting

T-DNA can not only be integrated by non-homologous recombination, but also at low frequency by homologous recombination (gene targeting). The number of gene targeting (GT) events was shown to be increased after disruption of NHEJ in lower eukaryotes, such as yeast and fungi (28;29;63;64). In order to test whether disruption of NHEJ also increased gene targeting frequency in plants NHEJ mutants were used in *Agrobacterium* floral dip transformation using a T-DNA with an incomplete mutated *PPO* gene with homology to the plant genome (Figure 2). If the targeted endogenous *PPO* gene is replaced by the mutated *PPO* of the T-DNA, the plants become resistant to butafenacil. If there are extra T-DNAs randomly inserted in other loci of the genome, the plants will also become resistant to phosphinotricin (ppt). Besides the Col-0 mutants characterized here, previously described

*Atku70* and *Atmre11* mutants were used of the ecotype Ws (9;41), because no *Atmre11* mutants could be obtained for the Col-0 ecotype.

**Table 2.** Transformation and gene targeting frequencies.

Plant lines	Transformants tested	Butafenacil resistant	ppt resistant	Transformation frequency
WT (Col-0)	2600	2	1	1
<i>Atku80</i> (Col-0)	1143	0	-	0.23
<i>Atku70</i> (Col-0)	1086	0	-	0.24
<i>Atlig4</i> (Col-0)	1537	0	-	0.66
WT (Ws)	10927	0	-	1
<i>Atku70</i> (Ws)	980	0	-	0.23
<i>Atmre11</i> (Ws)	3625	3	3	0.21

The numbers of different events found in gene targeting experiments. The transformation frequency was shown as the ratios compared with the wild-type and the value of the wild-type was set on 1.

Firstly, 1 g of seeds was used to determine the transformation frequency by plating on ppt media (Table 2). In all 5 mutants the frequency was lower compared to the wild-type as already described above for the three Col-0 mutants (Figure 10). The remaining of the seeds was plated with selection for butafenacil resistance. The theoretical number of transformants in these seed batches was calculated from the transformation frequency.

There were 2 butafenacil-resistant plants found in 2600 transformants of the wild-type of ecotype Col-0. PCR analysis showed that both plants represent true gene targeting (TGT) events (data not shown). One of these plants is also ppt resistant, indicating the presence of extra T-DNA copies. There were no GT events found in around 1000 transformants of the *Atku70*, *Atku80* and *Atlig4* Col-0 mutants (Table 2), indicating that the gene targeting frequency was not significantly increased in those mutants compared with the wild-type.

Subsequently, the Ws wild-type and mutants were used for a GT experiment. In about  $10^4$  wild-type transformants no GT event was observed. Since the transformation frequency of *Atku70* (ecotype Ws) was rather low only about 1000 transformants were obtained and no GT events were observed. However, there were 3 butafenacil-resistant plants found in 3625 transformants of the *Atmre11* mutant (ecotype Ws). Therefore, the frequency of gene targeting was increased at least 10 fold in the *Atmre11* mutant compared with that in the Ws wild-type. Initial PCR analysis showed that GT had occurred in these plants (results not shown). These plants were further analyzed by Southern blotting.

The genomic DNA of pools of progeny plants of the 3 plant lines was digested by KpnI and NcoI for Southern blotting (Figure 11). With the 5' *PPO* probe and the 3' *PPO* probe, a band of 11.6 kb was detected for the wild-type allele in all lanes. In most progeny plants of all three lines a band of 2 kb representing the gene targeting allele was detected with the 5'



*PPO* probe. With the 3' *PPO* probe, a band of 9.6 kb representing the gene targeting allele was only detected in line IV. The results showed that the plant lines III and V of *Atmre11* represented ectopic gene targeting (EGT) events, whereas plant IV represented a true gene targeting (TGT) event. All of the three plant lines had extra bands with the 3', the 5' and the *BAR* probe, and moreover, they were ppt-resistant, suggesting that they all contained extra T-DNA insertions. In principle, individual homozygous plants for the modified copy of the *PPO* locus would be segregated from the progenies in case of TGT. But it was strange that only the bands for T-DNA and 5' *PPO* segregated, and the bands for the wild-type *PPO* did not segregate.

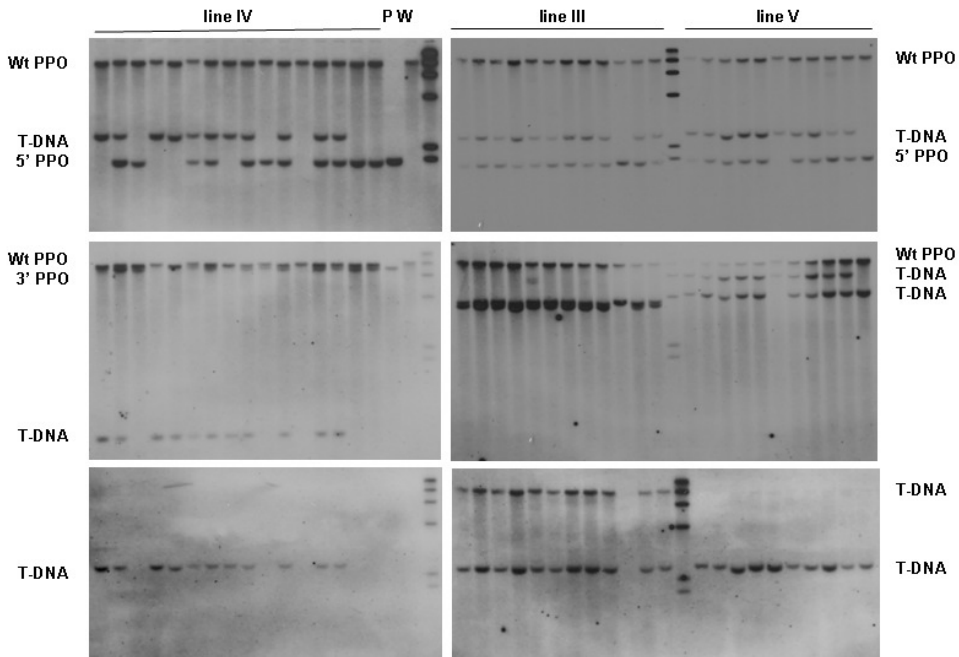


**Figure 11.** Gene targeting analysis of butafenacil resistant *Atmre11* lines.

Southern blot analysis was performed for progeny of the three individual plant lines (III, IV and V) of the *Atmre11* mutant. P is for positive control (*PPO* resistant plant) and W is for the wild-type. The probe used for the top panel is probe 5' *PPO*, the probe for the middle panel is probe 3' *PPO* and probe for the bottom panel is probe *Bar*. The sizes for the bands of the marker from the top to the bottom are as follows: 23130 kb, 9416 kb, 6557 kb, 4361 kb, 2322 kb, and 2027 kb.

## Discussion

Here, we isolated and characterized three *Arabidopsis thaliana* NHEJ mutants in which *AtKu80*, *AtKu70* and *AtLig4* were inactivated through a T-DNA insertion. The mouse is the only other multicellular organism in which the effects of inactivation of the *Ku80*, *Ku70* and *Lig4* genes have been studied in detail. Mice lacking *Ku80* or *Ku70* are fertile, but they show growth retardation and have immuno-deficiencies due to defects in V(D)J recombination.

Mice lacking Lig4 show late embryonic lethality associated with extensive apoptosis in the embryonic central nervous system (65-68). Yeasts and filamentous fungi with mutations in the NHEJ genes have no obvious growth phenotype (28;30;31;64;69). The *Arabidopsis thaliana* mutants homozygous for those mutations, which we obtained, showed no obvious growth phenotypes or sterility. Only the AtKu80 mutant showed a phenotype in which it differed from the wild-type, i.e. delayed germination. However, the NHEJ mutants all did show a clear hypersensitivity to the DNA damaging agent bleomycin. Thus, as in yeast and mammalian cells, *AtKu80*, *AtKu70* and *AtLig4* play a role in the repair of DNA damage, especially in DSBs repair. In mice, the *Ku80*, *Ku70* and *Lig4* genes are likewise involved in DNA damage repair; but here they may have additional functions that are necessary for normal development and may be involved in cell growth, DNA replication, G1-S transition and Bax mediated apoptosis (70-73). Lig4 was also found to play a role in apoptosis in mammalian cells (74). In plants and lower eukaryotes, *Ku80*, *Ku70* and *Lig4* genes may lack these additional functions and therefore show no phenotype under standard growth conditions. Three *Atmre11* mutants (ecotype Col-0) were also ordered by us from the Salk T-DNA collection (*Atmre11c-1*: SALK\_028450, *Atmre11c-2*: SALK\_0554418, *Atmre11c-3*: SALK\_067823). No homozygous mutant was obtained for the *Atmre11c-2* mutant. The homozygous *Atmre11c-1* and *Atmre11c-3* mutants were obtained. They were dwarf and sterile (data not shown), similar to the phenotype of the *Atmre11-1* mutant (ecotype Ws) described by Bundock *et al.* (9). Since no seeds were obtained from these *Atmre11* mutants (ecotype Col-0), no further analysis was done with these mutants. Therefore the *Atmre11* (ecotype Ws) mutant that was previously isolated was used for gene targeting experiments.

We have tested the role of *AtKu80*, *AtKu70* and *AtLig4* genes in DNA repair in *Arabidopsis thaliana* (ecotype Col-0) by comparing the response of the T-DNA insertion mutants and the wild-type to treatment with the DNA-damaging agents, bleomycin and MMS. The NHEJ mutants turned out to be hypersensitive to bleomycin. The *Atku70* and *Atlig4* mutants are also sensitive to MMS. Similar phenotypes have been observed for *Arabidopsis* (ecotype Ws) deficient in *AtKu80* (46), *AtKu70* (41) and *AtLig4* (43). *Atku80*, *Atku70* and *Atlig4* seedlings seem to be more sensitive to bleomycin than to MMS compared to wild-type plants. Bleomycin is a radiomimetic drug that will induce predominantly DSBs, whereas MMS is a methylating agent that will cause abasic sites and SSBs, that may be converted to DSBs during DNA replication in S phase (75). This indicated that *AtKu80*, *AtKu70* and *AtLig4* genes may play a more important role in DSBs repair than SSBs repair in plants. Previously, it was found that a *Atlig4* mutant is less sensitive to MMS than to X-rays, which also induces mainly DSBs (43). These results confirmed that Ku80, Ku70 and Lig4 all play a role in the repair of DSBs by NHEJ in plants, as they do in yeast and mammalian cells.

It has been reported that Ku80 and Ku70 need to be heterodimerized as a ring to bind DNA ends and repair DNA damage (11;76). We showed that dimerization is necessary for stabilization of the heterodimer. Therefore, the *Atku80* and *Atku70* mutants are expected to have similar phenotypes. However, *Atku70* plants seem to be more sensitive to bleomycin

than *Atku80* plants (Figure 6). It was also reported that there are some differences in the phenotype of *Ku70*- and *Ku80*-knockout mice (77). One recent report showed that deleting *Ku70* had milder effects than deleting *Ku80* in p53-mutant mice. The authors suggested that *Ku80* may function outside the *Ku* heterodimer to suppress cancer caused by translocation in mice (78). In plants, *Ku70* and *Ku80* may also have additional functions besides their role as *Ku* heterodimer in NHEJ. Since the T-DNA is inserted in the very end of the *AtKu80* gene in the *Atku80* mutant, it is possible that a small amount of truncated *Ku80* remaining in the *Atku80* mutant heterodimerized with *Ku70* to promote DNA end joining. We investigated the RNA expression of *AtKu80* in the *Atku80* mutant by RT-PCR using primers located in the N-terminal part of the coding region before the T-DNA insertion site. The results showed that there are products detectable (data not shown). Possibly a truncated protein, which still may retain partial function, is produced at low level causing the *Atku80* mutant to stand stress better than the *Atku70* mutant. Western blot was performed using the antibody that in principle could detect a C-terminal truncated *Ku80* protein. But no *Ku80*-related bands with a smaller MW were detectable on the western blot, indicating that no truncated protein was produced or that the amount was too low for detection. Alternatively, the presence of the complete or partial mRNAs may have a regulatory role in the plant cell.

Double strand break repair mechanisms are hypothesized to control the integration of *Agrobacterium* T-DNA in plants. In yeast non-homologous T-DNA is integrated by NHEJ (27), but the results obtained in plants so far are variable (43;45;59;62). In order to test whether *AtKu80*, *AtKu70* and *AtLig4* are involved in T-DNA integration, we performed root transformation assays and floral dip transformation and calculated the transformation frequency. The results of floral dip transformation showed that the transformation frequency is highly reduced in the *Atku70* and *Atku80* mutants. However, the results of root transformation showed that the NHEJ mutants have similar transformation frequency compared to the wild-type. Thus T-DNA integration occurs equally well in root cells of the wild-type and the NHEJ mutants. Li *et al.* (2005) also performed root transformation assays and they found that *Ku80*-deficient mutants have fewer tumors than wild-type plants (45). It could be that calli induced on the wound site of roots are derived from multiple cells and that high transformation frequencies mask differences between wild-type plants and mutants in our experiments. Previously, our group has shown the essential role of NHEJ proteins including the *Ku70/Ku80* complex and *Lig4* in T-DNA integration in the yeast *S.cerevisiae* (27;28). The *AtLig4* gene was not required for efficient integration of *Agrobacterium* T-DNA (ecotype Ws) (43). Recently, Windhofer *et al.* (2007) showed that low levels of DNA Ligase III and IV are sufficient for effective NHEJ in mammal cells (79). Plants may have similar mechanisms. When *AtLig4* is deficient, another DNA ligase of plants (such as DNA ligase I or VI) may take over the function of *AtLig4* in T-DNA integration.

Although the efficiencies of T-DNA integration in the *Atku70* and *Atku80* mutants are highly reduced, random T-DNA integration still occurs in these mutants. In addition, the frequency of gene targeting was not increased in these NHEJ mutants. In yeast and fungi,

the frequency of gene targeting was increased dramatically in absence of NHEJ components, such as Ku70/Ku80, Lig4, Mre11, Rad50, Xrs2 (28;29;31;63;64). It could be that C-NHEJ is the only NHEJ pathway in lower eukaryotes, whereas there must be one or several back-up NHEJ (B-NHEJ) pathways in plants. When C-NHEJ is blocked, the back-up pathways are still robust to take the function of DNA repair. Deficiency of AtMre11 resulted in an increase in gene targeting, suggesting the MRN complex could function at the initial step of end joining and be involved not only in C-NHEJ, but also in other pathways. We will explore B-NHEJ further in the future.

### Acknowledgements

Amke den Dulk-Ras, Joy Ramdjielal, Vanessa Costa and Tiia Husso for their technical assistance with the characterization of mutants and gene targeting events. This work was supported by the Chinese Scholarship Council (CSC) (QJ).

### Reference List

1. Bleuyard, J.Y., Gallego, M.E. and White, C.I. (2006) Recent advances in understanding of the DNA double-strand break repair machinery of plants. *DNA Repair (Amst)*, **5**, 1-12.
2. Branzei, D. and Foiani, M. (2008) Regulation of DNA repair throughout the cell cycle. *Nat. Rev. Mol. Cell Biol.*, **9**, 297-308.
3. Mahaney, B.L., Meek, K. and Lees-Miller, S.P. (2009) Repair of ionizing radiation-induced DNA double-strand breaks by non-homologous end-joining. *Biochem. J.*, **417**, 639-650.
4. Yano, K., Morotomi-Yano, K., Adachi, N. and Akiyama, H. (2009) Molecular mechanism of protein assembly on DNA double-strand breaks in the non-homologous end-joining pathway. *J. Radiat. Res. (Tokyo)*, **50**, 97-108.
5. Lieber, M.R. (1999) The biochemistry and biological significance of nonhomologous DNA end joining: an essential repair process in multicellular eukaryotes. *Genes Cells*, **4**, 77-85.
6. Helleday, T., Lo, J., van, G. and Engelward, B.P. (2007) DNA double-strand break repair: from mechanistic understanding to cancer treatment. *DNA Repair (Amst)*, **6**, 923-935.
7. Shrivastav, M., De Haro, L.P. and Nickoloff, J.A. (2008) Regulation of DNA double-strand break repair pathway choice. *Cell Res.*, **18**, 134-147.
8. Lamarche, B.J., Orazio, N.I. and Weitzman, M.D. (2010) The MRN complex in double-strand break repair and telomere maintenance. *FEBS Lett.*, **584**, 3682-3695.
9. Bundock, P. and Hooykaas, P. (2002) Severe developmental defects, hypersensitivity to DNA-damaging agents, and lengthened telomeres in Arabidopsis MRE11 mutants. *Plant Cell*, **14**, 2451-2462.
10. Critchlow, S.E. and Jackson, S.P. (1998) DNA end-joining: from yeast to man. *Trends Biochem. Sci.*, **23**, 394-398.
11. Lieber, M.R. (2008) The mechanism of human nonhomologous DNA end joining. *J. Biol. Chem.*, **283**, 1-5.
12. Koike, M. (2002) Dimerization, translocation and localization of Ku70 and Ku80 proteins. *J. Radiat. Res. (Tokyo)*, **43**, 223-236.
13. Muller, C., Paupert, J., Monferran, S. and Salles, B. (2005) The double life of the Ku protein: facing the DNA breaks and the extracellular environment. *Cell Cycle*, **4**, 438-441.

14. Koike,M. and Koike,A. (2005) The Ku70-binding site of Ku80 is required for the stabilization of Ku70 in the cytoplasm, for the nuclear translocation of Ku80, and for Ku80-dependent DNA repair. *Exp. Cell Res.*, **305**, 266-276.
15. Seluanov,A., Danek,J., Hause,N. and Gorbunova,V. (2007) Changes in the level and distribution of Ku proteins during cellular senescence. *DNA Repair (Amst)*, **6**, 1740-1748.
16. West,R.B., Yaneva,M. and Lieber,M.R. (1998) Productive and nonproductive complexes of Ku and DNA-dependent protein kinase at DNA termini. *Mol. Cell Biol.*, **18**, 5908-5920.
17. Meek,K., Douglas,P., Cui,X., Ding,Q. and Lees-Miller,S.P. (2007) trans Autophosphorylation at DNA-dependent protein kinase's two major autophosphorylation site clusters facilitates end processing but not end joining. *Mol. Cell Biol.*, **27**, 3881-3890.
18. Uematsu,N., Weterings,E., Yano,K., Morotomi-Yano,K., Jakob,B., Taucher-Scholz,G., Mari,P.O., van Gent,D.C., Chen,B.P. and Chen,D.J. (2007) Autophosphorylation of DNA-PKCS regulates its dynamics at DNA double-strand breaks. *J. Cell Biol.*, **177**, 219-229.
19. Nick McElhinny,S.A., Snowden,C.M., McCarville,J. and Ramsden,D.A. (2000) Ku recruits the XRCC4-ligase IV complex to DNA ends. *Mol. Cell Biol.*, **20**, 2996-3003.
20. Costantini,S., Woodbine,L., Andreoli,L., Jeggo,P.A. and Vindigni,A. (2007) Interaction of the Ku heterodimer with the DNA ligase IV/Xrcc4 complex and its regulation by DNA-PK. *DNA Repair (Amst)*, **6**, 712-722.
21. Wu,P.Y., Frit,P., Malivert,L., Revy,P., Biard,D., Salles,B. and Calsou,P. (2007) Interplay between Cernunnos-XLF and nonhomologous end-joining proteins at DNA ends in the cell. *J. Biol. Chem.*, **282**, 31937-31943.
22. Critchlow,S.E., Bowater,R.P. and Jackson,S.P. (1997) Mammalian DNA double-strand break repair protein XRCC4 interacts with DNA ligase IV. *Curr. Biol.*, **7**, 588-598.
23. Ma,Y., Lu,H., Tippin,B., Goodman,M.F., Shimazaki,N., Koiwai,O., Hsieh,C.L., Schwarz,K. and Lieber,M.R. (2004) A biochemically defined system for mammalian nonhomologous DNA end joining. *Mol. Cell*, **16**, 701-713.
24. Mahajan,K.N., Nick McElhinny,S.A., Mitchell,B.S. and Ramsden,D.A. (2002) Association of DNA polymerase mu (pol mu) with Ku and ligase IV: role for pol mu in end-joining double-strand break repair. *Mol. Cell Biol.*, **22**, 5194-5202.
25. Tsai,C.J., Kim,S.A. and Chu,G. (2007) Cernunnos/XLF promotes the ligation of mismatched and noncohesive DNA ends. *Proc. Natl. Acad. Sci. U. S. A.*, **104**, 7851-7856.
26. Wang,H., Perrault,A.R., Takeda,Y., Qin,W., Wang,H. and Iliakis,G. (2003) Biochemical evidence for Ku-independent backup pathways of NHEJ. *Nucleic Acids Res.*, **31**, 5377-5388.
27. van Attikum,H., Bundock,P. and Hooykaas,P.J.J. (2001) Non-homologous end-joining proteins are required for *Agrobacterium* T-DNA integration. *EMBO J.*, **20**, 6550-6558.
28. van Attikum,H. and Hooykaas,P.J.J. (2003) Genetic requirements for the targeted integration of *Agrobacterium* T-DNA in *Saccharomyces cerevisiae*. *Nucleic Acids Res.*, **31**, 826-832.
29. Kooistra,R., Hooykaas,P.J. and Steensma,H.Y. (2004) Efficient gene targeting in *Kluyveromyces lactis*. *Yeast*, **21**, 781-792.
30. Krappmann,S., Sasse,C. and Braus,G.H. (2006) Gene targeting in *Aspergillus fumigatus* by homologous recombination is facilitated in a nonhomologous end- joining-deficient genetic background. *Eukaryot. Cell*, **5**, 212-215.
31. Meyer,V., Arentshorst,M., El-Ghezal,A., Drews,A.C., Kooistra,R., van den Hondel,C.A. and Ram,A.F. (2007) Highly efficient gene targeting in the *Aspergillus niger* kusa mutant. *J. Biotechnol.*, **128**, 770-775.

32. Hanin,M., Volrath,S., Bogucki,A., Briker,M., Ward,E. and Paszkowski,J. (2001) Gene targeting in Arabidopsis. *Plant J.*, **28**, 671-677.
33. Halfter,U., Morris,P.C. and Willmitzer,L. (1992) Gene targeting in *Arabidopsis thaliana*. *Mol. Gen. Genet.*, **231**, 186-193.
34. de Pater,S., Neuteboom,L.W., Pinas,J.E., Hooykaas,P.J. and van der Zaal,B.J. (2009) ZFN-induced mutagenesis and gene-targeting in Arabidopsis through *Agrobacterium*-mediated floral dip transformation. *Plant Biotechnol. J.*, **7**, 821-835.
35. Hroudá,M. and Paszkowski,J. (1994) High fidelity extrachromosomal recombination and gene targeting in plants. *Mol. Gen. Genet.*, **243**, 106-111.
36. Lee,K.Y., Lund,P., Lowe,K. and Dunsmuir,P. (1990) Homologous recombination in plant cells after *Agrobacterium*-mediated transformation. *Plant Cell*, **2**, 415-425.
37. Miao,Z.H. and Lam,E. (1995) Targeted disruption of the TGA3 locus in *Arabidopsis thaliana*. *Plant J.*, **7**, 359-365.
38. Offringa,R., de Groot,M.J., Haagsman,H.J., Does,M.P., van den Elzen,P.J. and Hooykaas,P.J. (1990) Extrachromosomal homologous recombination and gene targeting in plant cells after *Agrobacterium* mediated transformation. *EMBO J.*, **9**, 3077-3084.
39. Paszkowski,J., Baur,M., Bogucki,A. and Potrykus,I. (1988) Gene targeting in plants. *EMBO J.*, **7**, 4021-4026.
40. Risseeuw,E., Offringa,R., Franke-van Dijk,M.E. and Hooykaas,P.J. (1995) Targeted recombination in plants using *Agrobacterium* coincides with additional rearrangements at the target locus. *Plant J.*, **7**, 109-119.
41. Bundock,P., van Attikum,H. and Hooykaas,P.J.J. (2002) Increased telomere length and hypersensitivity to DNA damaging agents in an Arabidopsis KU70 mutant. *Nucleic Acids Res.*, **30**, 3395-3400.
42. Tamura,K., Adachi,Y., Chiba,K., Oguchi,K. and Takahashi,H. (2002) Identification of Ku70 and Ku80 homologues in *Arabidopsis thaliana*: evidence for a role in the repair of DNA double-strand breaks. *Plant J.*, **29**, 771-781.
43. van Attikum,H., Bundock,P., Overmeer,R.M., Lee,L.Y., Gelvin,S.B. and Hooykaas,P.J.J. (2003) The Arabidopsis AtLIG4 gene is required for the repair of DNA damage, but not for the integration of *Agrobacterium* T-DNA. *Nucleic Acids Res.*, **31**, 4247-4255.
44. West,C.E., Waterworth,W.M., Jiang,Q. and Bray,C.M. (2000) Arabidopsis DNA ligase IV is induced by gamma-irradiation and interacts with an Arabidopsis homologue of the double strand break repair protein XRCC4. *Plant J.*, **24**, 67-78.
45. Li,J., Vaidya,M., White,C., Vainstein,A., Citovsky,V. and Tzfira,T. (2005) Involvement of KU80 in T-DNA integration in plant cells. *Proc. Natl. Acad. Sci. U. S. A.*, **102**, 19231-19236.
46. West,C.E., Waterworth,W.M., Story,G.W., Sunderland,P.A., Jiang,Q. and Bray,C.M. (2002) Disruption of the Arabidopsis AtKu80 gene demonstrates an essential role for AtKu80 protein in efficient repair of DNA double-strand breaks in vivo. *Plant J.*, **31**, 517-528.
47. Alonso,J.M., Stepanova,A.N., Lisse,T.J., Kim,C.J., Chen,H., Shinn,P., Stevenson,D.K., Zimmerman,J., Barajas,P., Cheuk,R. *et al.* (2003) Genome-wide insertional mutagenesis of *Arabidopsis thaliana*. *Science*, **301**, 653-657.
48. de Pater,S., Caspers,M., Kottenhagen,M., Meima,H., ter Stege,R. and de Vetten,N. (2006) Manipulation of starch granule size distribution in potato tubers by modulation of plastid division. *Plant Biotechnol. J.*, **4**, 123-134.
49. Laemmli,U.K. (1970) Cleavage of structural proteins during the assembly of the head of bacteriophage T4. *Nature*, **227**, 680-685.
50. Weijers,D., Franke-van,D.M., Vencken,R.J., Quint,A., Hooykaas,P. and Offringa,R. (2001) An Arabidopsis Minute-like phenotype caused by a semi-dominant mutation in a RIBOSOMAL PROTEIN S5 gene. *Development*, **128**, 4289-4299.



51. Murashige, T. and Skoog, F. (1962) A Revised Medium for Rapid Growth and Bio Assays with Tobacco Tissue Cultures. *Physiologia Plantarum*, **15**, 473-497.
52. Menke, M., Chen, I., Angelis, K.J. and Schubert, I. (2001) DNA damage and repair in *Arabidopsis thaliana* as measured by the comet assay after treatment with different classes of genotoxins. *Mutat. Res.*, **493**, 87-93.
53. Wang, S., Tiwari, S.B., Hagen, G. and Guilfoyle, T.J. (2005) AUXIN RESPONSE FACTOR7 restores the expression of auxin-responsive genes in mutant *Arabidopsis* leaf mesophyll protoplasts. *Plant Cell*, **17**, 1979-1993.
54. Nam, J., Mysore, K.S., Zheng, C., Knue, M.K., Matthyse, A.G. and Gelvin, S.B. (1999) Identification of T-DNA tagged *Arabidopsis* mutants that are resistant to transformation by *Agrobacterium*. *Mol. Gen. Genet.*, **261**, 429-438.
55. Bravo-Angel, A.M., Hohn, B. and Tinland, B. (1998) The omega sequence of VirD2 is important but not essential for efficient transfer of T-DNA by *Agrobacterium tumefaciens*. *Mol. Plant Microbe Interact.*, **11**, 57-63.
56. Clough, S.J. and Bent, A.F. (1998) Floral dip: a simplified method for *Agrobacterium*-mediated transformation of *Arabidopsis thaliana*. *Plant J.*, **16**, 735-743.
57. Masson, J. and Paszkowski, J. (1992) The Culture Response of *Arabidopsis-Thaliana* Protoplasts Is Determined by the Growth-Conditions of Donor Plants. *Plant Journal*, **2**, 829-833.
58. Koike, M., Shiomi, T. and Koike, A. (2001) Dimerization and nuclear localization of ku proteins. *J. Biol. Chem.*, **276**, 11167-11173.
59. Friesner, J. and Britt, A.B. (2003) Ku80- and DNA ligase IV-deficient plants are sensitive to ionizing radiation and defective in T-DNA integration. *Plant J.*, **34**, 427-440.
60. Burger, R.M., Peisach, J. and Horwitz, S.B. (1981) Activated bleomycin. A transient complex of drug, iron, and oxygen that degrades DNA. *J. Biol. Chem.*, **256**, 11636-11644.
61. O'Connor, P.J. (1981) Interaction of chemical carcinogens with macromolecules. *J. Cancer Res. Clin. Oncol.*, **99**, 167-186.
62. Gallego, M.E., Bleuyard, J.Y., Daoudal-Cotterell, S., Jallut, N. and White, C.I. (2003) Ku80 plays a role in non-homologous recombination but is not required for T-DNA integration in *Arabidopsis*. *Plant J.*, **35**, 557-565.
63. Ninomiya, Y., Suzuki, K., Ishii, C. and Inoue, H. (2004) Highly efficient gene replacements in *Neurospora* strains deficient for nonhomologous end-joining. *Proc. Natl. Acad. Sci. U. S. A.*, **101**, 12248-12253.
64. Nielsen, J.B., Nielsen, M.L. and Mortensen, U.H. (2008) Transient disruption of non-homologous end-joining facilitates targeted genome manipulations in the filamentous fungus *Aspergillus nidulans*. *Fungal Genet. Biol.*, **45**, 165-170.
65. Nussenzweig, A., Sokol, K., Burgman, P., Li, L. and Li, G.C. (1997) Hypersensitivity of Ku80-deficient cell lines and mice to DNA damage: the effects of ionizing radiation on growth, survival, and development. *Proc. Natl. Acad. Sci. U. S. A.*, **94**, 13588-13593.
66. Gu, Y., Seidl, K.J., Rathbun, G.A., Zhu, C., Manis, J.P., van der, S.N., Davidson, L., Cheng, H.L., Sekiguchi, J.M., Frank, K. *et al.* (1997) Growth retardation and leaky SCID phenotype of Ku70-deficient mice. *Immunity*, **7**, 653-665.
67. Barnes, D.E., Stamp, G., Rosewell, I., Denzel, A. and Lindahl, T. (1998) Targeted disruption of the gene encoding DNA ligase IV leads to lethality in embryonic mice. *Curr. Biol.*, **8**, 1395-1398.
68. Hakem, R. (2008) DNA-damage repair; the good, the bad, and the ugly. *EMBO J.*, **27**, 589-605.
69. Schorsch, C., Kohler, T. and Boles, E. (2009) Knockout of the DNA ligase IV homolog gene in the sphingoid base producing yeast *Pichia ciferrii* significantly increases gene targeting efficiency. *Curr. Genet.*

70. Rampakakis,E., Di,P.D. and Zannis-Hadjopoulos,M. (2008) Ku is involved in cell growth, DNA replication and G1-S transition. *J. Cell Sci.*, **121**, 590-600.
71. Rathaus,M., Lerrer,B. and Cohen,H.Y. (2009) DeubiKuitylation: a novel DUB enzymatic activity for the DNA repair protein, Ku70. *Cell Cycle*, **8**, 1843-1852.
72. Lloret,M., Lara,P.C., Bordon,E., Fontes,F., Rey,A., Pinar,B. and Falcon,O. (2009) Major vault protein may affect nonhomologous end-joining repair and apoptosis through Ku70/80 and bax downregulation in cervical carcinoma tumors. *Int. J. Radiat. Oncol. Biol. Phys.*, **73**, 976-979.
73. Trougakos,I.P., Lourda,M., Antonelou,M.H., Kletsas,D., Gorgoulis,V.G., Papassideri,I.S., Zou,Y., Margaritis,L.H., Boothman,D.A. and Gonos,E.S. (2009) Intracellular clusterin inhibits mitochondrial apoptosis by suppressing p53-activating stress signals and stabilizing the cytosolic Ku70-Bax protein complex. *Clin. Cancer Res.*, **15**, 48-59.
74. Friesen,C., Uhl,M., Pannicke,U., Schwarz,K., Miltner,E. and Debatin,K.M. (2008) DNA-ligase IV and DNA-protein kinase play a critical role in deficient caspases activation in apoptosis-resistant cancer cells by using doxorubicin. *Mol. Biol. Cell*, **19**, 3283-3289.
75. Moore,J.D., Yazgan,O., Ataian,Y. and Krebs,J.E. (2007) Diverse roles for histone H2A modifications in DNA damage response pathways in yeast. *Genetics*, **176**, 15-25.
76. Walker,J.R., Corpina,R.A. and Goldberg,J. (2001) Structure of the Ku heterodimer bound to DNA and its implications for double-strand break repair. *Nature*, **412**, 607-614.
77. Featherstone,C. and Jackson,S.P. (1999) Ku, a DNA repair protein with multiple cellular functions? *Mutat. Res.*, **434**, 3-15.
78. Li,H., Choi,Y.J., Hanes,M.A., Marple,T., Vogel,H. and Hastay,P. (2009) Deleting Ku70 is milder than deleting Ku80 in p53-mutant mice and cells. *Oncogene*, **28**, 1875-1878.
79. Windhofer,F., Wu,W. and Iliakis,G. (2007) Low levels of DNA ligases III and IV sufficient for effective NHEJ. *J. Cell Physiol*, **213**, 475-483.



# Chapter 3

Poly(ADP-ribose) polymerase facilitating back-up non-homologous end joining via micro-homologous sequences in plants

Qi Jia, B. Sylvia de Pater and Paul J.J. Hooykaas

## Abstract

Poly(ADP-ribose) polymerase 1 (Parp1) and Parp2 are ADP-ribose transferases, which are involved in single strand break repair (SSBR), base excision repair (BER) and back-up NHEJ (B-NHEJ) in animals. In order to investigate if Parp has similar functions in plants, two *Arabidopsis* lines with a T-DNA insertion in *AtParp1* and *AtParp2* were functionally characterized. The homozygous mutants of *Atparp1*, *Atparp2* and *Atparp1parp2* (*Atp1p2*) were phenotypically indistinguishable from the wild-type under normal growth conditions. However, the *Atparp1* and *Atp1p2* mutants were hypersensitive to the genotoxic agent MMS, but not to bleomycin, suggesting that AtParp1 has an important role in SSB DNA repair. *AtParp2* was up-regulated in NHEJ mutants, suggesting that AtParp2 may also be involved in double strand break (DSB) repair. Indeed the capacity of DNA end joining was slightly reduced in *Atparp* mutants. In the *Atp1p2* double mutant a clear shift in end-joining was seen, utilizing significantly less micro-homology mediated end joining (MMEJ) than the wild-type. This indicates that AtParp1 and AtParp2 are functionally redundant and may cooperate in MMEJ. *Agrobacterium* mediated T-DNA transformation via floral dip was hardly affected in the *Atparp* mutants, indicating that the classical NHEJ (C-NHEJ) and/or other components play the major role in that process.

## Introduction

Poly(ADP-ribose) polymerases (Parps) are ADP-ribose transferases that transfer ADP-ribose (PAR) from NAD<sup>+</sup> to target proteins (1;2). There are eighteen known members identified in the superfamily by *in silico* homology searching in animals (3). They share a conserved catalytic domain and an active site formed by a highly conserved sequence. Parp proteins have a major impact on various cellular processes, such as cell death, transcription, cell division, DNA repair and telomere integrity, via poly(ADP-ribosyl)ation (4). Only two of them are activated in response to DNA damage: Parp1 (113 kDa) and Parp2 (62 kDa) (5). Parp1 is involved in DNA single strand break repair (SSBR) and base excision repair (BER), preventing the formation of DNA double strand breaks (DSBs) (6-8). Parp can also attract Mre11 to sites of DNA damage to repair (9;10). Some reports also suggested that when the DNA-PK dependent classical non-homologous end joining (C-NHEJ) pathway is deficient, Parp together with Lig3 plays a role in DSB repair via back-up non-homologous end joining (B-NHEJ) (11-14). This alternative NHEJ pathway preferentially utilizes micro-homology for repair, and therefore has been called micro-homology mediated end joining (MMEJ).

Homologues of Parp1 and Parp2 have been identified in plants (15). One is the classical zinc finger containing polymerase (ZAP), which was first purified from maize seedlings and has a molecular mass of 113 kDa (16). It was also identified in *Arabidopsis*. ZAP has high similarity in the sequence and domain organization to Parp1 in animals (15). The other one

is a structurally non-classical Parp protein, called APP in Arabidopsis and NAP in *Zea mays* (17). It is a short version of Parp with the molecular mass of 72 kDa. The counterpart of it in animals has also been identified and was termed Parp2 (18). Since APP was identified earlier than ZAP in Arabidopsis, some people termed APP as Parp1 and ZAP as Parp2. Considering the similarity to the corresponding homologues in animals and avoiding confusion, in this chapter ZAP was termed as Parp1 and APP as Parp2. Many former reports on Parp1 and Parp2 in plants provide evidence for the function of Parp in stress tolerance and in the control of programmed cell death (19-21). As mentioned above, Parp1 and Parp2 take an important role in DNA repair in animals (4;5), whereas in plants this is still largely unknown. Parp1 and Parp2 are localized in the nucleus and are activated by DNA damage, hinting that they could also be involved in DNA repair in plants (15;22;23). In order to investigate the function of Parp proteins in DNA repair, two Col-0 Arabidopsis lines containing a T-DNA insertion in *AtParp1* or *AtParp2* genes were characterized here. The homozygous mutants of *Atparp1* and *Atparp2* were isolated and crossed with each other to obtain the homozygous double mutant of *Atparp1parp2* (*Atp1p2*). The single and double mutants were analyzed for the sensitivity to DNA damaging agents and the capacity for DNA end joining. How absence of the AtParp proteins affected *Agrobacterium*-mediated T-DNA integration via floral dip was also tested.

## Material and methods

### Plant material

*Atparp1* and *Atparp2* T-DNA insertion lines were obtained from the GABI-Kat T-DNA collection (GABI-Kat Line 692A05) or the SALK T-DNA collection (SALK\_640400), respectively. Information about them is available at <http://signal.salk.edu/cgi-bin/tdnaexpress> (24). The homozygotes of the *Atparp1* and *Atparp2* mutants were isolated. They were crossed to get the *Atparp1parp2* (*Atp1p2*) double mutant.

### Characterization of the *Atparp1* and *Atparp2* mutants

DNA was extracted from individual plants using the CTAB DNA isolation protocol (25). The T-DNA insertion sites of the mutants were mapped with a gene-specific primer (Sp167 or Sp168 for *Atparp1*, Sp219 or Sp222 for *Atparp2*) and a T-DNA specific primer (LBb1 or Sp173 for Left Border (LB), Sp200 for Right Border (RB)). PCR products were sequenced. Pairs of gene-specific primers around the insertion site were used to determine whether the plants were homozygous or heterozygous for the T-DNA insertion. The sequences of all the primers are listed in Table 1. For Southern blot analysis, DNA from the *Atparp1* mutant was digested with EcoRV or BglII, and DNA from the *Atparp2* mutant was digested with HindIII. DNA (5 µg) was ran on a 0.7% agarose gel and transferred onto positively charged Hybond-N membrane (Amersham Biosciences). The hybridization and detection procedures were done according to the DIG protocol from Roche Applied Sciences. The

DIG probe was produced using the PCR DIG Labeling Mix (Roche) with specific primers for each T-DNA (*Atparp1* (pGABI): Sp225 and Sp226; *Atparp2* (pROK2): pROK2 and Sp250).

**Table 1.** Sequences of primers used for characterization of T-DNA insertion lines and Q-PCR.

Name	Locus	Sequence
LBb1	T-DNA LB	5'-GCGTGGACCGCTTGCTGCAACT-3'
Sp173	T-DNA LB	5'-CCCATTTGGACGTGAATGTAGACAC-3'
Sp200	T-DNA RB	5'-GCTTGGCTGCAGGTCCGAC-3'
Sp167	<i>AtParp1</i>	5'-CATTGACGGAGATACAGAGG-3'
Sp168	<i>AtParp1</i>	5'-GGTGCAATTCTCAGTCCTTG-3'
Sp219	<i>AtParp2</i>	5'-GATGGGGAAGAGTTGGTGTG-3'
Sp222	<i>AtParp2</i>	5'-GAGTGTCTATAACAACTGGC-3'
pROK2	pROK2 probe	5'-GCGGACGTTTTTAATGTACTGGGG-3'
Sp250	pROK2 probe	5'-GGGAATGCAGTCACCTCTAT-3'
Sp225	pGABI1 probe	5'-AAATGTAGATGTCCGCAGCG-3'
Sp226	pGABI1 probe	5'-AGACGTGACGTAAGTATCCG-3'
Sp207	<i>AtKu80</i>	5'-GCGTCTTGGAGCAGGTCTCTTC-3'
Sp208	<i>AtKu80</i>	5'-GATGAAATCCCCAGCGTTCTCG-3'
q1	<i>AtKu70</i>	5'-TCTACCACTCAGTCAACCTG-3'
q2	<i>AtKu70</i>	5'-CAATAGACAAGCCATCACAG-3'
q6	<i>AtLig4</i>	5'-GACACCAACGGCACAAG-3'
q7	<i>AtLig4</i>	5'-AAGTTCAATGTATGTCAGTCCC-3'
Sp211	<i>AtParp1</i>	5'-CTCCACTCTGTATGCGTTGGG-3'
Sp212	<i>AtParp1</i>	5'-CCCTTCTATTCATCCTCATATATCCG-3'
Sp243	<i>AtParp2</i>	5'-CTCGGCAAGATAAGCAAGTCC-3'
Sp213	<i>AtXRCC1</i>	5'-CTTCACTACACGAGGGACAAAGC-3'
Sp214	<i>AtXRCC1</i>	5'-CAGAAACAAGGGGAACACCATCTACC-3'
Roc5.2	<i>Roc1</i>	5'-GAACGGAACAGGCGGTGAGTC-3'
Roc3.3	<i>Roc1</i>	5'-CCACAGGCTTCGTCCGCTTTC-3'
q8	BamHI	5'-GTGACATCTCCACTGACGTAAG-3'
q9	BamHI	5'-GATGAACTTCAGGGTCAGCTTG-3'
q10	GFP	5'-CAAGCTGACCCTGAAGTTCATC-3'
q11	GFP	5'-GTTGTGGCGGATCTTGAAG-3'
q30	pUC18P1/4	5'-GTTTCGGTGATGACGGTG-3'
q31	pUC18P1/4	5'-TGGCACGACAGGTTTCC-3'
q40	pUC18P1/4	5'-GCTGTAGGATGGTAGCTTGGCAC-3'
q41	pUC18P1/4	5'-ATCCTACAGCTGGAATTCGTAATC-3'

### Quantitative reverse-transcription PCR (Q-RT-PCR)

Leaves of 2-week-old wild-type (ecotype Columbia-0), *Atparp1*, *Atparp2*, *Atku80*, *Atku70* and *Atlig4* plants (chapter 2) were ground under liquid N<sub>2</sub> in a Tissue-Lyser (Retch). Total RNA was extracted from the leaf powder using the RNeasy kit (Qiagen) according to the supplied protocol. Residual DNA was removed from the RNA samples with DNaseI (Ambion) in the presence of RNase inhibitor (Promega). RNA was quantified and 1 µg of RNA was used to make cDNA templates using the iScript cDNA synthesis kit according to the manufacturer's instructions (Bio-Rad). Quantitative real-time PCR (Q-PCR) analyses were done using the iQ™ SYBR® Green Supermix (Bio-Rad). Specific fragments (about 200 bp) were amplified with pairs of primers around the T-DNA insertion sites using a DNA Engine Thermal Cycler (MJ Research) equipped with a Chromo4 real-time PCR detection system (Bio-Rad). The sequences of the primers are listed in Table 1. The cycling parameters were 95°C for 3 min, 40 cycles of (95°C for 1 min, 60°C for 40 s), 72°C for 10 min. All sample values were normalized to the values of the house keeping gene *Roc1* (primers Roc5.2, Roc3.3) and were presented as relative expression ratios. The value of the Col-0 wild-type was set on 1.

### Assays for sensitivity to bleomycin and methyl methane sulfonate (MMS)

Seeds of wild-type, *Atparp1*, *Atparp2*, and *Atp1p2* plants were surface-sterilized as described (26) and germinated on solid ½ MS medium. Four days after germination, the seedlings were transferred to liquid ½ MS medium without additions or ½ MS medium containing 0.2 µg/ml and 0.4 µg/ml Bleocin™ (Calbiochem), 0.007% and 0.01% (v/v) MMS (Sigma) and scored after 2 weeks. Fresh weight (compared with controls) was determined by weighing the seedlings in batches of 20 in triplicate, which were treated in 0%, 0.006%, 0.008% and 0.01% (v/v) MMS for 2 weeks.

### Comet assay

1-week-old seedlings were treated in liquid ½ MS containing 0.01% MMS for 0 h, 2 h and 24 h. Some seedlings with 24 h treatment were recovered in liquid ½ MS for another 24 h. DNA damage was detected by comet assays as described previously (27) with minor modifications. Since MMS mostly causes SSBs, DNA was exposed to high alkali prior to electrophoresis under neutral conditions (A/N protocol) to detect DNA SSBs preferentially. Plant nuclei were embedded in 1% low melting point Ultrapure™ agarose-1000 (Invitrogen) to make a mini gel on microscopic slides according to the protocol. Nuclei were subjected to lysis in high alkali (0.3 M NaOH, 5 mM EDTA pH13.5) for 20 min at room temperature (A/N protocol). Equilibration for 3 times 5 min in TBE buffer (90 mM Tris-borate, 2 mM EDTA, pH8.4) on ice was followed by electrophoresis at 4°C (cold room) in TBE buffer for 15 min at 30 V (1 V/cm), 15-17 mA. Dry agarose gels were stained with 15 µl ethidium bromide (5 µg/ml) and immediately evaluated with a Zeiss Axioplan 2 imaging fluorescence microscope (Zeiss, Germany) using the DsRed channel (excitation at 510

nm, emission at 595 nm). Images of comets were captured at a 40-fold magnification by an AxioCam MRc5 digital camera (Zeiss, Germany). The comet analysis was carried out by comet scoring software CometScore™ (Tritek Corporation). The fraction of DNA in comet tails (%tail-DNA) was used as a measure of DNA damage. Measures included 4 independent gel replicas totaling about 100 comets analyzed per experimental point. The results were presented by the mean value ( $\pm$ standard deviation = S.D.) from four gels, based on the median values of %tail-DNA of 25 individual comets per gel. The student's t-test was used to test for significant difference compared to the wild-type with the same treatment.

### **Histochemical GUS analysis**

The NHEJ mutants previously described (chapter 2) (*Atku80*, *Atku70* and *Atlig4*) were crossed with *AtParp2:GUS* reporter plants (15;28), which were kindly provided by De Veylder (Gent, Belgium). Ten-day-old seedlings were treated with 0 or 0.01% MMS for 2 h, followed by GUS staining as described previously (29). The GUS staining was examined under a Leica MZ12 microscope (Leica microsystems). Plants were photographed with a Leica DC 500 digital camera (Leica microsystems).

### **Isolation of Arabidopsis mesophyll protoplasts**

*Arabidopsis* was either grown in a greenhouse at 21°C (16 h photoperiod) or in a culture chamber (21°C, 50% relative humidity, 16 h photoperiod). Rosette leaves (~1 g) from plants that were 3 to 5 weeks old were collected, rinsed with deionized water and briefly dried. The leaves were cut into 0.5 to 1 mm strips with a razor blade, placed into a Petri dish containing 15 ml of filter-sterilized enzyme solution [1.5%(w/v) cellulose R10, 0.4%(w/v) macerozyme R10, 0.4 M mannitol, 20 mM KCl, 20 mM MES pH5.7, 10 mM CaCl<sub>2</sub>, 0.1%(w/v) BSA] and 2 to 3 h incubated in the dark at 28°C. Then the protoplasts were filtered with a 50  $\mu$ m mesh to remove the undigested material and transferred to a round bottom Falcon tube. The solution was centrifuged for 5 min at 600 rpm to pellet the protoplasts. The supernatant which contained broken cells was discarded. The protoplasts were gently washed twice with 15 ml cold W5 solution (154 mM NaCl, 125 mM CaCl<sub>2</sub>, 5 mM KCl, 2 mM MES pH5.7) and resuspended in cold W5 solution to a final concentration of  $2 \times 10^5$  cells/ml and kept on ice for 30 min. Just before starting transfection, protoplasts were collected from the W5 solution by centrifugation and were resuspended to a density of  $2 \times 10^5$  cells/ml in MMg solution (0.4 M mannitol, 15 mM MgCl<sub>2</sub>, 4 mM MES pH5.7) at room-temperature.

### **End joining assay**

Plasmid pART7-HA-GFP (S65T) was linearized by cleavage with BamHI (Figure1). Fresh protoplasts prepared from leaves were transformed with either linear or circular plasmid DNA by the polyethylene glycol (PEG) transformation protocol (30). In each experiment,  $2 \times 10^4$  protoplasts were transformed with 2  $\mu$ g of plasmid. Recircularization of the linear plasmid in

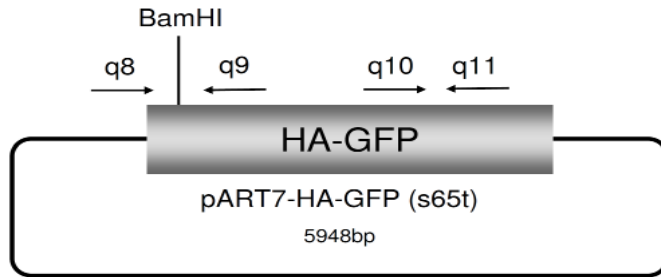


**Figure 1.** Schematic diagram of pART7-HA-GFP. The primers for Q-PCR are shown by arrows.

protoplasts by the NHEJ pathway was analyzed. DNA was extracted from protoplasts (at 0 h and 20 h) and was used to quantify rejoining by Q-PCR. The DNA extraction protocol and the cycling parameters of Q-PCR were the same as mentioned above. Two pairs of primers were used: one pair (q8+q9) was flanking both sites of the enzyme digestion site (BamHI); the other pair (q10+q11) was localized in GFP (Figure1). When the plasmid is circular, both pairs will give products. When the plasmid is cleaved by BamHI, the first pair of primers will not give a product, whereas the second will still give products. The efficiency of end joining is presented by the ratio of PCR products using q8+q9 primers and q10+q11 primers in comparison with the controls. The value of Col-0 wild-type was set on 1. Q-PCR was performed as three replicates and the assays were performed in triplicate. The PCR products with the primers of q8 and q9 were purified with QIAquick gel extraction kit (Qiagen), followed by cloning into pJET1.2/blunt Cloning Vector (CloneJET™ PCR Cloning Kit, Fermentas). Individual clones were first digested by BamHI. The clones resistant to the digestion of BamHI were sequenced by ServiceXS.

### MMEJ assay with active protein extract from leaves

Ten-day-old seedlings were ground under liquid N<sub>2</sub> in a Tissue-Lyser (Retch). One ml protein extraction buffer (50 mM Tris-HCl pH 7.5; 2 mM EDTA; 0.2 mM PMSF; 1 mM DTT; 1×Protease inhibitor cocktail Complete®, EDTA free) was added to 1 g of tissue powder. Soluble protein was isolated by centrifugation at 4°C. The protein concentration was determined using Bio-Rad protein assay reagent.

The DNA substrate (pUC18P1/4) for MMEJ was described and obtained from Liang et al (31;32). The construct can be cleaved with the restriction enzymes Eco47III and EcoRV to a 2.7 kb linear form with a 10 bp direct repeat (ATCCTACAGC) at both blunt ends (Figure2). Since it was hard to digest completely, the long linear DNA fragment was amplified by PCR with q40 and q41 primers.

According to the results from Liang et al. (31;32), high DNA/protein ratio was used for the high efficiency of end joining. The linear DNA substrates (300 ng) were incubated with 1 µg protein extract from leaves in 50 mM Tris-HCl (pH 7.6), 10mM MgCl<sub>2</sub>, 1mM dithiothreitol, 1 mM ATP and 25% (w/v) polyethylene glycol 2000 at 14 °C for 2 hour in a

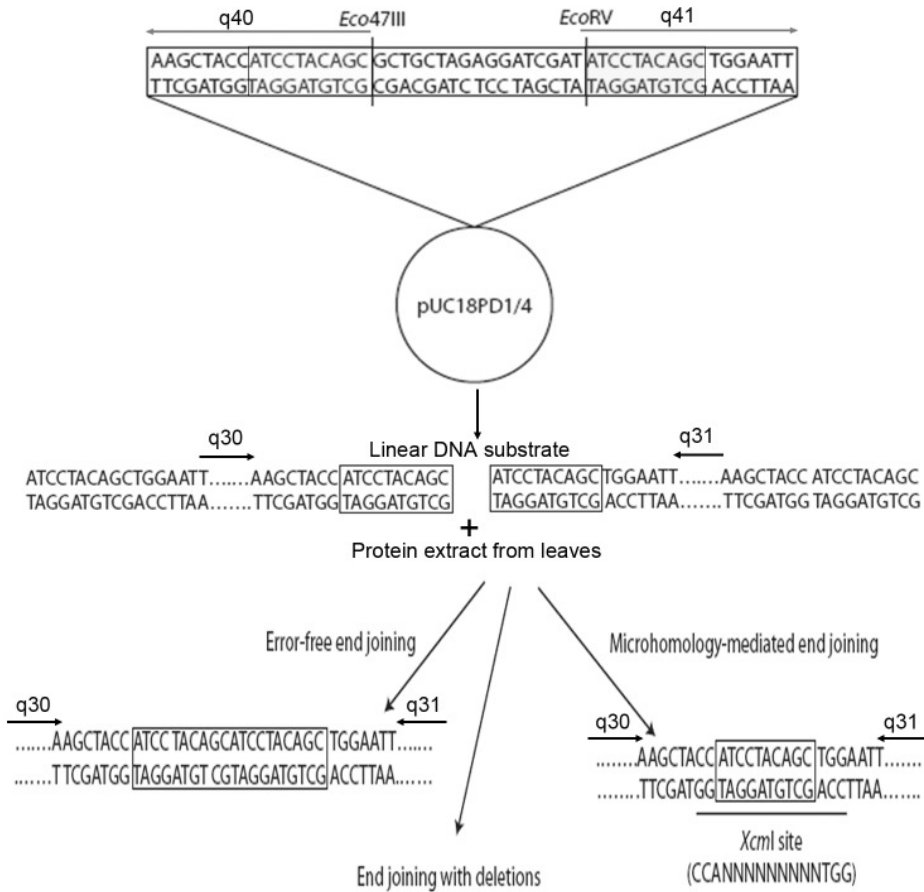


**Figure 2.** DNA substrates for MMEJ.

The plasmid PUC18PD1/4 has two 10 bp repeats around the digestion sites of Eco47III and EcoRV. The 2.7 kb linear fragment was PCR amplified with the primers (q40+q41). An XcmI restriction site will be generated after end joining via MMEJ. The primers are indicated by arrows.

volume of 20  $\mu$ l. DNA products were deproteinized and purified by electrophoresis through 0.6% agarose gels. A 600-bp fragment containing the end-joined junction was amplified by PCR with q30 and q31 primers flanking the junction. When end-joining had occurred via MMEJ using the 10 bp microhomology, an XcmI site (CCAN9TGG) was generated. PCR products were digested by XcmI, followed by electrophoresis on a 1.5% agarose gel. The presence of an XcmI site will result in a 400 bp and a 200 bp fragment. The intensity of DNA bands was quantified by using ImageJ software. The relative contribution of end-joining via the 10 bp repeat was calculated as the percentage of the XcmI-digested fragments of total PCR products (sum of the XcmI- digested and undigested fragments).

### Floral dip transformation

Floral dip transformation was performed according to the procedure described by Clough and Bent (33). The *Agrobacterium* strain AGL1 (pSDM3834) (34) was used for infection.



Plasmid pSDM3834 is a pCambia 1200 derivative (hpt selection marker). Seeds were harvested from the dry plants after maturation, surface-sterilized and plated on solid MA without sucrose containing 15 µg/ml hygromycin, 100 µg/ml timentin (to kill *Agrobacterium* cells) and 100 µg/ml nystatin (to prevent growth of fungi). Hygromycin-resistant seedlings were scored 2 weeks after germination and transformation frequency was determined (50 seeds is 1mg) (35).

## Results

### Isolation and characterization of the *Atparp1* and *Atparp2* mutants

Arabidopsis mutants with mutations in *Atparp1* and *Atparp2* were obtained from the GABI-Kat or Salk collection, respectively. We identified homozygous mutants by PCR harboring a T-DNA insertion for each gene in the next generation. When two gene-specific primers flanking the insertion site were used, PCR products were amplified for wild-type and heterozygotes. No PCR products were obtained for homozygous mutants by using these two gene-specific primers, because the PCR products in the mutant would be >10 kb in size and would be not detectable. When a T-DNA-specific primer from LB or RB was used in combination with one gene-specific primer, PCR products for the T-DNA insertion mutants were amplified, whereas no PCR products were obtained for the wild-type. The insertion point was mapped by sequencing of the PCR products generated using one of T-DNA specific primers in combination with one of the gene-specific primers. The combination of the primers for each gene is shown in the Figure 3. There were PCR products of LB and RB fragments for the *Atparp1* mutant and PCR products of two LB fragments for the *Atparp2* mutant, indicating that one T-DNA was inserted in the *AtParp1* locus and at least 2 T-DNA copies were inserted as an inverted repeat in the *AtParp2* locus. Sequencing results indicated that the T-DNAs were all inserted at the position as described in the internet database. A detailed characterization of the T-DNA insertions is shown in Figure 3. The T-DNA of *Atparp1* was integrated in exon 14 and had 240 base pairs (bps) filler DNA. The *Atparp2* line contained at least 2 T-DNA copies inserted as an inverted repeat. The T-DNA of *Atparp2* was integrated into intron 6, having 5 bps filler DNA.

The genomic DNA was digested by restriction enzymes (EcoRV or BglII for *Atparp1*, HindIII for *Atparp2*) for Southern blotting (Figure 3). If there is one T-DNA inserted in the correct locus, it can be expected that bands with the following sizes will be detected on the blot: *Atparp1*: 1350bp (EcoRV), 2716bp (BglII); *Atparp2*: 3600bp and 5476bp (HindIII). If T-DNAs are inserted in other loci, additional bands probably with different sizes will be detected. The results showed that the *Atparp1* line contained one T-DNA insertion. The expected 3600bp band for the *Atparp2* line was clearly visible, but the expected band of 5476bp for the *Atparp2* mutant was very faint, suggesting that this T-DNA was probably not intact or the digestion site of HindIII was mutated and could not be cleaved. There were four additional bands for the *Atparp2* line, indicating that this line had multiple T-DNA

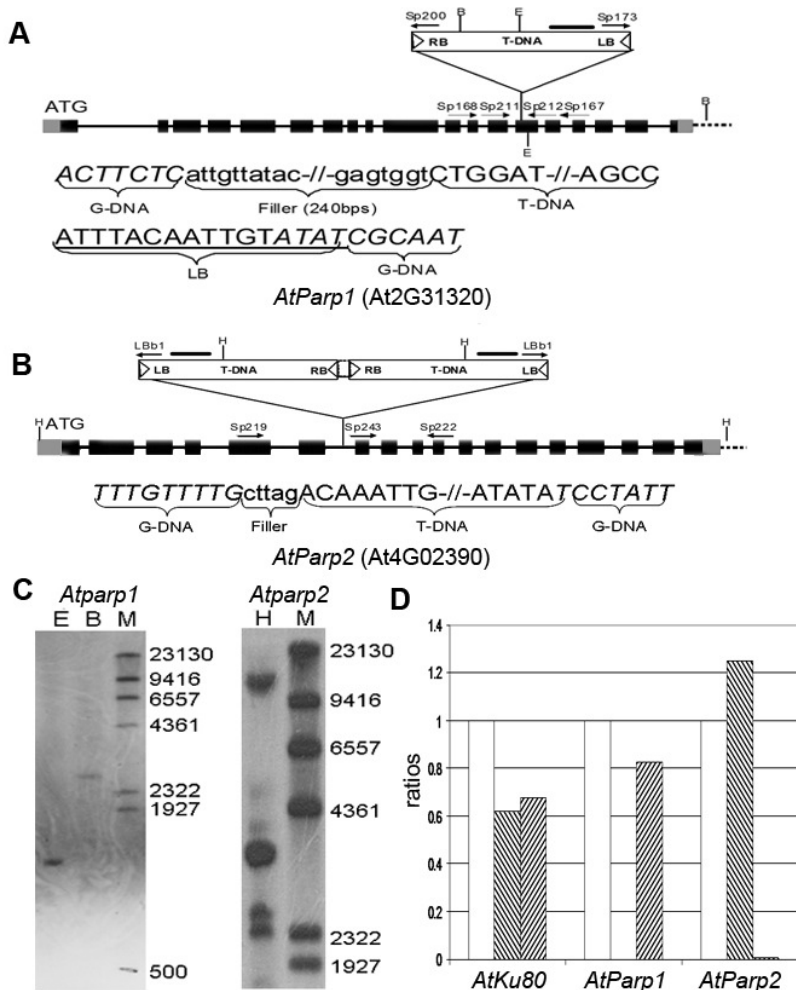


**Figure 3.** Molecular analysis of the T-DNA insertion in the *AtParp1* and *AtParp2* loci. Genomic organization of the *AtParp1* (A) and *AtParp2* (B) locus are indicated with the positions of the inserted T-DNAs. Exons are shown as black boxes. 3' and 5' UTRs are shown as gray boxes. Introns are shown as lines. The primers used for genotyping and Q-RT-PCR analysis, the probes (—) and the restriction enzyme digestion sites used for Southern blot analysis are indicated. Genomic DNA sequences (g-DNA) flanking the T-DNA insertion are shown in italic. (C) Southern blot analysis of the T-DNA insertion. The genomic DNA of the *Atparp1* mutant was digested by EcoRV (E) or BglII (B) and the DNA of the *Atparp2* mutant by HindIII (H). M:  $\lambda$ HindIII Marker. (D) RNA expression of the *AtKu80*, *AtParp1* and *AtParp2* genes were determined by Q-RT-PCR in wild-type, *Atparp1* and *Atparp2* plants. All the sample values were normalized to *Roc* values. The values of the wild-type were set on 1. (□ wild-type (WT); ▨ *Atparp1*; ▩ *Atparp2*)

copies in *AtParp2* and/or extra copies located somewhere else in the genome. One band probably represents the band derived from the T-DNA copy in *Atparp2* for which no band of correct size was detected.

In order to find out whether the mutated loci still produce mRNA, Q-RT-PCR analysis was performed for the *Atparp1* and *Atparp2* T-DNA insertion lines using primers flanking the insertion site. This resulted in a product for each gene in the wild-type, but not in the corresponding T-DNA insertion mutant (Figure 3). The mRNA expression of *ku80* was also checked here as a reference. This indicated that neither of the two T-DNA insertion mutants produces a stable mRNA of the mutated gene and that the plants are homozygous mutants indeed. The *Atparp1* mutant was crossed with the *Atparp2* mutant in order to obtain double mutants. In the second generation of this cross indeed, homozygous *Atp1p2* double mutants were obtained. No obvious differences in growth were observed between the *Atparp* single or double mutants and the wild-type.

### Sensitivity to bleomycin and MMS

Since more and more biochemical evidence in mammals showed that Parp1 and Parp2 are involved in DNA repair processes, we investigated whether the two Parp proteins also have a similar function in plants. To this end, the *Atparp* mutants were tested for the sensitivity to two genotoxic agents (bleomycin and MMS). The radiomimetic chemical bleomycin induces mainly DNA double strand breaks (DSBs) (36). The monofunctional alkylating agent MMS induces mainly base methylation and as a consequence DNA single strand breaks (SSBs) that can be converted into DSBs during replication (37). As shown in Figure 4, the *Atparp1* and *Atp1p2* mutants tolerated the damage induced by bleomycin equally well as the wild-type, but turned out to be hypersensitive to MMS. The *Atparp2* mutant seemed to tolerate the damage induced by both MMS and bleomycin equally well as the wild-type. This indicated that AtParp1 had an important role in SSBs repair. To quantify the effect of MMS treatment on growth, the fresh weight of seedlings was determined after 2 weeks of continuous MMS treatment. After growth on the highest concentration of MMS (0.01%) all the plant lines had become very sick and stopped growing. Lower concentrations (0.006% and 0.008%) of MMS led to growth retardation of the *Atparp1* and *Atp1p2* mutants. After growth in the presence of 0.008% MMS, the fresh weight of the *Atparp1* mutant was reduced to 2/3 of the weight of the wild-type and the fresh weight of the *Atp1p2* mutant was about 1/2 of that of the wild-type. The *Atparp2* mutant had more or less the same weight as the wild-type in all the MMS treatments. It seems that the role of AtParp2 only becomes apparent in the absence of AtParp1. When *AtParp1* is mutated as well, the effect of a mutation in *AtParp2* can be observed, since the fresh weight of the *Atp1p2* double mutant was less than that of the *Atparp1* single mutant after MMS treatment. This is in accordance with previous reports about the collaboration of Parp1 and Parp2 in efficient base excision DNA repair in mammals (38).

In order to quantify the DNA damage in these mutants after MMS treatment, comet assays (A/N protocol) were performed, measuring SSBs and DSBs. For each treatment, around 100 nuclei from 4 independent mini gel replicas were analyzed at random by using CometScore™. Without any treatment, the *Atparp1* and *Atp1p2* mutants had already more

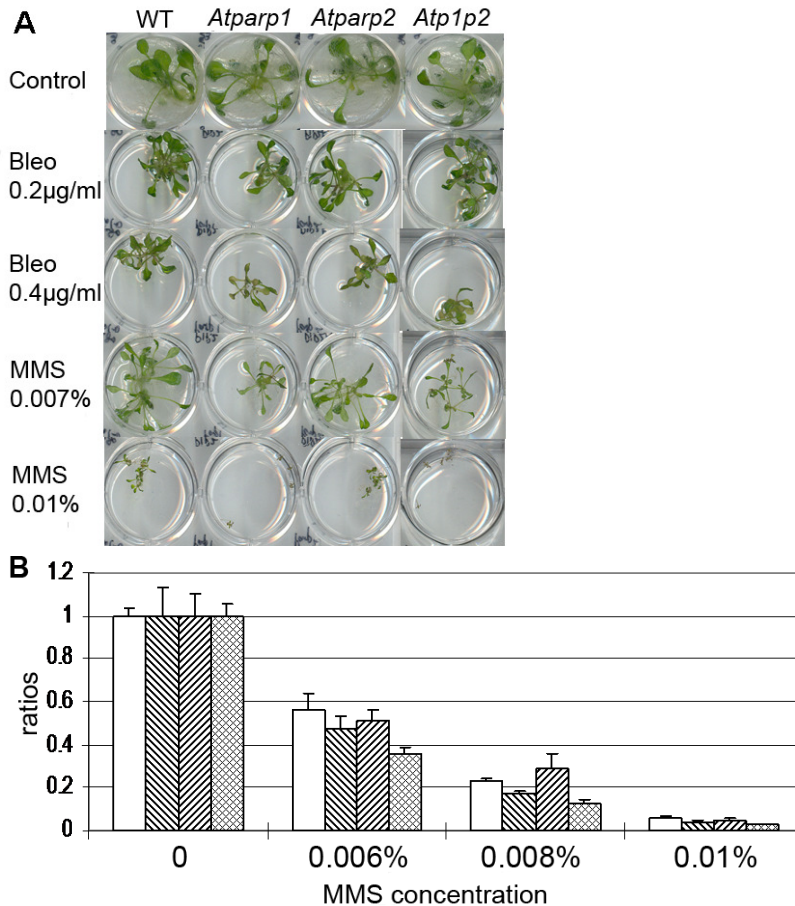


**Figure 4.** Response of *Atparp* mutants to DNA-damaging treatments.

(A) Phenotypes of wild-type (Col-0) plants and *Atparp1*, *Atparp2* and *Atp1p2* mutants to bleomycin or MMS treatment. Four-day-old seedlings were transferred to liquid  $\frac{1}{2}$  MS medium (control) or  $\frac{1}{2}$  MS medium containing different concentrations of bleomycin (Bleo) or MMS and were scored 2 weeks after germination.

(B) Fresh weight of 2-week-old wild-type plants and *Atparp1*, *Atparp2* and *Atp1p2* mutants treated with 0, 0.006%, 0.008% or 0.010% MMS. For each treatment 20 seedlings were weighed in triplicate. Fresh weight of the wild-type and the mutants grown for 2 weeks without MMS was set at 1. (□ WT; ▨ *Atparp1*; ▩ *Atparp2*; ▤ *Atp1p2*)

DNA damage than the wild-type, demonstrating that AtParp1 is involved in DNA repair (Figure 5). After 2h MMS treatment, all the mutants have more DNA damage compared to the wild-type, indicating that AtParp1 and AtParp2 are both involved in DNA repair. But the *Atparp1* and *Atp1p2* mutants had a higher level of nuclear DNA damage than the *Atparp2* mutant, suggesting that AtParp1 may have a more crucial function in SSBs repair. In both the wild-type and the mutants, the level of DNA damage after 24h MMS treatment plus 24h recovery was reduced indicative of DNA repair. Recovery was slower in the mutants than in the wild-type, and the *p1p2* mutant had slower recovery than the single *Atparp1* and

*Atparp2* mutants. It seems that AtParp1 and AtParp2 have redundant functions, and that in the *Atp1p2* double mutant this function is abolished.

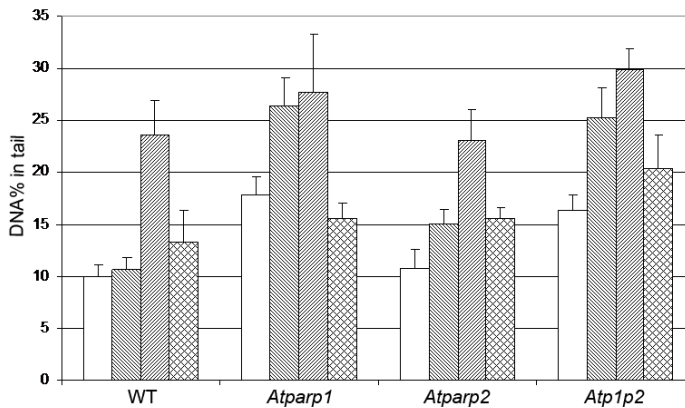


**Figure 5.** Comet assay.

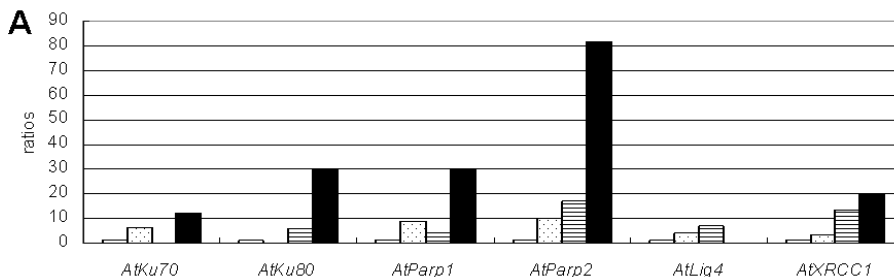
The fraction of DNA in comet tails (%tail-DNA) was used as a measure of DNA damage in wild-type, *Atparp1*, *Atparp2* and *Atp1p2* plants. Around 100 nuclei for each treatment were analyzed at random. The means of %tail-DNA after MMS treatment are shown.

(□ t=0; ▨ t=2h; ▩ t=24h; ▧ 24h recovery)

### The expression of *AtParp2*

Microarray analysis showed that the transcript level of *AtParp2* is induced in *Atku80* mutants and the bleomycin treated wild-type plants (23). This suggests that AtParp2 may be involved in a DNA DSB repair pathway, possibly the B-NHEJ pathway. To confirm this hypothesis, RNA expression levels of *AtParp2* and some other genes involved in DSB repair was analyzed using Q-RT-PCR in the C-NHEJ mutants (*Atku70*, *Atku80* and *Atlig4*). The results showed that the mRNA expression levels of DNA repair genes are increased in NHEJ mutants. *AtParp2* expression is increased in all mutants, and especially in the *Atlig4* mutant (Figure 6). This demonstrated that AtParp2 could be an indicator for DNA damage.

We also analyzed the expression in a *AtParp2:GUS* reporter line, which carried as transgene the *AtParp2* gene promoter fused to GUS (15;28). We crossed the *Atlig4* mutant with the *AtParp2:GUS* reporter line. The homozygous *Atlig4* mutant containing the *AtParp2:GUS* construct was obtained. MMS could induce the expression of *AtParp2* throughout the plant,





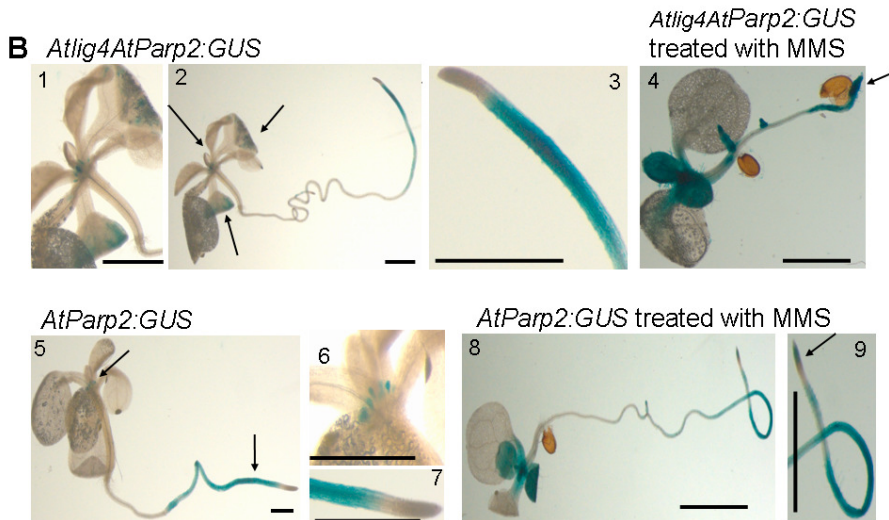


**Figure 6.** Parp2 expression in NHEJ mutants.

(A) RNA expression of the NHEJ genes (*AtKu70*, *AtKu80*, *AtParp1*, *AtParp2*, *AtLig4* and *AtXRCC1*) determined by Q-RT-PCR in wild-type and NHEJ mutant plants. All the values were normalized to Roc values and the ratios were obtained in triplicate. The values of the wild-type were set on 1. (□ WT; ▤ *Atku80*; ▨ *Atku70*; ■ *Atlig4*)

(B) Histochemical staining for GUS activity in *lig4* and wild-type seedlings harboring the *AtParp2* promoter fused to the *GUS* gene (*AtParp2:GUS*). Ten-day-old seedlings were stained for GUS expression without treatment (panel 1-3: *Atlig4AtParp2:GUS*, panel 5-7: *AtParp2:GUS*) or treated with 0.01% MMS for 2h prior to staining (panel 4: *Atlig4AtParp2:GUS*, panel 8,9: *AtParp2:GUS*). The arrows indicated the GUS expression. Bars are 3 mm.

especially in the root tip (Figure 6). The GUS staining was not significantly higher in the *Atlig4* mutant than in the wild-type (Figure 6). It may be that the *AtParp2* coding region or the sequences not present in the *AtParp2:GUS* construct are important for increased expression levels in the C-NHEJ mutants.

### End joining activity

To directly test the function of *AtParp1* and *AtParp2* in NHEJ, an *in vivo* plasmid rejoining assay was utilized to quantify the capacity of the *Atparp1* and *Atparp2* mutants to repair DSBs generated by restriction enzymes. To this end, we transformed protoplasts from leaves with circular (control) or BamHI linearized plasmid DNA. BamHI digests the plasmid DNA in the N-terminal part of the GFP coding sequence. Rejoining of linear plasmid by the NHEJ pathway *in vivo* will result in GFP expression. GFP fluorescence was indeed detected in the wild-type protoplasts which were transformed with the linearized plasmid. But it was difficult to quantify the difference in GFP expression between the wild-type and the mutants under the fluorescence microscope. Therefore, we analyzed the rejoining efficiency by Q-PCR, using primers around the BamHI site and compared with primers in the GFP coding region. The results showed that the rejoining efficiencies were reduced mildly in the *Atparp* single and double mutants (Figure 7). To check if different repair pathways are used

in the different plant lines, the rejoining region was sequenced. Most of the ends had been joined precisely, but in some 1-3 bp had been deleted. No differences were observed between the *Atparp* mutants and the wild-type (data not shown). AtParp proteins have been shown to be involved in B-NHEJ in mammalian cells (11;14). When the C-NHEJ is functional, the deficiency in *AtParp* genes only has a minor influence on the end joining capacity of the cell.

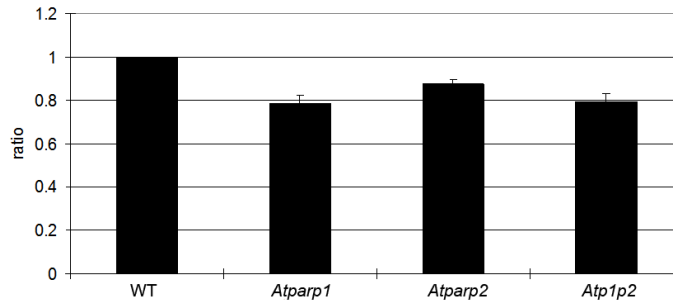


**Figure 7.** Plasmid end-joining assay.

Rejoined plasmid DNA with respect to total plasmid DNA in wild-type protoplasts was set on 1. Values of end joining in protoplasts from the mutants are given relative to that of the wild-type.

### MMEJ assay

Since recent reports showed that Parp proteins are involved in B-NHEJ in mammalian cells (4;11;39;40) and that B-NHEJ is prone to utilize microhomology (41-43), we hypothesized that Parp proteins may be involved in MMEJ in plants as well. To test whether Parp proteins contribute to MMEJ, a MMEJ assay was performed. We expected to find less MMEJ products when Parp proteins are absent. Three hundred  $\mu\text{g}$  linear DNA substrates containing 10 bp repeats at the ends (Figure 2) were incubated without or with 1  $\mu\text{g}$  protein extract from leaves of the *Atparp1*, *Atparp2*, *Atp1p2* mutants or the wild-type. The joined region was amplified by PCR with the primers flanking the junction (q30+q31), and with all extracts PCR products were obtained. No products were obtained in the absence of protein extract (data not shown). When end-joining occurs via MMEJ using the 10 bp microhomology, an XcmI site (CCAN9TGG) will be generated (Figure 2). To determine the fraction of the products joined via MMEJ using the 10 bp microhomology, the PCR products were digested with XcmI (Figure 8). We repeatedly saw a significant reduction in the amount of MMEJ products in the *Atp1p2* double mutant, corroborating with the requirement of AtParp proteins for MMEJ.

### T-DNA integration

Double strand break repair mechanisms are hypothesized to control the integration of *Agrobacterium* T-DNA in plants. Though there is evidence to the contrary (35;44), some reports points to a role of C-NHEJ components in T-DNA integration in plants like this is the case in yeast (45;46). Our own previous data showed that in the *Atku80* and *Atku70* mutants the floral dip transformation frequency is significantly reduced compared with that



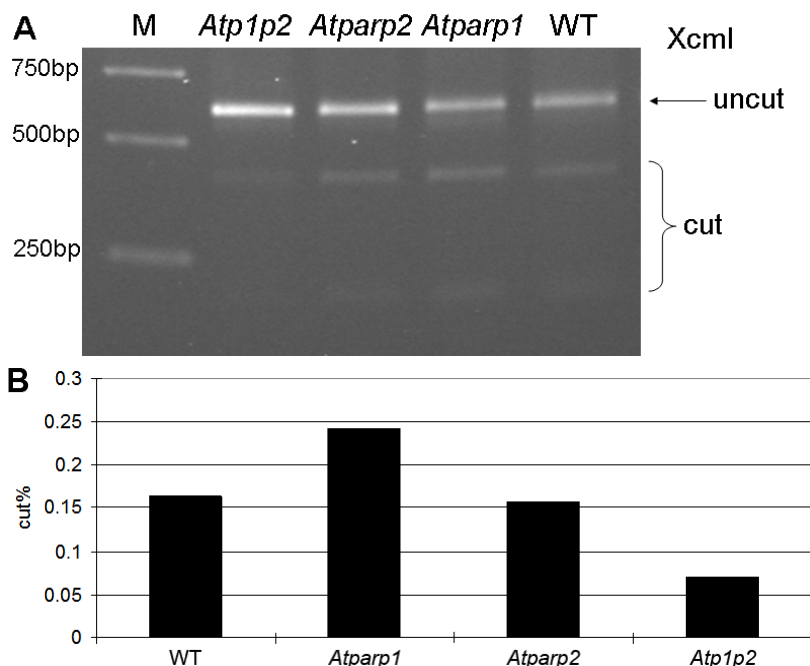


**Figure 8.** MMEJ catalyzed by protein extracts from leaves.

(A) A 600-bp fragment was PCR-amplified on the end-joined products and subsequently digested with XcmI. Only the products via MMEJ can be digested with XcmI resulting in two fragments of 400bp and 200bp.

(B) Quantification of MMEJ activity from (A). The relative contribution of MMEJ was calculated as the percentage of the XcmI-digested fragments of total PCR products (sum of the XcmI-digested and undigested fragments).

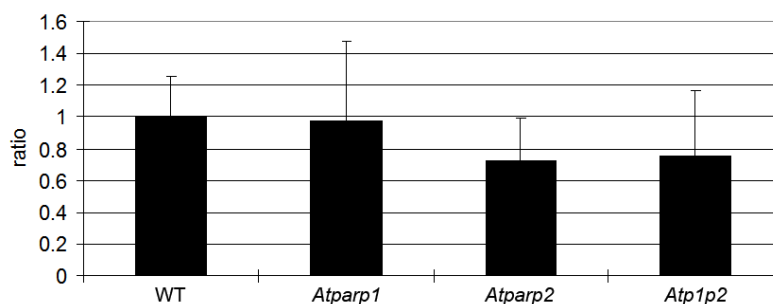


**Figure 9.** Transformation frequencies using the floral dip assay.

One gram of seeds from the wild-type and the NHEJ mutants obtained after floral dip transformations were selected on hygromycin. The number of hygromycin resistant seedlings was scored 2 weeks after germination. The transformation frequency is presented as the ratio of the percentage of hygromycin resistant seedlings in the mutants and the wild-type.

in the wild-type (chapter 2), but root transformation of the *Atku80*, *Atku70* and *Atlig4* mutants was as efficient as that of the wild-type (chapter2). To determine whether components which are involved in B-NHEJ, like AtParp1 and AtParp2, would also influence T-DNA

integration in plants, wild-type and *Atparp* mutants were transformed by *Agrobacterium* using the floral dip method. The transformation frequency was determined as the number of Hpt-resistant seedlings per total number of plated seeds. The transformation frequencies of the *Atparp* mutants were not significantly reduced compared with the wild-type (Figure 9), indicating that AtParp1 and AtParp2 are not essential for efficient T-DNA integration in germline cells. Since C-NHEJ is the major pathway of DSBs repair and consequently may have a major role in T-DNA integration as well, the influence of B-NHEJ is neglectable when C-NHEJ is functional.

## Discussion

3

Here two T-DNA insertion mutants of AtParp1 and AtParp2 were isolated and characterized. There was no phenotypical difference under normal growth conditions between the *Atparp* mutants and the wild-type plants. Some former researchers showed that AtParp proteins were involved in programmed cell death (PCD) process and play a role in the stress tolerance (19-21). Our *Atparp* mutants were tested by drought, salt and cold stress, but no obvious differences were observed (data not shown) in contrast to the *Atparp*-deficient plants used by de Block *et al.* (19). These latter were however made by overexpression of *dsRNA-Atparp* constructs and this may have caused their different behavior.

Like their counterparts in animals, AtParp proteins were found to be involved in the process of DNA repair in Arabidopsis. The *Atparp1* mutant was hypersensitive to MMS, which mainly causes SSB, but was tolerant to bleomycin, which mainly causes DSB, indicating that AtParp1 plays an important role in SSB repair. Since all the components of C-NHEJ were present in the *Atparp* mutants, DSBs can be efficiently repaired via C-NHEJ and consequently the *Atparp* mutants could stand the stress from bleomycin. The *Atparp2* mutant could tolerate the genotoxic stress equally well as the wild-type, but the *Atp1p2* double mutant was more sensitive than the *Atparp1* mutant. It means that AtParp2 probably plays a minor role in DNA repair and its function only becomes apparent in the absence of AtParp1. In mice, single mutants of Parp1 or Parp2 can survive, but the double mutant is embryo lethal, suggesting that Parp1 and Parp2 are functionally redundant (47). Microarray data show that the expression level of *AtParp2* is increased in the *Atku80* mutant and in the wild-type after the treatment of bleomycin (23). The expression of *AtParp2* is thus possibly induced when there is DNA damage due to the absence of C-NHEJ. This was confirmed by the Q-RT-PCR results for RNA expression of *AtParp2* in NHEJ mutants. We also found similar enhanced expression of *AtParp1* and *AtXrcc1* in these NHEJ mutants. This would be in line with a response to the presence of DSBs and a role of AtParp and the scaffold protein AtXrcc1 in a backup pathway of DNA end joining.

Since C-NHEJ is still functional in the *Atparp* mutants, the end joining capacity was not significantly diminished in these mutants. Still the way the ends are joined is different from the wild-type. In the wild-type, two DNA ends containing micro-homology can be

joined using MMEJ. In the *Atp1p2* mutant, the products of MMEJ were obtained much less frequently than in the wild-type. In the *Atparp1* and *Atparp2* single mutants, more products of MMEJ were obtained than in the *Atp1p2* mutant. This indicated that the two AtParp proteins together play an important role in MMEJ and function redundantly. Recently Mansour *et al.* (14) reported that in mammals back-up NHEJ required Parp1, but was independent on microhomologies. Further work is needed to find out whether this is the case in plants as well. An analysis of the effect of the *Atparp* mutants in the background of C-NHEJ mutants may generate such insight. Blocking both the C-NHEJ and B-NHEJ pathways may also open possibilities to increase the efficiency of homologous recombination and thus of gene-targeting.

### Reference List

1. Burzio,L.O., Riquelme,P.T. and Koide,S.S. (1979) ADP ribosylation of rat liver nucleosomal core histones. *J. Biol. Chem.*, **254**, 3029-3037.
2. Riquelme,P.T., Burzio,L.O. and Koide,S.S. (1979) ADP ribosylation of rat liver lysine-rich histone *in vitro*. *J. Biol. Chem.*, **254**, 3018-3028.
3. Ame,J.C., Spenlehauer,C. and de Murcia,G. (2004) The PARP superfamily. *Bioessays*, **26**, 882-893.
4. Yelamos,J., Schreiber,V. and Dantzer,F. (2008) Toward specific functions of poly(ADP-ribose) polymerase-2. *Trends Mol. Med.*, **14**, 169-178.
5. Woodhouse,B.C. and Dianov,G.L. (2008) Poly ADP-ribose polymerase-1: an international molecule of mystery. *DNA Repair (Amst)*, **7**, 1077-1086.
6. Cistulli,C., Lavrik,O.I., Prasad,R., Hou,E. and Wilson,S.H. (2004) AP endonuclease and poly(ADP-ribose) polymerase-1 interact with the same base excision repair intermediate. *DNA Repair (Amst)*, **3**, 581-591.
7. Satoh,M.S. and Lindahl,T. (1992) Role of poly(ADP-ribose) formation in DNA repair. *Nature*, **356**, 356-358.
8. Woodhouse,B.C., Dianova,I.I., Parsons,J.L. and Dianov,G.L. (2008) Poly(ADP-ribose) polymerase-1 modulates DNA repair capacity and prevents formation of DNA double strand breaks. *DNA Repair (Amst)*, **7**, 932-940.
9. Haince,J.F., McDonald,D., Rodrigue,A., Dery,U., Masson,J.Y., Hendzel,M.J. and Poirier,G.G. (2008) PARP1-dependent kinetics of recruitment of MRE11 and NBS1 proteins to multiple DNA damage sites. *J. Biol. Chem.*, **283**, 1197-1208.
10. Bryant,H.E., Petermann,E., Schultz,N., Jemth,A.S., Loseva,O., Issaeva,N., Johansson,F., Fernandez,S., McGlynn,P. and Helleday,T. (2009) PARP is activated at stalled forks to mediate Mre11-dependent replication restart and recombination. *EMBO J.*, **28**, 2601-2615.
11. Audebert,M., Salles,B. and Calsou,P. (2004) Involvement of poly(ADP-ribose) polymerase-1 and XRCC1/DNA ligase III in an alternative route for DNA double-strand breaks rejoining. *J. Biol. Chem.*, **279**, 55117-55126.
12. Audebert,M., Salles,B. and Calsou,P. (2008) Effect of double-strand break DNA sequence on the PARP-1 NHEJ pathway. *Biochem. Biophys. Res. Commun.*, **369**, 982-988.
13. Mortusewicz,O., Ame,J.C., Schreiber,V. and Leonhardt,H. (2007) Feedback-regulated poly(ADP-ribosylation) by PARP-1 is required for rapid response to DNA damage in living cells. *Nucleic Acids Res.*, **35**, 7665-7675.
14. Mansour,W.Y., Rhein,T. and Dahm-Daphi,J. (2010) The alternative end-joining pathway for repair of DNA double-strand breaks requires PARP1 but is not dependent upon microhomologies. *Nucleic Acids Res.*, **38**, 6065-6077.

15. Babiychuk,E., Cottrill,P.B., Storozhenko,S., Fuangthong,M., Chen,Y., O'Farrell,M.K., Van Montagu,M., Inze,D. and Kushnir,S. (1998) Higher plants possess two structurally different poly(ADP-ribose) polymerases. *Plant J.*, **15**, 635-645.
16. Chen,Y.M., Shall,S. and O'Farrell,M. (1994) Poly(ADP-ribose) polymerase in plant nuclei. *Eur. J. Biochem.*, **224**, 135-142.
17. Lepiniec,L., Babiychuk,E., Kushnir,S., van Montagu,M. and Inze,D. (1995) Characterization of an *Arabidopsis thaliana* cDNA homologue to animal poly(ADP-ribose) polymerase. *FEBS Lett.*, **364**, 103-108.
18. Ame,J.C., Rolli,V., Schreiber,V., Niedergang,C., Apiou,F., Decker,P., Muller,S., Hoger,T., Murcia,J.M. and de Murcia,G. (1999) PARP-2, A novel mammalian DNA damage-dependent poly(ADP-ribose) polymerase. *J. Biol. Chem.*, **274**, 17860-17868.
19. De Block,M., Verduyn,C., De Brouwer,D. and Cornelissen,M. (2005) Poly(ADP-ribose) polymerase in plants affects energy homeostasis, cell death and stress tolerance. *Plant J.*, **41**, 95-106.
20. Amor,Y., Babiychuk,E., Inze,D. and Levine,A. (1998) The involvement of poly(ADP-ribose) polymerase in the oxidative stress responses in plants. *FEBS Lett.*, **440**, 1-7.
21. Vanderauwera,S., De Block,M., Van de Steene,N., van de Cotte,B., Metzloff,M. and Van Breusegem,F. (2007) Silencing of poly(ADP-ribose) polymerase in plants alters abiotic stress signal transduction. *Proc. Natl. Acad. Sci. U. S. A.*, **104**, 15150-15155.
22. Doucet-Chabeaud,G., Godon,C., Brutesco,C., de Murcia,G. and Kazmaier,M. (2001) Ionising radiation induces the expression of PARP-1 and PARP-2 genes in *Arabidopsis*. *Mol. Genet. Genomics*, **265**, 954-963.
23. West,C.E., Waterworth,W.M., Sunderland,P.A. and Bray,C.M. (2004) *Arabidopsis* DNA double-strand break repair pathways. *Biochem. Soc. Trans.*, **32**, 964-966.
24. Alonso,J.M., Stepanova,A.N., Lisse,T.J., Kim,C.J., Chen,H., Shinn,P., Stevenson,D.K., Zimmerman,J., Barajas,P., Cheuk,R. *et al.* (2003) Genome-wide insertional mutagenesis of *Arabidopsis thaliana*. *Science*, **301**, 653-657.
25. de Pater,S., Caspers,M., Kottenhagen,M., Meima,H., ter Stege,R. and de Vetten,N. (2006) Manipulation of starch granule size distribution in potato tubers by modulation of plastid division. *Plant Biotechnol. J.*, **4**, 123-134.
26. Weijers,D., Franke-van Dijk,M., Vencken,R.J., Quint,A., Hooykaas,P. and Offringa,R. (2001) An *Arabidopsis* Minute-like phenotype caused by a semi-dominant mutation in a RIBOSOMAL PROTEIN S5 gene. *Development*, **128**, 4289-4299.
27. Menke,M., Chen,I., Angelis,K.J. and Schubert,I. (2001) DNA damage and repair in *Arabidopsis thaliana* as measured by the comet assay after treatment with different classes of genotoxins. *Mutat. Res.*, **493**, 87-93.
28. Takahashi,N., Lammens,T., Boudolf,V., Maes,S., Yoshizumi,T., de Jaeger,G., Witters,E., Inze,D. and de Veylder,L. (2008) The DNA replication checkpoint aids survival of plants deficient in the novel replisome factor ETG1. *EMBO J.*, **27**, 1840-1851.
29. Lindhout,B.I., Pinas,J.E., Hooykaas,P.J. and van der Zaal,B.J. (2006) Employing libraries of zinc finger artificial transcription factors to screen for homologous recombination mutants in *Arabidopsis*. *Plant J.*, **48**, 475-483.
30. Wang,S., Tiwari,S.B., Hagen,G. and Guilfoyle,T.J. (2005) AUXIN RESPONSE FACTOR7 restores the expression of auxin-responsive genes in mutant *Arabidopsis* leaf mesophyll protoplasts. *Plant Cell*, **17**, 1979-1993.
31. Liang,L., Deng,L., Nguyen,S.C., Zhao,X., Maulion,C.D., Shao,C. and Tischfield,J.A. (2008) Human DNA ligases I and III, but not ligase IV, are required for microhomology-mediated end joining of DNA double-strand breaks. *Nucleic Acids Res.*, **36**, 3297-3310.
32. Liang,L., Deng,L., Chen,Y., Li,G.C., Shao,C. and Tischfield,J.A. (2005) Modulation of DNA end joining by nuclear proteins. *J. Biol. Chem.*, **280**, 31442-31449.
33. Clough,S.J. and Bent,A.F. (1998) Floral dip: a simplified method for *Agrobacterium*-

- mediated transformation of *Arabidopsis thaliana*. *Plant J.*, **16**, 735-743.
34. de Pater,S., Neuteboom,L.W., Pinas,J.E., Hooykaas,P.J. and van der Zaal,B.J. (2009) ZFN-induced mutagenesis and gene-targeting in *Arabidopsis* through *Agrobacterium*-mediated floral dip transformation. *Plant Biotechnol. J.*, **7**, 821-835.
  35. van Attikum,H., Bundock,P., Overmeer,R.M., Lee,L.Y., Gelvin,S.B. and Hooykaas,P.J. (2003) The *Arabidopsis* AtLIG4 gene is required for the repair of DNA damage, but not for the integration of *Agrobacterium* T-DNA. *Nucleic Acids Res.*, **31**, 4247-4255.
  36. Burger,R.M., Peisach,J. and Horwitz,S.B. (1981) Activated bleomycin. A transient complex of drug, iron, and oxygen that degrades DNA. *J. Biol. Chem.*, **256**, 11636-11644.
  37. O'Connor,P.J. (1981) Interaction of chemical carcinogens with macromolecules. *J. Cancer Res. Clin. Oncol.*, **99**, 167-186.
  38. Schreiber,V., Ame,J.C., Dolle,P., Schultz,I., Rinaldi,B., Fraulob,V., Murcia,J.M. and de Murcia,G. (2002) Poly(ADP-ribose) polymerase-2 (PARP-2) is required for efficient base excision DNA repair in association with PARP-1 and XRCC1. *J. Biol. Chem.*, **277**, 23028-23036.
  39. Robert,I., Dantzer,F. and Reina-San-Martin,B. (2009) Parp1 facilitates alternative NHEJ, whereas Parp2 suppresses IgH/c-myc translocations during immunoglobulin class switch recombination. *J. Exp. Med.*, **206**, 1047-1056.
  40. Wang,M., Wu,W., Wu,W., Rosidi,B., Zhang,L., Wang,H. and Iliakis,G. (2006) PARP-1 and Ku compete for repair of DNA double strand breaks by distinct NHEJ pathways. *Nucleic Acids Res.*, **34**, 6170-6182.
  41. Verkaik,N.S., Esveldt-van Lange,R.E., van Heemst,D., Bruggenwirth,H.T., Hoeijmakers,J.H., Zdzienicka,M.Z. and van Gent,D.C. (2002) Different types of V(D)J recombination and end-joining defects in DNA double-strand break repair mutant mammalian cells. *Eur. J. Immunol.*, **32**, 701-709.
  42. Simsek,D. and Jasin,M. (2010) Alternative end-joining is suppressed by the canonical NHEJ component Xrcc4-ligase IV during chromosomal translocation formation. *Nat. Struct. Mol. Biol.*, **17**, 410-416.
  43. Fattah,F., Lee,E.H., Weisensel,N., Wang,Y., Lichter,N. and Hendrickson,E.A. (2010) Ku regulates the non-homologous end joining pathway choice of DNA double-strand break repair in human somatic cells. *PLoS. Genet.*, **6**, e1000855.
  44. Gallego,M.E., Bleuyard,J.Y., Daoudal-Cotterell,S., Jallut,N. and White,C.I. (2003) Ku80 plays a role in non-homologous recombination but is not required for T-DNA integration in *Arabidopsis*. *Plant J.*, **35**, 557-565.
  45. Li,J., Vaidya,M., White,C., Vainstein,A., Citovsky,V. and Tzfira,T. (2005) Involvement of KU80 in T-DNA integration in plant cells. *Proc. Natl. Acad. Sci. U. S. A.*, **102**, 19231-19236.
  46. Friesner,J. and Britt,A.B. (2003) Ku80- and DNA ligase IV-deficient plants are sensitive to ionizing radiation and defective in T-DNA integration. *Plant J.*, **34**, 427-440.
  47. Menissier de Murcia,J., Ricoul,M., Tartier,L., Niedergang,C., Huber,A., Dantzer,F., Schreiber,V., Ame,J.C., Dierich,A., LeMeur,M. *et al.* (2003) Functional interaction between PARP-1 and PARP-2 in chromosome stability and embryonic development in mouse. *EMBO J.*, **22**, 2255-2263.

## **Chapter 4**

AtKu80 and AtParp are involved  
in distinct NHEJ pathways

Qi Jia, Amke den Dulk-Ras, B. Sylvia de Pater and  
Paul J.J. Hooykaas

## Abstract

Besides the Ku-dependent classical non-homologous end joining (C-NHEJ) pathway, an alternative NHEJ pathway has been identified in mammalian systems, which is often called the back-up NHEJ (B-NHEJ) pathway. The single-strand break repair factor poly (ADP-ribose) polymerase (Parp) was found to be involved in B-NHEJ in mammalian cells. In B-NHEJ, micro-homology is often used for repair. In order to investigate alternative pathways for NHEJ in Arabidopsis, the *Atparp1parp2ku80* (*Atp1p2k80*) mutant was obtained and functionally characterized along with the *Atku80* and *Atparp1parp2* (*Atp1p2*) mutants. Due to the absence of both the C-NHEJ factor AtKu80 and the putative B-NHEJ factors AtParp1 and AtParp2, the *Atp1p2k80* mutant was hypersensitive to DNA damage agents resulting in more DNA damage, but it still had the ability to repair DNA damage as measured in comet assays. The absence of AtParp proteins restored end joining in the background of AtKu80-deficient plants, suggesting the presence of another alternative NHEJ pathway, which is suppressed by AtKu and AtParp proteins under normal conditions. End joining assays with different linear DNA substrates with different ends in cell-free leaf protein extracts showed that AtKu played a role in DNA end protection and AtParp proteins were involved in micro-homology mediated end joining (MMEJ). The *Atp1p2k80* mutant showed a reduced T-DNA integration efficiency after floral dip transformation. The gene targeting frequency of the triple mutant was not significantly different from that of the wild-type.

## Introduction

For living organisms, DNA double strand breaks (DSBs) are one of the most harmful lesions that can promote mutation and induce cell death. There are two primary pathways to repair DNA DSBs: non-homologous end joining (NHEJ) and homologous recombination (HR). NHEJ is a DNA repair pathway, which rejoins the DNA ends directly and does not depend on homology. HR utilizes a homologous stretch of DNA as a template to align and join the DNA ends. HR is the major pathway used in lower eukaryotes like yeast, whereas NHEJ is the prevailing pathway in higher eukaryotes, such as mammals and plants. DNA transformation also depends on integration of the newly transformed genes by HR or NHEJ (1-3). When NHEJ is blocked in yeast, integration occurs exclusively by HR (2;3). This could open a possibility for increasing the frequency of gene targeting (GT) in plants and mammals. GT is a useful technique for the modification of endogenous genes using HR, but unfortunately occurs with a very low frequency in higher eukaryotes.

Distinct NHEJ pathways have been identified in mammals. One is the classical NHEJ (C-NHEJ) pathway, which is dependent on Ku70/Ku80 and DNA-PKcs. DNA ligase IV (Lig4), XRCC4 and XLF/Cernunnos are also utilized as central components in C-NHEJ.



In the absence of C-NHEJ core factors, back-up NHEJ (B-NHEJ) pathways were identified (4). Some proteins were shown to be involved in B-NHEJ, such as Parp1, Parp2, DNA ligase III (Lig3) and XRCC1 (5;6). In the absence of C-NHEJ, micro-homologous sequences (5-25 bps) flanking the break are more frequently used to join the DNA ends, resulting in deletions. This error-prone pathway has been called micro-homology mediated end joining (MMEJ). It seemed that MMEJ is the predominant pathway among the B-NHEJ pathways. Most components involved in MMEJ are still elusive.

In plants, homologs for most mammalian C-NHEJ factors have been identified, suggesting a similar NHEJ mechanism. However, the existence of B-NHEJ pathways and the proteins involved is still unclear. Here we hypothesized that Parp proteins were also involved in B-NHEJ in plants as in mammals. The triple mutant *Atparp1parp2ku80* (*Atp1p2k80*) was obtained and functionally characterized. The sensitivity to DNA damage and the end joining activity were tested for this triple mutant, and T-DNA integration and gene targeting were also analyzed.

## 4

### Material and methods

#### Plant material

The *Atparp1*, *Atparp2* and *Atku80* T-DNA insertion lines were obtained from the GABI-Kat T-DNA collection (GABI-Kat Line 692A05) or the SALK T-DNA collection (SALK\_640400, SALK\_016627), respectively. Information about it is available at <http://signal.salk.edu/cgi-bin/tdnaexpress> (7). The homozygotes of those mutants isolated in our lab (chapter 2 and 3) were crossed and the homozygous *Atparp1parp2* (*Atp1p2*) double mutant and the homozygous *Atparp1parp2ku80* (*Atp1p2k80*) triple mutant were obtained.

#### Assays for sensitivity to bleomycin and methyl methane sulfonate (MMS)

Seeds of wild-type, *Atp1p2*, *Atp1p2k80* and *Atku80* plants were surface-sterilized as described (8) and germinated on solid ½ MS medium (9). Four days after germination, the seedlings were transferred to liquid ½ MS medium without additions or ½ MS medium containing 0.2 µg/ml and 0.4 µg/ml Bleocin<sup>TM</sup> (Calbiochem), 0.007% and 0.01% (v/v) MMS (Sigma). The seedlings were scored after 2 weeks of growth. Fresh weight (compared with controls) was determined by weighing the seedlings in batches of 20 in triplicate, which were treated in 0%, 0.006%, 0.008% and 0.01% (v/v) MMS for 2 weeks.

#### Comet assay

One-week-old seedlings were treated in liquid ½ MS containing 0.01% MMS for 0 h, 2 h and 24 h. Some seedlings with 24 h treatment were recovered in liquid ½ MS for another 24 h. DNA damage was detected by comet assays using the A/N protocol as described in chapter 3. The fraction of DNA in comet tails (%tail-DNA) was used as a measure of DNA damage (10). Measures included 4 independent gel replicas totaling about 100 comets

analyzed per experimental point. The result was represented by the mean value ( $\pm$ standard deviation = S.D.) from four gels, based on the median values of %tail-DNA of 25 individual comets per gel. The student's t-test was used to test for significant difference compared to the wild-type with the same treatment.

### ***In vivo* end joining assay**

Arabidopsis mesophyll protoplasts isolation and protoplasts DNA transformation using the polyethylene glycol (PEG) transformation protocol (11) were described in chapter 2. In each experiment,  $2 \times 10^4$  protoplasts were transformed with 2  $\mu$ g of circular or linear plasmid pART7-HA-GFP(S65T) (Figure 1), which was cleaved with BamHI. Recircularization of

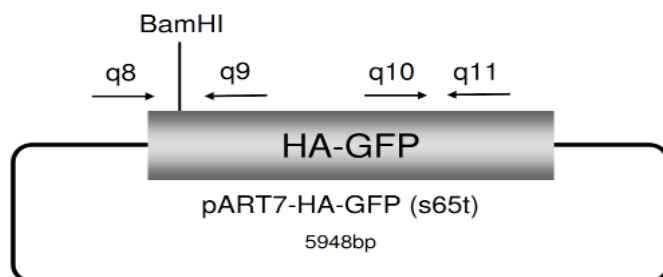


**Figure 1.** Schematic diagram of pART7-HA-GFP.

The primers for Q-PCR are shown by arrows.

**Table 1.** Sequences of primers used for end joining assays.

Name	Sequence
q8	5'-GTGACATCTCCACTGACGTAAG-3'
q9	5'-GATGAACTTCAGGGTCAGCTTG-3'
q10	5'-CAAGCTGACCCTGAAGTTCATC-3'
q11	5'-GTTGTGGCGGATCTTGAAG-3'
q30	5'-GTTTCGGTGATGACGGTG-3'
q31	5'-TGGCACGACAGGTTTCC-3'
q40	5'-GCTGTAGGATGGTAGCTTGGCAC-3'
q41	5'-ATCCTACAGCTGGAATTCGTAATC-3'
q46	5'-TGGAATTCGTAATCATGGTCATAGC-3'
q47	5'-CGTTGGATCCGAATTCGTAATCATGGTCATAGC-3'
q48	5'-CGTTGGTACCGAATTCGTAATCATGGTCATAGC-3'
q49	5'-CGTTGAGCTCGAATTCGTAATCATGGTCATAGC-3'
q50	5'-CGATGGATCCGCTGTAGGATGGTAGCTTG-3'
q51	5'-CGTTGGTACCGCTGTAGGATGGTAGCTTG-3'
q52	5'-CGTTGAGCTCGCTGTAGGATGGTAGCTTG-3'
q53	5'-CGTTGAATTCGCTGTAGGATGGTAGCTTG-3'
PPO-PA	5'-GTGACCGAGGCTAAGGATCGTGT-3'
PPO-1	5'-GCAAGGAGTTGAAACATTAG-3'
PPO-4	5'-CATGAAGTTGTTGACCTCAATC-3'
Sp319	5'-CTATCAAAGAGCACAGACAGC-3'

the linear plasmid in protoplasts was analyzed by Q-PCR with two pairs of primers: q8+q9 and q10+q11 (chapter 2). The sequences of the primers are listed in Table 1. The efficiency of end joining is presented by the ratio of PCR products using q8+q9 primers and q10+q11 primers in comparison with the controls. The value obtained with wild-type protoplasts was set on 1. Q-PCR was performed as three replicates and the assays were performed in triplicate. The PCR products with the primers of q8 and q9 were purified with QIAquick gel extraction kit (Qiagen) and cloned into pJET1.2/blunt Cloning Vector (CloneJET™ PCR Cloning Kit, Fermentas). Individual clones were first digested by BamHI. The clones resistant to digestion by BamHI were sequenced by ServiceXS.

### *In vitro* end joining assay

Protein extracts were obtained from leaves as described in chapter 3. The DNA substrates with different ends were amplified by PCR with different sets of primers. The template for all the PCRs was the 3kb plasmid pUC18P1/4 (chapter 3), which was obtained from Liang (12;13). Phusion™ DNA high-fidelity polymerase (Finnzymes) was used for PCR to generate blunt ends. Sticky ends were generated by digesting the PCR products with different restriction enzymes. The different ends are also listed in Table 2.

**Table 2.** Different ends for end joining assay.

End type			Restriction enzyme	Recognize site	Primers
Sticky ends	Compatible	3'-overhangs	KpnI	GGTAC^C	q48+q51
		5'-overhangs	BamHI	G^GATCC	q47+q50
	Incompatible	3'-overhangs +5'-overhangs	KpnI EcoRI	GGTAC^C G^AATTC	q48+q51
Blunt ends	With micro-homology (10bp)				q40+q41
	Without micro-homology				q40+q46

The linear DNA substrates (300 ng) were incubated with 1 µg protein extract from leaves in 50 mM Tris-HCl (pH7.6), 10mM MgCl<sub>2</sub>, 1mM dithiothreitol, 1 mM ATP and 25% (w/v) polyethylene glycol 2000 at 14°C for 2 hour in a volume of 20 µl. DNA products were purified by electrophoresis through 0.6% agarose gels. A 600-bp fragment containing the end-joined junction was amplified with q30 and q31 primers flanking the junction by PCR, followed by purification and cloning into pJET1.2/blunt Cloning Vector as mentioned above. Individual clones were first digested by corresponding restriction enzymes to check if they were joined precisely or via MMEJ. The clones resistant to the digestion were sequenced by ServiceXS.

### Floral dip transformation and gene targeting

Floral dip transformation was performed according to the procedure described by Clough and Bent (14). The *Agrobacterium* strain AGL1 (pSDM3834) (15) was used for infection. Plasmid pSDM3834 is a pCambia 1200 derivative (hpt selection marker). Seeds were harvested from the dry plants after maturation and plated on solid MA medium (16) without sucrose containing 15 µg/ml hygromycin, 100 µg/ml timentin (to kill *Agrobacterium* cells) and 100 µg/ml nystatin (to prevent growth of fungi). Hygromycin-resistant seedlings were scored 2 weeks after germination and transformation frequency was determined (50 seeds is 1 mg) (17).

In order to test the frequency of gene targeting in the mutants, the same procedure was performed with *Agrobacterium* strain AGL1 (pSDM3900) using the protoporphyrinogen oxidase (PPO) system (18). Plasmid pSDM3900 is a pCambia 3200 derivative (phosphinothricin (ppt) selection marker). About 1 gram seeds were plated on solid MA without sucrose containing 15 µg/ml ppt, 100 µg/ml timentin and 100 µg/ml nystatin to determine the transformation frequency. The rest of the seeds were all sowed on solid MA without sucrose containing 50 µM butafenacil, 100 µg/ml timentin and 100 µg/ml nystatin to identify gene targeting events. The butafenacil-resistant plants were analyzed with PCR to determine if they represent true gene targeting (TGT) events (Figure 2).

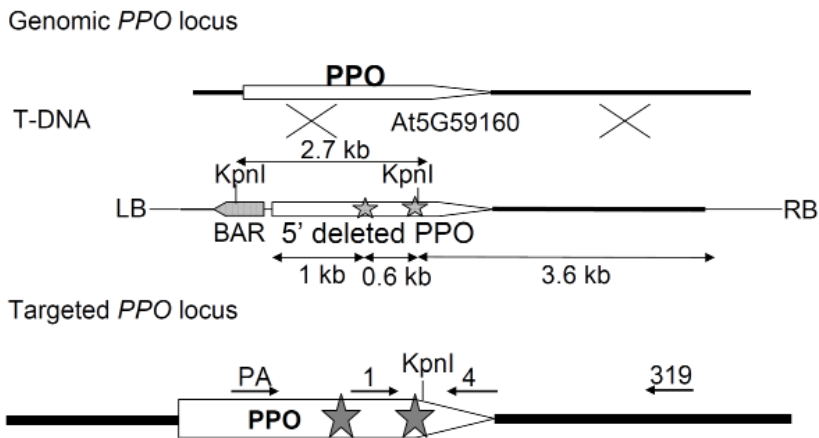


**Figure 2.** The design for the targeted modification of the Arabidopsis *PPO* locus. The white box marked *PPO* represents the *PPO* coding region, and the black lines represents flanking plant genomic DNA. The two mutations conferring butafenacil resistance are indicated as stars. The T-DNA repair construct contains the *BAR* resistance gene linked to the truncated 5'Δ*PPO* (LB for left border and RB for right border). The primers for PCR analysis of the gene targeting events are indicated by arrows.

## Results

### DNA damage response of the *Atku80*, *Atp1p2* and *Atp1p2k80* mutants

In order to study whether the AtParp proteins and the AtKu80 protein function in

different or similar DNA repair pathways, the *Atp1p2k80* triple mutant was obtained and the homozygotes were identified using PCR analysis (chapter 2 and 3). The *Atp1p2k80* mutant had no obvious phenotype under normal growth conditions as compared with the wild-type. When it was treated with genotoxic agents (bleomycin or MMS), it was more sensitive to both agents than the *Atp1p2* and *Atku80* mutants (Figure 3). The radiomimetic chemical bleomycin induces mainly DNA double strand breaks (DSBs) (19), whereas the monofunctional alkylating agent MMS induces mainly DNA single strand breaks (SSBs)

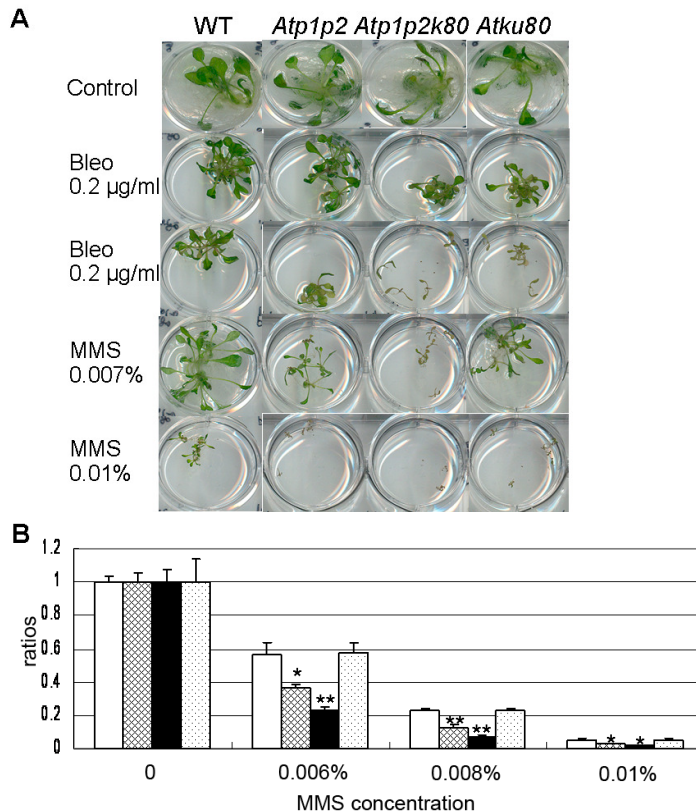


**Figure 3.** Response to DNA-damaging treatments.

(A) Phenotypes of wild-type plants and *Atp1p2*, *Atp1p2k80* and *Atku80* mutants after bleomycin or MMS treatment. Four-day-old seedlings germinated on solid ½ MS were transferred to liquid ½ MS medium (control) or ½ MS medium containing different concentrations of bleomycin (Bleo) or MMS and were scored 2 weeks after germination.

(B) Fresh weight of 2-week-old wild-type plants, *Atp1p2*, *Atp1p2k80* and *Atku80* mutants treated with 0, 0.006%, 0.008% or 0.01% MMS. For each treatment 20 seedlings were weighed in triplicate. Fresh weight of the wild-type grown for 2 weeks without MMS was set at 1. Student's test: \*  $P < 0.05$ , \*\*  $P < 0.001$  (comparing mutants with the wild-type of the same treatment).

(□ wild-type (WT); ▨ *Atp1p2*; ■ *Atp1p2k80*; ▤ *Atku80*)

that can be converted into DSBs during replication (20). As discussed previously in chapter 2 and 3, the AtKu80 protein functions mainly in DSBs repair via C-NHEJ, whereas the AtParp proteins play an important role in SSBs repair and probably in B-NHEJ as well.

To quantify the effect of MMS treatment, the fresh weight of seedlings was determined after 2 weeks of continuous MMS treatment (Figure 3). With the highest concentration of MMS (0.01%), all the plant lines were very sick and did not grow at all. With the lower concentrations of MMS (0.006% and 0.008%), the growth of the *Atp1p2* and *Atp1p2k80* mutants was retarded more than the growth of the wild-type and the *Atku80* mutant. In the presence of 0.008% MMS, the fresh weight of the *Atp1p2k80* mutant was reduced to half of the weight of the *Atp1p2* mutant, or one fourth of the weight of the *Atku80* mutant. As expected, the *Atp1p2k80* triple mutant was most sensitive to the exposure of MMS among all the plant lines, probably due to the deficiency of multiple DNA repair pathways in this triple mutant.

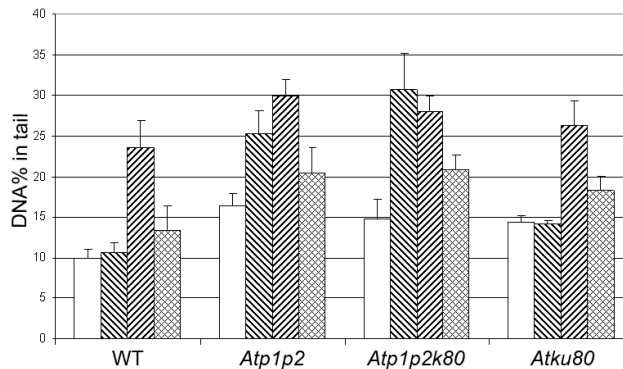


**Figure 4.** Quantification of DNA damage by Comet assay.

The fraction of DNA in comet tails (%tail-DNA) was used as a measure of DNA damage in wild-type plants and *Atp1p2*, *Atp1p2k80* and *Atku80* mutants. Around 100 nuclei for each treatment were analyzed. The means of %tail-DNA after MMS treatment are shown.

(□ t=0; ▨ t=2h; ▩ t=24h; ▤ 24h+24h recovery)

In order to quantify the DNA damage in these mutants after MMS treatment, comet assays (A/N protocol) were performed, that identify SSBs and DSBs. For each treatment, around 100 randomly chosen nuclei from 4 independent mini gel replicas were analyzed by using CometScore™. Without any treatment, the genomic DNA of the *Atp1p2*, *Atp1p2k80* and *Atku80* mutants already had more DNA damage than that of the wild-type, demonstrating that AtParp proteins and AtKu80 are involved in DNA repair systems (Figure 4). The *Atp1p2* and *Atp1p2k80* mutants had a higher level of nuclear DNA damage than the wild-type and the *Atku80* mutant after 2 h MMS treatment, which can be explained by the essential role of the AtParp proteins in SSBs repair. The *Atp1p2k80* triple mutant had more DNA damage than the *Atp1p2* mutant, in accordance with the result of the fresh weight measurements after the MMS treatment. After 24 h MMS treatment, the differences among the various plant lines were not significant, since 24 h MMS treatment was very deleterious to all of them. After 24 h of recovery the DNA damage was repaired in the wild-type to the situation before the treatment. In the mutants about half of the DNA damage was repaired after 24 h recovery compared to the situation before treatment. Since AtKu80 is a major

component of C-NHEJ, DNA repair capacity was expected to be reduced in the *Atku80* mutant. Interestingly, even in the *Atp1p2k80* triple mutant, half of the additional DNA damage was repaired, suggesting the existence of another SSBR pathway besides the AtParp mediated SSBR.

### End joining in the *Atku80*, *Atp1p2* and *Atp1p2k80* mutants

To directly test the function of AtParp proteins and AtKu80 in NHEJ, an *in vivo* plasmid rejoining assay was utilized to quantify the capacity of the *Atparp* and *Atku80* mutants to repair DSBs generated by restriction enzymes. To this end, we transformed protoplasts from leaves with circular (control) or BamHI linearised plasmid DNA. BamHI digests the plasmid DNA in the N-terminal part of the GFP coding sequence. Rejoining of linear plasmid by the NHEJ pathway *in vivo* will result in GFP expression. GFP fluorescence was indeed detected in the wild-type protoplasts which were transformed with the linearized plasmid. But it was difficult to quantify the difference in GFP expression between the wild-type and the mutants under the fluorescence microscope. Therefore, we analyzed the rejoining efficiency by Q-PCR, using primers around the BamHI site compared to primers in the GFP coding region. The results showed that the rejoining efficiency was reduced by half in the *Atku80* mutant compared with the wild-type, whereas the efficiencies were reduced mildly in the *Atp1p2* mutant (Figure 5). This demonstrated that AtKu80, a core component in C-NHEJ, played a crucial role in NHEJ. AtParp proteins could be participants in B-NHEJ. When the C-NHEJ was well functioning, the deficiency in *AtParp* genes did not much influence the capacity of end joining. Surprisingly, the *Atp1p2k80* triple mutant had nearly the same ability of end joining as the wild-type. This suggests that there may be other robust alternative NHEJ pathways in plants, which probably are inhibited by both Ku-dependent C-NHEJ and Parp-dependent B-NHEJ and only become active in the absence of these pathways.

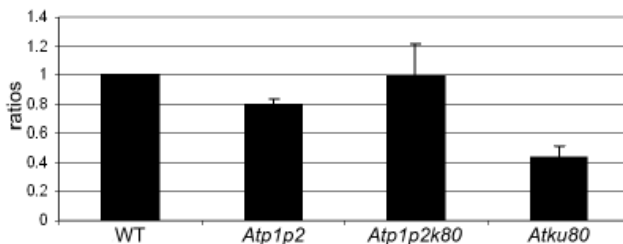


**Figure 5.** Plasmid end joining assay with protoplasts.

Fraction of rejoining plasmid DNA was determined by PCR. The value obtained in wild-type protoplasts was set on 1. Values of end joining in protoplasts from the mutants are given relative to that of the wild-type.

### End joining products of the *Atku80*, *Atp1p2* and *Atp1p2ku80* mutants

In order to investigate the mutagenic potential of the different NHEJ pathways, the spectra of end-joining products with DNA substrates with different type of DNA ends was tested with



cell-free protein extracts from leaves of the wild-type and the mutants. Analysis of the joined products showed that the joining was accurate for the DNA substrates with compatible ends of 5'-overhangs, whereas the joining was prone to be inaccurate for the other types of ends, such as compatible 3'-overhangs, incompatible ends and blunt ends (Figure 6). In most cases deletions were produced for inaccurate end joining, suggesting that the DNA substrates

----G GATCC---- ----CCTAG G----	5' overhangs (BamHI)				----TACAGC TGGAA---- ----ATGTCG ACCTTA----	Blunt ends (no homology)			
	WT	<i>Atp1p2</i>	<i>Atp1p2k80</i>	<i>Atku80</i>		WT	<i>Atp1p2</i>	<i>Atp1p2k80</i>	<i>Atku80</i>
BamHI sensitive	13/15	17/17	19/19	14/14	XcmI sensitive	8/15	4/16	1/11	7/19
small deletion<10bp	2/15				small deletion<10bp	5/15	11/16	7/11	9/19
----GGTAC C---- ----C CATGG----	3' overhangs (KpnI)				---TACCATCCTACAGC ATCCTACAGCTGGA--- ---ATGGTAGGATGTCG TAGGATGTCGACCT---	Blunt ends (10bp homology)			
	WT	<i>Atp1p2</i>	<i>Atp1p2k80</i>	<i>Atku80</i>		WT	<i>Atp1p2</i>	<i>Atp1p2k80</i>	<i>Atku80</i>
KpnI sensitive	6/9	7/12	7/11	7/13	joined precisely	7/36	7/23	3/17	2/20
small deletion<10bp	2/9	1/12	2/11	1/13	small deletion<10bp	5/36	10/23	7/17	3/20
large deletion>10bp	1/9			2/13	insertion		3/23	2/17	
insertion		3/12	2/11	3/13	MMEJ (XcmI sensitive)	24/36	3/23	5/17	15/20
substitution		1/12				WT	<i>Atp1p2</i>	<i>Atp1p2k80</i>	<i>Atku80</i>
MMEJ (large deletion)				1/13 (8bp)	Total large deletion (>10bp)	3/76	2/53	5/56	8/67
----GGTAC AATTC---- ----C G----	3' overhang (KpnI) + 5' overhang (EcoRI)								
Filled in	5/16	5/12	2/17	3/15					
small deletion<10bp	11/16	6/12	13/17	9/15					
large deletion>10bp		1/12	2/17	3/15					

**Figure 6.** Plasmid end joining assay with protein extracts.

DNA substrates with compatible 5'-overhangs, compatible 3'-overhangs, incompatible ends, blunt ends without micro-homology and blunt ends with 10 bp micro-homology were used. Spectra of the junctions are shown generated from DNA substrates with different ends in protein extracts from leaves of the wild-type and *Atp1p2*, *Atp1p2k80* or *Atku80* mutants. After end joining, the junction was amplified by PCR and cloned. The number of plasmids with specific types of junctions was shown compared to the total number analyzed.

were prone to be resected. Small deletions (<10 bp) were often seen among the products from all the different plant lines. Large deletions (>10 bp) were rarely obtained for the wild-type and the *Atp1p2* mutant. The number of large deletions, some of which utilized micro-homology, was increased in the *Atku80* and *Atp1p2k80* mutants, suggesting that AtKu80 protected the DNA ends from resection and prevented the formation of deletions. The sequencing results of the different ends are shown in Table 3. The sequencing results of the end joining assay for 5'-overhangs in leaf protoplasts revealed that most of the ends had been joined precisely, except for some small deletions, which occurred in all the different

plant lines. One junction, the result of a large deletion (29-125 bps) on sites of 8 bp micro-homology, was found in the *Atku80* mutant. This also pointed out that AtKu80 may inhibit MMEJ by protecting the DNA ends from resection.

**Table 3.** Sequence results for the in vitro end joining assay.

<b>5' overhangs (BamHI)</b>
CAAGTACCATCCTCAGC <b>G</b> <sup>^</sup> <b>GATCC</b> GAATTCGTAATCATGGTCATAGC
WT
CAAGTACCATCCTCAGC · · <b>ATCC</b> GAATTCGTAATCATGGTCATAGC
CAAGTACCATCCTCAG · · · <b>ATCC</b> GAATTCGTAATCATGGTCATAGC
<b>3' overhangs (KpnI)</b>
CAAGTACCATCCTACAGC <b>GGTAC</b> <sup>^</sup> <b>CGAATTC</b> GTAATCATGGTCATAGC
WT
CAAGTACCATCCTACAGC <b>GGTAC</b> · GAATTCGTAATCATGGTCATAGC (2)
CAAGTACCATCCTACAGC <b>GGT</b> · · -145bp · · · ACTGCCCGCTTCCAGT
<i>Atp1p2</i>
CAAGTACCATCCTACAGC <b>GGTAC</b> · GAATTCGTAATCATGGTCATAGC
CAAGTACCATCCTACAGC <b>GGTAC</b> AGAATTCGTAATCATGGTCATAGC
CAAGTACCATCCTACAGC <b>GGTAC</b> AAC <b>CGAATTC</b> GTAATCATGGTCATAG
CAAGTACCATCCTACAGC <b>GGTAC</b> GTAC <b>CGAATTC</b> GTAATCATGGTCAT (2)
<i>Atp1p2k80</i>
CAAGTACCATCCTACAGC <b>GGTAC</b> · GAATTCGTAATCATGGTCATAGC (2)
CAAGTACCATCCTACAGC <b>GGTAC</b> GTAC <b>CGAATTC</b> GTAATCATGGTCAT (2)
<i>Atku80</i>
CAAGTACCATCCTACAGC <b>GGTAC</b> · GAATTCGTAATCATGGTCATAGC
CAAGTACCATCCTACAGC <b>GGTAC</b> G <b>CGAATTC</b> GTAATCATGGTCATAGC
CAAGTACCATCCTACAGC <b>GGTAC</b> GTAC <b>CGAATTC</b> GTAATCATGGTCAT (2)
AAAATACCGC · · · · · -336bp · · · <b>TACCGAATTC</b> GTAATCATGGTCAT
TCGCTATTACGCCAGCTG · · · · · -291bp · · · · · CATTAATGAATCGGCCAACCGC
<b>3' overhangs (KpnI) +5' overhangs (EcoRI)</b>
CAAGTACCATCCTACAGC <b>GGTAC</b> <sup>^</sup> <b>C G</b> <sup>^</sup> <b>AATTC</b> GTAATCATGGTCATAGC
CAAGTACCATCCTACAGC <b>GGTACAATTC</b> GTAATCATGGTCATAGC
WT
CAAGTACCATCCTACAGC <b>GGTA</b> · <b>AATTC</b> GTAATCATGGTCATAGC (2)
CAAGTACCATCCTACAGC <b>GGTAC</b> · <b>ATTC</b> GTAATCATGGTCATAGC (3)
CAAGTACCATCCTACAGC <b>GGTA</b> · · <b>ATTC</b> GTAATCATGGTCATAGC
CAAGTACCATCCTACAGC <b>GGTAC</b> · · · <b>TCGTAATCATGGTCATAGC</b>
CAAGTACCATCCTACAGC <b>GGTAC</b> · · · · <b>CGTAATCATGGTCATAGC</b>
CAAGTACCATCCTACAGC <b>GGTAC</b> · · · · · <b>GTAATCATGGTCATAGC</b> (2)
CAAGTACCATCCTACAGC <b>G</b> · · · · · <b>GTAATCATGGTCATAGC</b>
<i>Atp1p2</i>
CAAGTACCATCCTACAGC <b>GGTA</b> · <b>AATTC</b> GTAATCATGGTCATAGC (2)
CAAGTACCATCCTACAGC <b>GGTAC</b> · <b>ATTC</b> GTAATCATGGTCATAGC
CAAGTACCATCCTACAGC <b>GGTAC</b> · · · · · <b>GTAATCATGGTCATAGC</b> (2)
CAAGTACCATCCTACAGC <b>GGTA</b> · · · · · <b>GTAATCATGGTCATAGC</b>
CAAGTACCATCCTACAGC <b>G</b> · · · -75bp · · · <b>GTCACAATTCACACAA</b>

*Atp1p2k80*

CAAGCTACCATCCTACAGC**GGTA**·**AATTC**CGTAATCATGGTCATAGC  
 CAAGCTACCATCCTACAGC**GGTAC**·**ATTC**CGTAATCATGGTCATAGC (3)  
 CAAGCTACCATCCTACAGC**GGTAC**··**TTC**CGTAATCATGGTCATAGC  
 CAAGCTACCATCCTACAGC**GGTAC**···**TCG**TAATCATGGTCATAGC  
 CAAGCTACCATCCTACAGC**GGTAC**····**CG**TAATCATGGTCATAGC (3)  
 CAAGCTACCATCCTACAGC**GGTAC**·····**G**TAATCATGGTCATAGC (4)  
 CAAGCTACCATCCTACAGC**GGTAC**····-12bp···**AT**GGTCATAGC  
 CAAGCTACCATCCTACAGC**GGTAC**·····-14bp····**GG**TCATAGC

*Atku80*

CAAGCTACCATCCTACAGC**GGTA**·**AATTC**CGTAATCATGGTCATAGC  
 CAAGCTACCATCCTACAGC**GGTAC**·····**G**TAATCATGGTCATAGC (4)  
 CAAGCTACCATCCTACAGC**GGTA**·····**G**TAATCATGGTCATAGC (3)  
 CAAGCTACCATCCTACAGC**GGTA**·······**A**ATCATGGTCATAGC  
 CAAGCTACCATCCTACAGC**GGTAC**·····-14bp····**GG**TCATAGC  
 CAAGCTACCATCCTACAGC**GGTAC**·····-41bp·····**TTATCCGC**  
 CAAGCTACCATCCTACAGC**GGTAC**·····-118bp·····**TAATGAG**

**Blunt ends without micro-homology**

GTGCCAAGCTACCATCCTACAGC<sup>^</sup>TGGAATTCGTAATCATGGTCATAGC

## WT

GTGCCAAGCTACCATCCTACA····**GAATTC**CGTAATCATGGTCATAGC  
 GTGCCAAGCTACCATCCTAC·····**GAATTC**CGTAATCATGGTCATAGC (2)  
 GTGCCAAGCTACCATCCTACAG····**AATTC**CGTAATCATGGTCATAGC  
 GTGCCAAGCTACCATCC·······**GAATTC**CGTAATCATGGTCATAGC  
 GTGCCAAGCTACCATCCTA·····-91bp····**AGTG**TAAAGCCTGGG  
 TCAGAGCAGATTG····-251bp···**GAATTC**CGTAATCATGGTCATAGC

*Atp1p2*

GTGCCAAGCTACCATCCTACAG··**GGAATTC**CGTAATCATGGTCATAGC (2)  
 GTGCCAAGCTACCATCCTACAG···**GAATTC**CGTAATCATGGTCATAGC  
 GTGCCAAGCTACCATCCTACA···**GGAATTC**CGTAATCATGGTCATAGC (4)  
 GTGCCAAGCTACCATCCTAC····**GGAATTC**CGTAATCATGGTCATAGC (2)  
 GTGCCAAGCTACCATCCTA·····**GAATTC**CGTAATCATGGTCATAGC  
 GTGCCAAGCTACCATCCTACA·····**ATT**CGTAATCATGGTCATAGC  
 GCCAAGCTACC·····-11bp····**GGAATTC**CGTAATCATGGTCATAG

*Atp1p2k80*

GTGCCAAGCTACCATCCTACAG·**TGGAATTC**CGTAATCATGGTCATAGC (1)  
 GTGCCAAGCTACCATCCTACAGC··**GAATTC**CGTAATCATGGTCATAGC (2)  
 GTGCCAAGCTACCATCCTACAG···**GAATTC**CGTAATCATGGTCATAGC  
 GTGCCAAGCTACCATCCTACAG····**AATTC**CGTAATCATGGTCATAGC  
 GTGCCAAGCTACCATCCTACA····**GAATTC**CGTAATCATGGTCATAGC (2)  
 GTGCCAAGCTACCATCCT········-24bp·······**C**ATAGC  
 GTGCCAAGCTACCATCCTA········-28bp········**C**  
 GTGCCAAGCTACCATCCTACAGC·····-78bp·····**CCGGAAGCAT**

<p><i>Atku80</i></p> <p>GTGCCAAGCTACCATCCTACAGC · · GAATTCGTAATCATGGTCATAGC  GTGCCAAGCTACCATCCTACAG · · GGAATTCGTAATCATGGTCATAGC  GTGCCAAGCTACCATCCTACAG · · · GAATTCGTAATCATGGTCATAGC  GTGCCAAGCTACCATCCTACA · · · GGAATTCGTAATCATGGTCATAGC  GTGCCAAGCTACCATCCTAC · · · · GGAATTCGTAATCATGGTCATAGC  GTGCCAAGCTACCATCCTAC · · · · · GAATTCGTAATCATGGTCATAGC (2)  GTGCCAAGCTACCATCCTAC · · · · · AATTCGTAATCATGGTCATAGC  GTGCCAAGCTACCATCC · · · · · GAATTCGTAATCATGGTCATAGC  GCCAAGCTACCATC · · · · · -22bp · · · · · ATGGTCATAGC  CCAGTGCCAAGCTACCATCC · · · -56bp · · · GCTCACAATTCCACACAACA  ACGCCAGGGTTTTCCCAGTC · · · -204bp · · · GGGAAACCTGTCGTGCCAG</p>
<p><b>Blunt ends with micro-homology</b></p> <p>GTGCCAAGCTACCATCCTACAGC <u>^ATCCTACAGCTGGAATTCGTAATCA</u>  WT  GTGCCAAGCTACCATCCTACAG · ATCCTACAGCTGGAATTCGTAATCA (5)</p>
<p><i>Atp1p2</i></p> <p>GTGCCAAGCTACCATCCTACAG · ATCCTACAGCTGGAATTCGTAATCA (8)  GTGCCAAGCTACCATCCTA · · · · ATCCTACAGCTGGAATTCGTAATCA (2)  GTGCCAAGCTACCATCCTACAGCAATCCTACAGCTGGAATTCGTAATCA  GTGCCAAGCTACCATCCTACAGCGGATCCTACAGCTGGAATTCGTAATCA  GTGCCAAGCTACCATCCTACAGCGTGATCCTACAGCTGGAATTCGTAATC</p>
<p><i>Atp1p2k80</i></p> <p>GTGCCAAGCTACCATCCTACAG · ATCCTACAGCTGGAATTCGTAATCA (5)  GTGCCAAGCTACCATCCTAC · · · ATCCTACAGCTGGAATTCGTAATCA  GTGCCAAGCTACCATCCTA · · · · ATCCTACAGCTGGAATTCGTAATCA  GTGCCAAGCTACCATCCTACAGCATCCTACAGCTGGAATTCGTAATCA  GTGCCAAGCTACCATCCTACAGCTGGGAATCCTACAGCTGGAATTCGTAA</p>
<p><i>Atku80</i></p> <p>GTGCCAAGCTACCATCCTACAG · ATCCTACAGCTGGAATTCGTAATCA (2)  GTGCCAAGCTACCATCCTA · · · · ATCCTACAGCTGGAATTCGTAATCATG</p>

The recognition sequences for restriction enzymes are shown as bold letters. The number in brackets indicates multiple clones obtained for that sequence. The dots represent the deletion and the italic letters represent the insertion. The micro-homologous sequences are underlined.

In order to test whether AtParp proteins are involved in MMEJ, a DNA substrate with blunt ends containing 10 bp micro-homology sequences was used for end-joining assays in the wild-type and *Atp1p2*, *Atku70*, *Atku80* and *Atp1p2k80* mutants as described for the *Atparp* mutants in chapter 3. When end joining occurs via MMEJ using the 10 bp microhomology, an XcmI site (CCAN9TGG) will be generated (chapter 3). To determine the fraction of the products joined via MMEJ using the 10 bp microhomology, the PCR products were digested with XcmI. Compared with the wild-type, the *Atp1p2* and *Atp1p2k80* mutants had about two fold less MMEJ products, whereas the *Atku* mutants had about two fold more MMEJ products, indicating that the AtParp proteins are involved in MMEJ (chapter 3), while the AtKu proteins prevent MMEJ by the AtParp proteins (Figure 7). This

suggested that there is a competition between AtParp and AtKu proteins to regulate the use of different NHEJ pathways. The products that were not repaired via MMEJ were also sequenced and these turned out to contain small deletion or insertions.

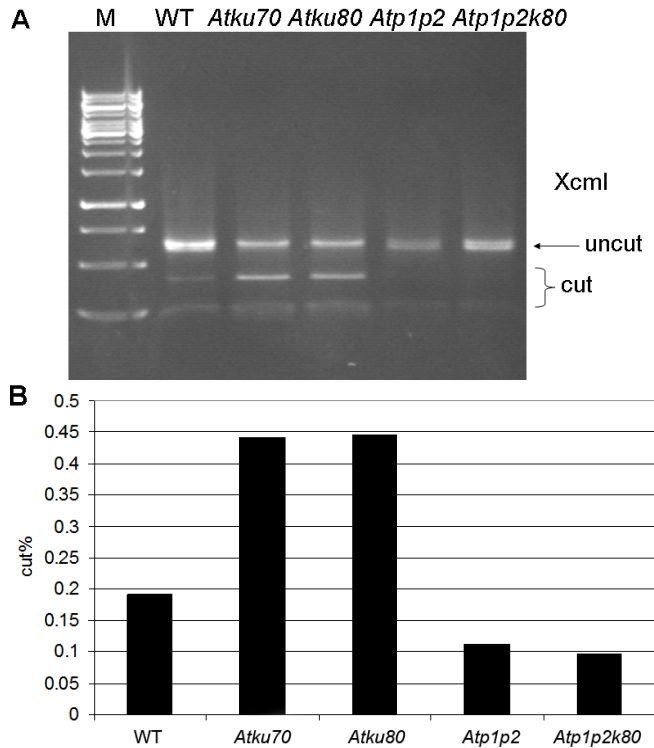


**Figure 7.** MMEJ catalyzed by protein extracts from leaves.

(A) After incubation of linear DNA substrate with protein extracts, a 600-bp fragment was PCR-amplified on the end-joined products and subsequently digested with XcmI. Only the products joined via MMEJ can be digested with XcmI resulting in two fragments of 400 bp and 200 bp. (B) Quantification of MMEJ activity from (A). The relative contribution of the 10-bp MMEJ was calculated as the percentage of the XcmI-digested fragments of total PCR products (sum of the XcmI-digested and undigested fragments).

### T-DNA integration and gene targeting in the *Atku80*, *Atp1p2* and *Atp1p2k80* mutants

Double strand break repair mechanisms are hypothesized to control the integration of *Agrobacterium* T-DNA in plants. In chapter 2, we found that the *Atku* mutations significantly reduced the floral dip transformation frequency as compared to the wild-type, and in chapter 3 that the absence of AtParp proteins did not cause a significant decrease in T-DNA integration frequency via floral dip. To test if T-DNA integration still can happen when both C-NHEJ and B-NHEJ are blocked, the *Atp1p2k80* mutant was transformed by *Agrobacterium* using the floral dip method. The transformation frequency was determined as the number of Hpt-resistant seedlings per total number of plated seeds. The transformation frequencies of the *Atp1p2k80* mutant was significantly reduced compared with the wild-type, and was even lower than that of the *Atku80* mutant (Figure 8). However T-DNA

integration still happened in the triple mutant when both NHEJ pathways were inactivated.

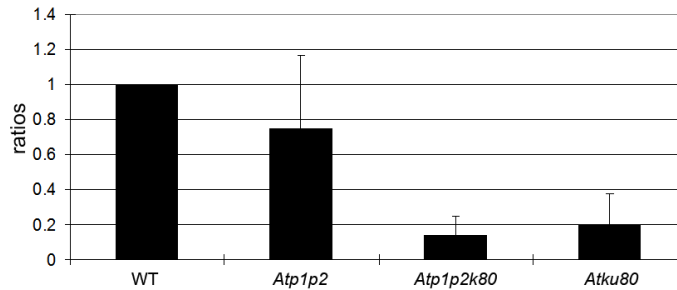


**Figure 8.** Transformation frequencies using the floral dip assay. One gram of seeds from the wild-type and the *Atp1p2*, *Atp1p2ku80* or *Atku80* mutants obtained after floral dip transformations were selected on hygromycin. The number of hygromycin resistant seedlings was scored 2 weeks after germination. The transformation frequency is presented as the ratio of the percentage of hygromycin resistant seedlings in the mutants and the wild-type.

If NHEJ is blocked, the chance for DNA repair via HR could be increased, so that the frequency of gene targeting could also be increased (2;3;21;22). The frequency of gene targeting was tested in the wild-type, the *Atp1p2*, *Atp1p2ku80*, and *Atku80* mutants. About 1 butafenacil-resistant plant in 1000 transformants was found in the wild-type (chapter 2). There were 1 or 2 butafenacil-resistant plants found in around 1000 transformants of the *Atp1p2*, *Atku80* and *Atp1p2ku80* mutants. The butafenacil-resistant plants were analyzed by PCR to determine whether they indeed represented gene targeting events. In case of a GT event, PCR products obtained with the combination of the PPO primers (Figure 2) can be digested by KpnI. The butafenacil-resistant plants of the wild-type were GT events (data not shown). However, the PCR products of the butafenacil-resistant plants of the *Atku80* and *Atp1p2ku80* mutants were resistant to KpnI digestion, indicating they were escapes (data not shown). The butafenacil-resistant plants of the *Atp1p2* mutants were too small for PCR analysis. It seemed that the gene targeting frequency was not significantly increased in the triple mutant compared with the wild-type, suggesting that inactivation of components from both the C-NHEJ and the B-NHEJ pathways did not induce the HR pathway. Together with the results from the T-DNA integration experiments, this indicated that an additional pathway of NHEJ must exist.

## Discussion

Here the *Atp1p2ku80* triple mutant, which was deficient in both Ku-dependent C-NHEJ and Parp-involved B-NHEJ pathways, was obtained and functionally characterized. The triple mutant was more sensitive to the stress of SSBs and DSBs than the wild-type, the *Atp1p2* and *Atku80* mutants, but it could still repair DNA damage to some extent according to the comet assay. The data from end joining assays and floral dip transformations showed that the *Atp1p2ku80* mutant still had ability for end joining and T-DNA integration. All

these results suggested that either there is another alternative NHEJ in plants or that the C-NHEJ and B-NHEJ were not completely inactive in the triple mutant. The end joining capacity of the *Atku80* mutant was much lower than that of the wild-type, while the end joining capacity of the *Atp1p2* mutant was only mildly affected (Figure 5). However, unexpectedly the *Atp1p2k80* triple mutant had a similar end joining capacity as the wild-type. This suggests that indeed an additional pathway is present, which is suppressed under normal conditions, and becomes active when both the C-NHEJ and B-NHEJ are blocked. This hypothesis also explains the residual T-DNA integration and low GT frequency in the triple mutant. Recently, a similar result was also reported from the DNA repair kinetics after  $\gamma$ -irradiation in the *Atku80xcorr1* mutant by Charbonnel et al. (23). Though the *Atp1p2k80* mutant did not reduce the end joining frequency in the leaf protoplasts, it still had lower T-DNA integration frequency via floral dip transformation, compared with the wild-type. Possibly, the additional pathway is less active in the gametophytic cells (used in floral dip transformation) than in the somatic leaf cells (used in the end joining assay). Alternatively, T-DNA integration in chromosomes may be more dependent on C-NHEJ than end joining of naked plasmid molecules.

Results from end joining assays with different DNA ends in cell-free extracts revealed that in the *Atku80* mutant more large deletions were found than in the wild-type, suggesting that Ku80 plays a role in keeping genome integrity in plants. This is in accordance with some reports in mammals, which also showed that Ku may serve as an alignment factor that not only increases NHEJ efficiency but also accuracy (24-28). Though NHEJ is an error-prone DNA repair pathway compared with HR, it still results in a high fidelity when Ku-dependent C-NHEJ is active. Mutation of C-NHEJ core factors resulted in loss of the accuracy of DNA repair (27). As in the results described here, the C-NHEJ deficient mutants preferred end joining using micro-homology so that the chance for deletions was highly increased and the genome was unstable (25;27). Of the known end-joining pathways, C-NHEJ is relatively fast and accurate, so that it is the first choice for the organisms to repair DNA DSBs.

The *Atp1p2* and *Atp1p2k80* mutants gave less MMEJ products than the wild-type, whereas the *Atku80* mutant gave more MMEJ products than the wild-type in the *in vitro* end joining assays (Figure 7). The latter is not consistent with the percentages of the different joined products from the results of sequencing (Figure 6). Sequencing indicated that the *Atku80* mutant formed a similar percentage of MMEJ products as the wild-type. It is possible that the PCR products in Figure 7 were not completely digested. But both experiments indicated that AtParp1 and AtParp2 are involved in MMEJ (chapter 3) and AtKu80 can inhibit MMEJ. These results point to a regulatory mechanism, in which competition between Parp and Ku determines whether C-NHEJ or B-NHEJ is used, as was found for mammalian systems (6). When the Ku protein is absent, Parp may bind the DNA ends and direct the DNA repair pathway to B-NHEJ, which more often uses micro-homology. Katsura *et al.* (29) reported that Ku80 could also be involved in MMEJ, but



MMEJ is less dependent on Ku80 than NHEJ. Recently, it was shown that Ku regulated the choice of repair pathway by inhibition of end processing and thus by repression on HR and MMEJ (30;31). MMEJ leads to deletion and is therefore mutagenic and may be harmful for the genome stability. When the major DNA DSB repair pathway, C-NHEJ, is available, MMEJ is suppressed by C-NHEJ for optimal genome stability. Ku and Parp proteins could be involved in regulating this. The *Atp1p2k80* triple mutant might be used as a tool to further investigate the mechanism of the regulation and to identify components of the additional NHEJ pathways in future.

### Reference List

1. van Attikum,H., Bundock,P. and Hooykaas,P.J. (2001) Non-homologous end-joining proteins are required for *Agrobacterium* T-DNA integration. *EMBO J.*, **20**, 6550-6558.
2. van Attikum,H. and Hooykaas,P.J. (2003) Genetic requirements for the targeted integration of *Agrobacterium* T-DNA in *Saccharomyces cerevisiae*. *Nucleic Acids Res.*, **31**, 826-832.
3. Kooistra,R., Hooykaas,P.J. and Steensma,H.Y. (2004) Efficient gene targeting in *Kluyveromyces lactis*. *Yeast*, **21**, 781-792.
4. Wang,H., Perrault,A.R., Takeda,Y., Qin,W., Wang,H. and Iliakis,G. (2003) Biochemical evidence for Ku-independent backup pathways of NHEJ. *Nucleic Acids Res.*, **31**, 5377-5388.
5. Audebert,M., Salles,B. and Calsou,P. (2004) Involvement of poly(ADP-ribose) polymerase-1 and XRCC1/DNA ligase III in an alternative route for DNA double-strand breaks rejoining. *J. Biol. Chem.*, **279**, 55117-55126.
6. Wang,M., Wu,W., Wu,W., Rosidi,B., Zhang,L., Wang,H. and Iliakis,G. (2006) PARP-1 and Ku compete for repair of DNA double strand breaks by distinct NHEJ pathways. *Nucleic Acids Res.*, **34**, 6170-6182.
7. Alonso,J.M., Stepanova,A.N., Leisse,T.J., Kim,C.J., Chen,H., Shinn,P., Stevenson,D.K., Zimmerman,J., Barajas,P., Cheuk,R. *et al.* (2003) Genome-wide insertional mutagenesis of *Arabidopsis thaliana*. *Science*, **301**, 653-657.
8. Weijers,D., Franke-van Dijk,M., Vencken,R.J., Quint,A., Hooykaas,P. and Offringa,R. (2001) An Arabidopsis Minute-like phenotype caused by a semi-dominant mutation in a RIBOSOMAL PROTEIN S5 gene. *Development*, **128**, 4289-4299.
9. Murashige,T. and Skoog,F. (1962) A Revised Medium for Rapid Growth and Bio Assays with Tobacco Tissue Cultures. *Physiologia Plantarum*, **15**, 473-497.
10. Kozak,J., West,C.E., White,C., da Costa-Nunes,J.A. and Angelis,K.J. (2009) Rapid repair of DNA double strand breaks in *Arabidopsis thaliana* is dependent on proteins involved in chromosome structure maintenance. *DNA Repair (Amst)*, **8**, 413-419.
11. Wang,S., Tiwari,S.B., Hagen,G. and Guilfoyle,T.J. (2005) AUXIN RESPONSE FACTOR7 restores the expression of auxin-responsive genes in mutant Arabidopsis leaf mesophyll protoplasts. *Plant Cell*, **17**, 1979-1993.
12. Liang,L., Deng,L., Nguyen,S.C., Zhao,X., Maulion,C.D., Shao,C. and Tischfield,J.A. (2008) Human DNA ligases I and III, but not ligase IV, are required for microhomology-mediated end joining of DNA double-strand breaks. *Nucleic Acids Res.*, **36**, 3297-3310.
13. Liang,L., Deng,L., Chen,Y., Li,G.C., Shao,C. and Tischfield,J.A. (2005) Modulation of DNA end joining by nuclear proteins. *J. Biol. Chem.*, **280**, 31442-31449.
14. Clough,S.J. and Bent,A.F. (1998) Floral dip: a simplified method for *Agrobacterium*-mediated transformation of *Arabidopsis thaliana*. *Plant J.*, **16**, 735-743.
15. de Pater,S., Neuteboom,L.W., Pinas,J.E., Hooykaas,P.J. and van der Zaal,B.J. (2009)

- ZFN-induced mutagenesis and gene-targeting in Arabidopsis through *Agrobacterium*-mediated floral dip transformation. *Plant Biotechnol. J.*, **7**, 821-835.
16. Masson, J. and Paszkowski, J. (1992) The Culture Response of *Arabidopsis-Thaliana* Protoplasts Is Determined by the Growth-Conditions of Donor Plants. *Plant Journal*, **2**, 829-833.
  17. van Attikum, H., Bundock, P., Overmeer, R.M., Lee, L.Y., Gelvin, S.B. and Hooykaas, P.J. (2003) The Arabidopsis AtLIG4 gene is required for the repair of DNA damage, but not for the integration of *Agrobacterium* T-DNA. *Nucleic Acids Res.*, **31**, 4247-4255.
  18. Hanin, M., Volrath, S., Bogucki, A., Briker, M., Ward, E. and Paszkowski, J. (2001) Gene targeting in Arabidopsis. *Plant J.*, **28**, 671-677.
  19. Burger, R.M., Peisach, J. and Horwitz, S.B. (1981) Activated bleomycin. A transient complex of drug, iron, and oxygen that degrades DNA. *J. Biol. Chem.*, **256**, 11636-11644.
  20. O'Connor, P.J. (1981) Interaction of chemical carcinogens with macromolecules. *J. Cancer Res. Clin. Oncol.*, **99**, 167-186.
  21. Abdel-Banat, B.M., Nonklang, S., Hoshida, H. and Akada, R. (2010) Random and targeted gene integrations through the control of non-homologous end joining in the yeast *Kluyveromyces marxianus*. *Yeast*, **27**, 29-39.
  22. Krappmann, S., Sasse, C. and Braus, G.H. (2006) Gene targeting in *Aspergillus fumigatus* by homologous recombination is facilitated in a nonhomologous end-joining-deficient genetic background. *Eukaryot. Cell*, **5**, 212-215.
  23. Charbonnel, C., Gallego, M.E. and White, C.I. (2010) Xrcc1-dependent and Ku-dependent DNA double-strand break repair kinetics in Arabidopsis plants. *Plant J.*, **64**, 280-290.
  24. Feldmann, E., Schmiemann, V., Goedecke, W., Reichenberger, S. and Pfeiffer, P. (2000) DNA double-strand break repair in cell-free extracts from Ku80-deficient cells: implications for Ku serving as an alignment factor in non-homologous DNA end joining. *Nucleic Acids Res.*, **28**, 2585-2596.
  25. Verkaik, N.S., Esveldt-van Lange, R.E., van Heemst, D., Bruggenwirth, H.T., Hoeijmakers, J.H., Zdzienicka, M.Z. and van Gent, D.C. (2002) Different types of V(D)J recombination and end-joining defects in DNA double-strand break repair mutant mammalian cells. *Eur. J. Immunol.*, **32**, 701-709.
  26. Chen, S., Inamdar, K.V., Pfeiffer, P., Feldmann, E., Hannah, M.F., Yu, Y., Lee, J.W., Zhou, T., Lees-Miller, S.P. and Povirk, L.F. (2001) Accurate in vitro end joining of a DNA double strand break with partially cohesive 3'-overhangs and 3'-phosphoglycolate termini: effect of Ku on repair fidelity. *J. Biol. Chem.*, **276**, 24323-24330.
  27. Kuhfittig-Kulle, S., Feldmann, E., Odersky, A., Kuliczowska, A., Goedecke, W., Eggert, A. and Pfeiffer, P. (2007) The mutagenic potential of non-homologous end joining in the absence of the NHEJ core factors Ku70/80, DNA-PKcs and XRCC4-LigIV. *Mutagenesis*, **22**, 217-233.
  28. Osakabe, K., Osakabe, Y. and Toki, S. (2010) Site-directed mutagenesis in Arabidopsis using custom-designed zinc finger nucleases. *Proc. Natl. Acad. Sci. U. S. A.*, **107**, 12034-12039.
  29. Katsura, Y., Sasaki, S., Sato, M., Yamaoka, K., Suzukawa, K., Nagasawa, T., Yokota, J. and Kohno, T. (2007) Involvement of Ku80 in microhomology-mediated end joining for DNA double-strand breaks in vivo. *DNA Repair (Amst)*, **6**, 639-648.
  30. Fattah, F., Lee, E.H., Weisensel, N., Wang, Y., Lichter, N. and Hendrickson, E.A. (2010) Ku regulates the non-homologous end joining pathway choice of DNA double-strand break repair in human somatic cells. *PLoS. Genet.*, **6**, e1000855.
  31. Roberts, S.A., Strande, N., Burkhalter, M.D., Strom, C., Havener, J.M., Hasty, P. and Ramsden, D.A. (2010) Ku is a 5'-dRP/AP lyase that excises nucleotide damage near broken ends. *Nature*, **464**, 1214-1217.

# **Chapter 5**

## Characterization of the plant specific DNA ligase AtLig6

Qi Jia, B. Sylvia de Pater and Paul J.J. Hooykaas

## Abstract

DNA ligases catalyze the joining of DNA ends and thus play important roles in DNA replication and DNA repair. Eukaryotes possess multiple ATP-dependent DNA ligases with distinct roles in DNA metabolism. Some of them have been well characterized, such as DNA ligase I (Lig1) and DNA ligase IV (Lig4). A novel plant-specific DNA ligase has been identified, termed DNA ligase VI (Lig6), but its function is still unclear. The expression pattern analyzed via Genevestigator showed that the expression level of *AtLig6* was lower than that of *AtLig1* and *AtLig4* and was especially induced at the stages of seed germination and flowering. Two homozygous mutants of *AtLig6* were isolated and crossed with the *Atlig4* mutant to obtain the double mutants (*Atlig4lig6-1*, *Atlig4lig6-2*). All these four homozygous ligase mutants were phenotypically indistinguishable from the wild-type under normal growth conditions. The two *Atlig6* single mutants could tolerate bleomycin treatment equally well as the wild-type. The *Atlig4lig6-1* and *Atlig4lig6-2* double mutants were hypersensitive to bleomycin, but no difference was observed from the *Atlig4* single mutant. The frequency of T-DNA integration was also not disturbed by the deficiency of *AtLig6*, and the frequency of gene targeting seems not to be increased in absence of both *AtLig6* and *AtLig4*. This indicates that other ligases function in NHEJ when *AtLig6* and *AtLig4* are inactive. One candidate was identified by *in silico* searching for homologs of ATP-dependent DNA ligases in Arabidopsis, which may represent a novel plant specific DNA ligase involved in back-up non-homologous end joining (B-NHEJ) for DSB DNA repair.

## Introduction

DNA ligases seal broken DNA molecules with 3' OH and 5' PO<sub>4</sub> ends, which is essential for many biological processes, including DNA replication, DNA repair and DNA recombination (1). On the basis of the different cofactor preferences, the large family of DNA ligases is divided into two groups (2;3). The first group consists of the NAD<sup>+</sup>-dependent DNA ligases, which are utilized by most eubacteria. The second comprises the ATP-dependent DNA ligases, which are utilized mainly by eukaryotes (4). Eukaryotic organisms have evolved multiple ATP-dependent ligase isoforms, including DNA ligase I (Lig1), DNA ligase III (Lig3), DNA ligase IV (Lig4) and DNA ligase VI (Lig6). Lig1 and Lig4 are expressed and conserved in all eukaryotes, whereas Lig3 is unique to vertebrates and Lig6 is plant-specific (4;5). Each ligase has a distinct function in DNA metabolism for the maintenance of genomic integrity (6).

Lig1 plays a vital role in DNA replication by joining the Okazaki fragments and also in DNA repair pathways, such as nucleotide excision repair (NER), base excision repair (BER), single strand break (SSB) repair and probably double strand break (DSB) repair (3;7). Lig4 mediates the final ligation step in the classical non-homologous end joining (C-NHEJ)

pathway (8;9), which is the predominant mechanism for DSB repair in mammals and plants. C-NHEJ joins the DNA ends directly independent of sequence homology by utilizing Ku70/80 proteins and the Lig4/XRCC4/XLF complex. The vertebrate-specific Lig3 has two variants, Lig3 $\alpha$  and Lig3 $\beta$ . Lig3 $\alpha$  is ubiquitously distributed, whereas Lig3 $\beta$  has only been found in testes and may function in meiotic recombination (10). Lig3 $\alpha$  plays a role in BER and SSB repair and interacts with XRCC1 (11). Evidence also points to Lig3 to be involved in the back-up NHEJ (B-NHEJ), which was identified to repair DSBs in absence of the major components of C-NHEJ (12;13). The B-NHEJ pathway is prone to use micro-homology, and is therefore sometimes referred to as the micro-homology mediated end joining (MMEJ) pathway (14). In mammals both Lig3 and Lig1 are involved in MMEJ, but Lig4 is not (15).

Lig6 is a novel DNA ligase that was recently discovered in higher plants by the analysis of plant genomic databases (5;16). Due to its domain structure, it is distinct from the other DNA ligases. It displays a significant sequence similarity to Lig1 (5) and contains three conserved regions in the N-terminus, which are characteristic for Pso2/Snm1 proteins. These proteins belong to the  $\beta$ -CASP family and play an important role in interstrand DNA crosslink repair (5;16;17). Recently, Waterworth *et al.* (17) reported that *Arabidopsis thaliana* Lig6 is required for rapid seed germination and it is a determinant of seed longevity and quality. AtLig6 is probably involved in a rapid and strong DNA DSB response, activated in the earliest stages of seed imbibitions to repair DNA damage that accumulated over time. In order to further analyze its role in DNA repair, we isolated the *Atlig6* and *Atlig4lig6* double mutants and determined the effects of the mutations on T-DNA integration and gene targeting frequencies. Further *in silico* studies on homologs of DNA ligase in *Arabidopsis* were also done to find other putative DNA ligases.

## Material and methods

### Plant materials

Two T-DNA Col-0 insertion lines of *Atlig6* were obtained from the SALK T-DNA collection (*Atlig6-1*: SALK\_065307, *Atlig6-2*: SALK\_079499). Information about them is available at <http://signal.salk.edu/cgi-bin/tdnaexpress> (18). The homozygous mutants were isolated. They were crossed with *Atlig4* (chapter 2) to get the *Atlig4lig6-1* (*Atlig6-1* crossed with *Atlig4*) and *Atlig4lig6-2* (*Atlig6-2* crossed with *Atlig4*) double mutants.

### Expression profiling with Genevestigator tools

The expression pattern of three ligase genes (*AtLig6*: At1G66730, *AtLig4*: At5G57160, *AtLig1*: At1G08130) in *Arabidopsis* were analyzed with Genevestigator analysis tools (<https://www.genevestigator.com/gv/index.jsp>) using publicly available microarray data. The data were selected from the 22k Affymetrix ATH1 Genechip arrays of high quality, totaling 5747 arrays and including datasets obtained from all available datasets online.

### Characterization of two *Arabidopsis* T-DNA insertion mutants of *AtLig6*

DNA was extracted from individual plants using the CTAB DNA isolation protocol (19). The T-DNA insertion site was mapped with a T-DNA Left Border (LB) specific primer LBa1 and a gene-specific primer. Pairs of gene-specific primers around the insertion site were used to determine whether the plants were homozygous or heterozygous for the T-DNA insertion, and the PCR products were sequenced. Southern blot analysis was performed as described in chapter 2. The DIG probe was produced using the PCR DIG Labeling Mix (Roche) with specific primers SP271 and SP272 that amplified an 850-bp fragment from the T-DNA of pROK2. The RNA expression of *AtLig6* in the two mutants was also analyzed (chapter 2). Specific fragments (about 200 bp) were amplified from cDNA with pairs of primers around the T-DNA insertion sites. All sample values were normalized to the values of the house keeping gene *Roc1* (Primers Roc5.2, Roc3.3) and were presented as relative expression ratios. The value of the wild-type was set on 1. The sequences of all the primers are listed in Table 1.

**Table 1.** Sequences of primers used for characterization of the two *Atlig6* mutants and Q-PCR.

Name	Locus	Sequence
LBb1	T-DNA LB	5'-GCGTGGACCGCTTGCTGCAACT-3'
Sp264	<i>Atlig6-1</i>	5'- GTCAACTCTGTCAATGGTCC -3'
Sp265	<i>Atlig6-1</i>	5'- AATATCAAACACGAAGACGCAGAC -3'
Sp266	<i>Atlig6-2</i>	5'- TAAGTGCTACGGTAGTTTCTC -3'
Sp267	<i>Atlig6-2</i>	5'- CTGTTCTGTAGTAAGGCGGC -3'
Sp271	pROK2 Probe	5'-CCCGTGTCTCTCCAAATG-3'
Sp272	pROK2 probe	5'-CAGGTCCCCAGATTAGCC-3'
q5	<i>Atlig6-1</i>	5'- ATCAAGTAACTTATGGATCTGG -3'
q4	<i>Atlig6-2</i>	5'- CAAGGTTAAGCGAGATTATG -3'
q3	<i>Atlig6-2</i>	5'- GACACGGCAGACACTCTG -3'
q1	<i>Atku70</i>	5'-TCTACCACTCAGTCAACCTG-3'
q2	<i>Atku70</i>	5'-CAATAGACAAGCCATCACAG-3'
q6	<i>Atlig4</i>	5'-GACACCAACGGCACAAG-3'
q7	<i>Atlig4</i>	5'-AAGTTCAATGTATGTCAGTCCC-3'
Roc5.2	<i>Roc1</i>	5'-GAACGGAACAGGCGGTGAGTC-3'
Roc3.3	<i>Roc1</i>	5'-CCACAGGCTTCGTCCGCTTTC-3'
PPO-PA	<i>PPO</i>	5'-GTGACCGAGGCTAAGGATCGTGT-3'
PPO-1	<i>PPO</i>	5'-GCAAGGAGTTGAAACATTAG-3'
PPO-4	<i>PPO</i>	5'-CATGAAGTTGTTGACCTCAATC-3'
Sp319	<i>PPO</i>	5'-CTATCAAAGAGCACAGACAGC-3'

### Assays for sensitivity to genotoxic agents

Seeds from wild-type, *Atlig6-1*, *Atlig6-2*, *Atlig4lig6-1* and *Atlig4lig6-2* were surface-

sterilized as described (20) and were germinated on solidified ½ MS medium (21) without additions or containing 0.1 µg/ml, 0.2 µg/ml, 0.3 µg/ml and 0.4 µg/ml Bleocin™ antibiotic (Calbiochem). The seedlings were scored after 3 weeks of growth.

### Floral dip transformation and gene targeting

In order to test the frequency of T-DNA integration and gene targeting in the *Atlig6* mutants, floral dip transformation was performed, as described by Clough and Bent (22), with the *Agrobacterium* strain AGL1 (pSDM3900) for gene targeting using the protoporphyrinogen oxidase (PPO) system (23). Plasmid pSDM3900 is a pCambia 3200 derivative (phosphinothricin (ppt) selection marker). About 1 gram seeds were plated on solid MA medium (24) without sucrose containing 15 µg/ml ppt, 100 µg/ml timentin and 100 µg/ml nystatin to determine the transformation frequency. Phosphinothricin-resistant seedlings were scored 2 weeks after germination and the relative transformation frequency was determined compared to the wild-type. The value of the wild-type was set on 1. The rest of the seeds were all sowed on solid MA medium without sucrose containing 50 µM butafenacil, 100 µg/ml timentin (to kill *Agrobacterium* cells) and 100 µg/ml nystatin (to prevent growth of fungi) to identify gene targeting events. The butafenacil-resistant plants were analyzed with PCR to determine if they represent true gene targeting (TGT) events (Figure 1).

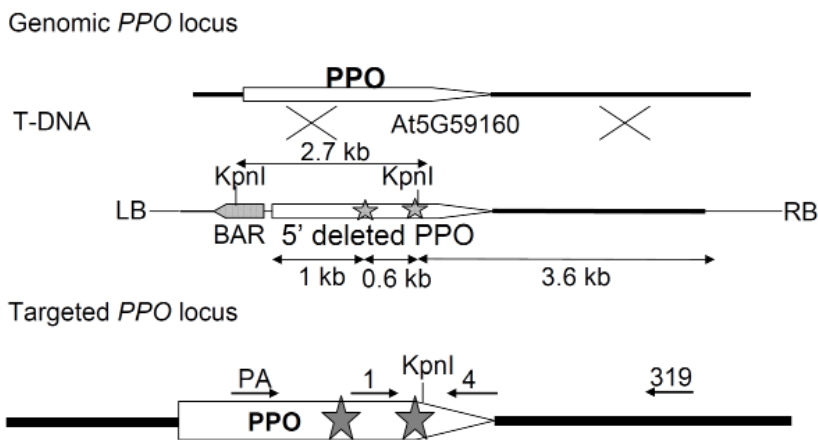


**Figure 1.** The design for the targeted modification of the *Arabidopsis PPO* locus. The white box marked *PPO* represents the *PPO* coding region, and the black lines represents flanking plant genomic DNA. The two mutations conferring butafenacil resistance are indicated as stars. The *BAR* resistance gene is linked to the truncated 5'Δ*PPO* of the T-DNA (LB for left border and RB for right border). The primers for PCR analysis of the gene targeting events are indicated by arrows.

### Sequence analysis and phylogeny

The protein sequences of DNA ligases were searched using the BLAST program on the National Center for Biotechnological Information (NCBI) web page (<http://www.ncbi.nlm.nih.gov/>). AtLig1 (At1G08130), AtLig4 (At5G57160), AtLig6 (At1G66730) and DNA



ligase 3 of *Homo sapiens* (GI 73747829) were used as a query to find possible homologous proteins. Multiple sequence alignments were built using Jalview software (<http://www.jalview.org/>) with default settings. The algorithm used here is neighbour joining using % identity.

## Results

### Isolation and characterization of the two *Atlig6* mutants

In yeast and fungi, deletion of Lig4 leads to a disruption of NHEJ and an almost complete loss of T-DNA integration (25). In plants this is not the case (8). In the *Atlig4* mutant T-DNA is integrated with equal efficiency as in the wild-type suggesting that another ligase is responsible for T-DNA integration. Recently the plant specific ligase Lig6 was discovered (5). In order to investigate *Atlig6* functions in T-DNA integration, we ordered seeds from T-DNA insertion mutants from the Salk collection and propagated these in order to obtain homozygous *Atlig6-1* and *Atlig6-2* mutants. The homozygotes were identified by PCR analysis. When two gene-specific primers flanking the insertion site were used, PCR products were amplified for wild-type and heterozygotes. No PCR products were obtained for homozygous mutants by using these two gene-specific primers, because the PCR products in the mutants would be >10 kb in size and will not be amplified with the PCR condition used here. When a T-DNA-specific primer from left border (LB) or right border (RB) was used in combination with one gene-specific primer, PCR products for the T-DNA insertion mutants were amplified, whereas no PCR products were obtained for the wild-type. We identified homozygous mutants harboring a T-DNA insertion in the *Atlig6* gene in the offspring of the heterozygous plants obtained from the Salk collection. The insertion point was mapped by sequencing of the PCR products generated using one of the T-DNA specific primers in combination with one of the gene-specific primers. For the *Atlig6-1* and *Atlig6-2* mutants, there were PCR products produced with LBa1 and both gene-specific primers (*Atlig6-1*: Sp264 and Sp265, *Atlig6-2*: Sp266 and Sp267), indicating that at least 2 T-DNA copies were inserted as an inverted repeat in the *Atlig6* locus. The combination of the primers is shown in the Figure 2. The genomic DNA was digested by HindIII for Southern blotting (Figure 2). With T-DNAs inserted in the loci identified by PCR, the amplified bands will be detected on the blot with the following sizes: for *Atlig6-1*: 2677 bp and 3584 bp and for *Atlig6-2*: 3742 bp and 4058 bp. If T-DNAs are inserted in other loci, additional bands probably with different sizes will be detected. If there are 2 or more T-DNAs inserted in one locus as direct repeat, an additional band of 4317 bp, representing a complete T-DNA, will be detected. If there are 2 or more T-DNAs inserted in one locus as inverted repeat, an additional band of 3634 bp will be detected with LBs in tail to tail orientation. Sequencing results and Southern blot analysis indicated that the T-DNAs were all inserted at the position as reported by the Salk database. A detailed characterization of the T-DNA insertions is shown in Figure 2. There were additional bands for both *Atlig6*

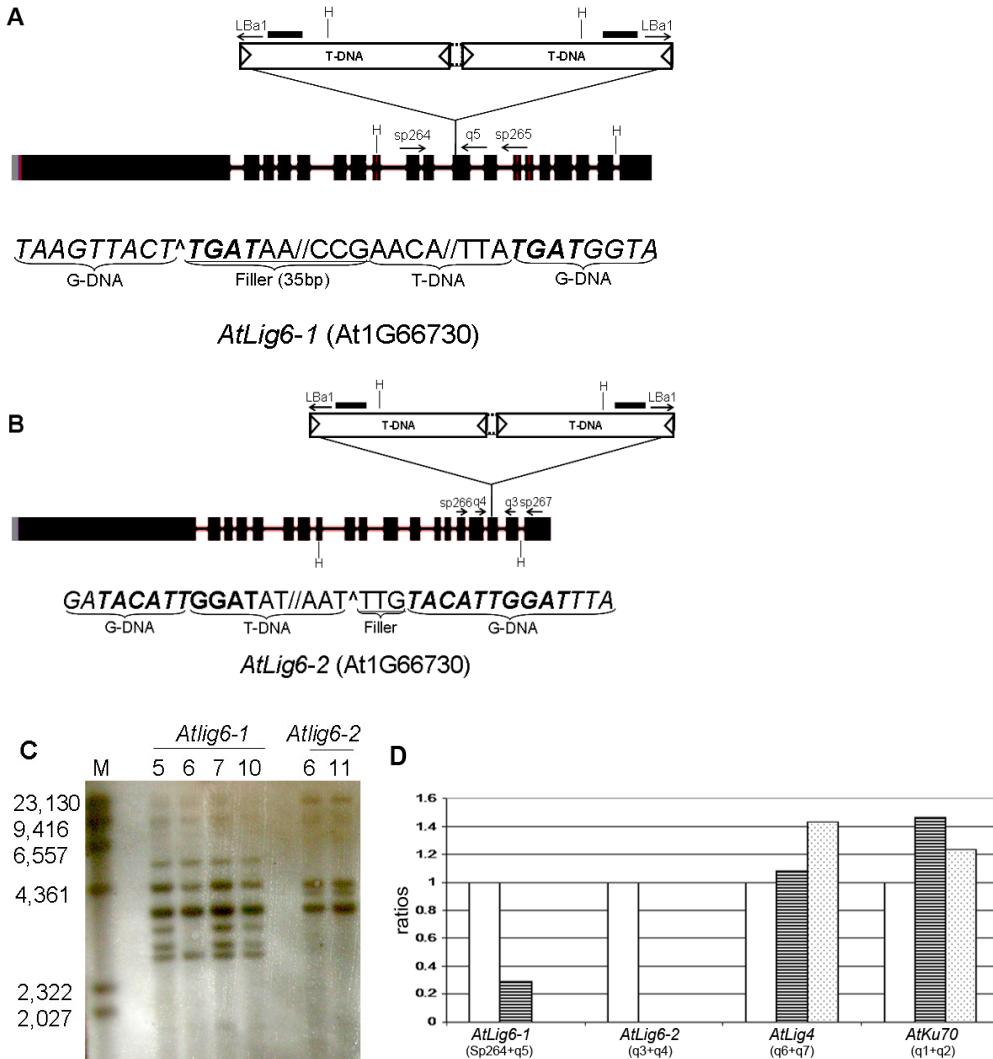


**Figure 2.** Molecular analysis of the T-DNA insertion in the *AtLig6* locus.

Genomic organization of the *AtLig6* locus is indicated with the positions of the inserted T-DNAs in *Atlig6-1* (A) and *Atlig6-2* (B). Exons are shown as black boxes. 3' and 5' UTRs are shown as gray boxes. Introns are shown as lines. The primers used for genotyping and Q-RT-PCR analysis are indicated. The probes (—) and the restriction enzyme digestion sites used for Southern blot analysis are also indicated. Genomic DNA sequences (g-DNA) flanking the T-DNA insertion are shown in italic. (C) Southern blot analysis of the T-DNA insertion. The genomic DNA was digested by HindIII. M:  $\lambda$ HindIII Marker, H: HindIII. (D) RNA expression of the *AtLig6*, *AtLig4* and *AtKu70* genes were determined by Q-RT-PCR in wild-type, *Atlig6-1* and *Atlig6-2* plants. Expression of *Atlig6* was analyzed with two different sets of primers. All the sample values were normalized to *Roc* values. The values of the wild-type were set on 1.

(□ wild-type; ▨ *Atlig6-1*; ▩ *Atlig6-2*)

mutants on the Southern blot, indicating that more than 2 T-DNAs were inserted in the genome. The T-DNA of *AtLig6-1* was integrated in exon 11 and had 35 bp filler DNA. The

two bands had segregated in the individual plant 6 of *Atlig6-1*, indicating that this plant lost two additional T-DNAs inserted in other loci, and therefore it was chosen for further research. The T-DNA of *AtLig6-2* was integrated in exon 17 and had 3 bp filler DNA. An additional band of around 4300 bp was shown for both *Atlig6* mutants, suggesting that they contained additional T-DNA copies in direct repeat.

Q-RT-PCR analysis was performed for the *Atlig6-1* and *Atlig6-2* T-DNA insertion lines using primers flanking the respective insertion sites (*Atlig6-1*: Sp264+q5, *Atlig6-2*: q3+q4). This resulted in a product with the two pairs of primers for *AtLig6* in the wild-type, but no correct products in the *Atlig6-1* and *Atlig6-2* mutants with the respective pairs of primers flanking the insertion (Figure 2). In the *Atlig6-1* mutant, a small amount of PCR product was seen, but this was shown to be of the wrong size through agarose gel electrophoresis (data not shown), suggesting that it was a non-specific PCR product. This indicated that the plants are homozygous mutants indeed. The expression levels of the *AtKu70* and *AtLig4* gene were also checked in the wild-type and the two *Atlig6* mutants as a reference. The *Atlig6* mutants had similar expression levels for the *AtKu70* and *AtLig4* genes as the wild-type.

The two *Atlig6* mutants were crossed with the *Atlig4* mutant (chapter 2) and homozygous *Atlig4lig6-1* and *Atlig4lig6-2* mutants were obtained. No obvious differences in growth were observed in these mutants compared with the wild-type under normal growth conditions.

### Expression profiling of *AtLig6*

We compared the expression of the three ligase genes of *A. thaliana*, i.e. *AtLig1*, *AtLig4* and *AtLig6*, using the genevestigator analysis tool (Figure 3). The expression levels of the three ligase genes were quite low in all organs, except for sperm cells where the expression levels of *AtLig1* and *AtLig6* were extremely high, indicating that *AtLig6* may play a role in meiosis as does *AtLig1*. The data also revealed that the developmental expression pattern of the three ligases was broadly similar to each other and that the expression level of *AtLig6* was rather low compared with *AtLig4* and *AtLig1* during the whole plant life cycle. The highest expression of *AtLig6* occurred during seed germination and flower development. In order to find out whether the expression level of *AtLig6* responds to certain stimuli, the genevestigator data relating to the abiotic stimuli were analyzed. This showed that the expression of all the three ligase genes hardly changed upon genotoxic stresses, but it changed about 2-fold for some other abiotic stresses. For *AtLig6*, its expression was induced by high light or heat.

### Sensitivity to genotoxic agents

Since *AtLig4* (chapter 2) and *AtLig1* (7) are involved in DNA repair, we hypothesized that the plant specific *AtLig6* would also be involved in this process. Therefore, we determined whether the *Atlig6* mutants were more sensitive to DNA damaging agents than the wild-type. The wild-type and the *Atlig6-1*, *Atlig6-2*, *Atlig4lig6-1* and *Atlig4lig6-2* mutants were treated with the DNA-damaging agent bleomycin. After 3 weeks, the *Atlig4*, *Atlig4lig6-1* and *Atlig4lig6-2* mutants turned out to be hypersensitive to bleomycin compared with the



sensitive to bleomycin than the *Atlig4* single mutant, suggesting that if any, *AtLig6* has only a minor role in the process of DSB DNA repair.

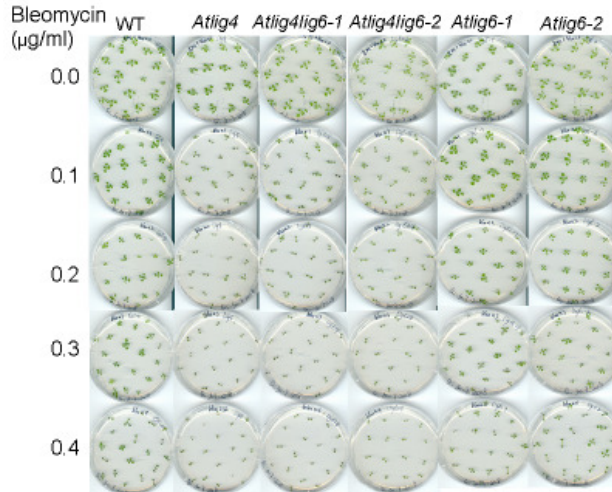


**Figure 4.** Response of *Atlig6* mutants to the DNA-damaging agent bleomycin. The wild-type, the *Atlig6-1*, *Atlig6-2*, *Atlig4lig6-1* and *Atlig4lig6-2* mutants were treated with different concentrations of bleomycin on the solid ½ MS media and were scored 2 weeks after germination.

### T-DNA integration and gene targeting in the *Atlig6* mutants

Our previous study showed that host proteins involved in DNA repair were involved in *Agrobacterium* T-DNA integration via floral dip transformation, and thus *AtLig6* could also be involved in that process. Our group has found that *Lig4* is essential for T-DNA integration in yeast and fungi, but not in plants. It might be that this was due to redundancy of *Lig4* with the plant-specific *Lig6*. Therefore, we determined T-DNA transformation in the *Atlig6* and *Atlig4Atlig6* double mutants, and also established whether the gene targeting efficiency was increased in these mutants. The floral dip transformation experiments were done at least 3 times independently for each mutant. The transformation frequencies of the

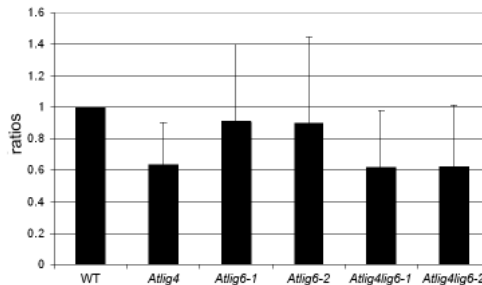


**Figure 5.** Transformation frequencies using the floral dip assay. One gram of seeds from the wild-type and the NHEJ mutants obtained after floral dip transformations were selected on ppt. The number of ppt resistant seedlings was scored 2 weeks after germination. The transformation frequency is presented as the percentage of ppt resistant seedlings compared with the wild-type, and the value of the wild-type is set on 1.

*Atlig6-1* and *Atlig6-2* mutants were at the same level as that of the wild-type (Figure 5). The transformation frequency of the *Atlig4* mutant was reduced mildly compared with the wild-type (chapter 2), and the transformation frequencies of the *Atlig4lig6-1* and *Atlig4lig6-2* mutants were similar to that of the *Atlig4* mutant (Figure 5). This indicated that AtLig6, like AtLig4 (chapter 2), was not required for efficient *Agrobacterium* T-DNA integration in plant germline cells.

Subsequently, the frequency of gene targeting was determined with the same mutants. About 1 butafenacil-resistant plant in 1000 transformants of the wild-type (chapter 2) were obtained. One butafenacil-resistant plant in 744 transformants of the *Atlig4lig6-1* mutant, and none butafenacil-resistant plants were found in 1000 or more transformants for the *Atlig4*, *Atlig6-1*, *Atlig6-2* and *Atlig4lig6-2* mutants (Table 2). The butafenacil-resistant plants

**Table 2.** The numbers of different events found in gene targeting experiments.

Plant lines	Transformants tested	Butafenacil resistant	ppt resistant	Transformation frequency
WT	2600	2	1	1
<i>Atlig4</i>	1537	0	-	0.64
<i>Atlig6-1</i>	1820	0	-	0.91
<i>Atlig6-2</i>	1998	0	-	0.90
<i>Atlig4lig6-1</i>	744	1	1	0.62
<i>Atlig4lig6-2</i>	996	0	-	0.63

The transformation frequency was shown as the ratios compared with the wild-type and the value of the wild-type was set on 1.

were analyzed by PCR to determine whether they were indeed the result of gene targeting (GT) events. The PCR products with the primers PPO-PA and PPO-4 were sensitive to KpnI, indicating that the 5' end of *PPO* is replaced via HR (Figure 6A). This was confirmed by KpnI digestion for the PCR products of nested PCR reactions with the primer PPO-1 and PPO-4 (Figure 6B). In order to test whether the 3' end of *PPO* is also replaced via HR, PCR products with the primers PPO-PA and Sp319 were cleaved by KpnI. The butafenacil-resistant plants of the wild-type represented true gene targeting (TGT) plants (chapter 2). However, the PCR products from the butafenacil resistant *Atlig4lig6-1* plant were resistant to KpnI, indicating it represented an ectopic gene targeting (EGT) event. The number of transformants tested of the double mutants was too low to make a solid conclusion, but it seemed that the absence of both AtLig4 and AtLig6 did not increase the gene targeting efficiency.

## Discussion

Under both normal growth conditions and under genotoxic stress, no specific phenotype



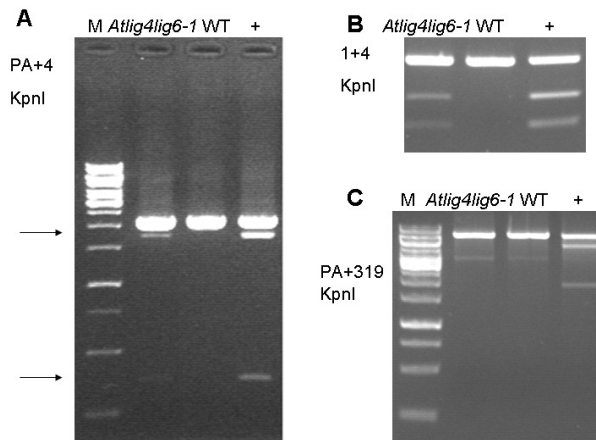


**Figure 6.** Gene targeting analysis for the butafanecil-resistant plant of *Atlig4lig6-1* mutant. PCR products were amplified with primers on *PPO* gene or non-coding regions (A: PPO-PA+4, B: PPO-1+PPO-4, C: PPO-PA+Sp319) followed by digesting with KpnI. The two lanes for *Atlig4lig6-1* in (A) are PCR products from the same butafanecil-resistant *Atlig4lig6-1* plant. WT: wild-type. +: positive control for true gene targeting event.

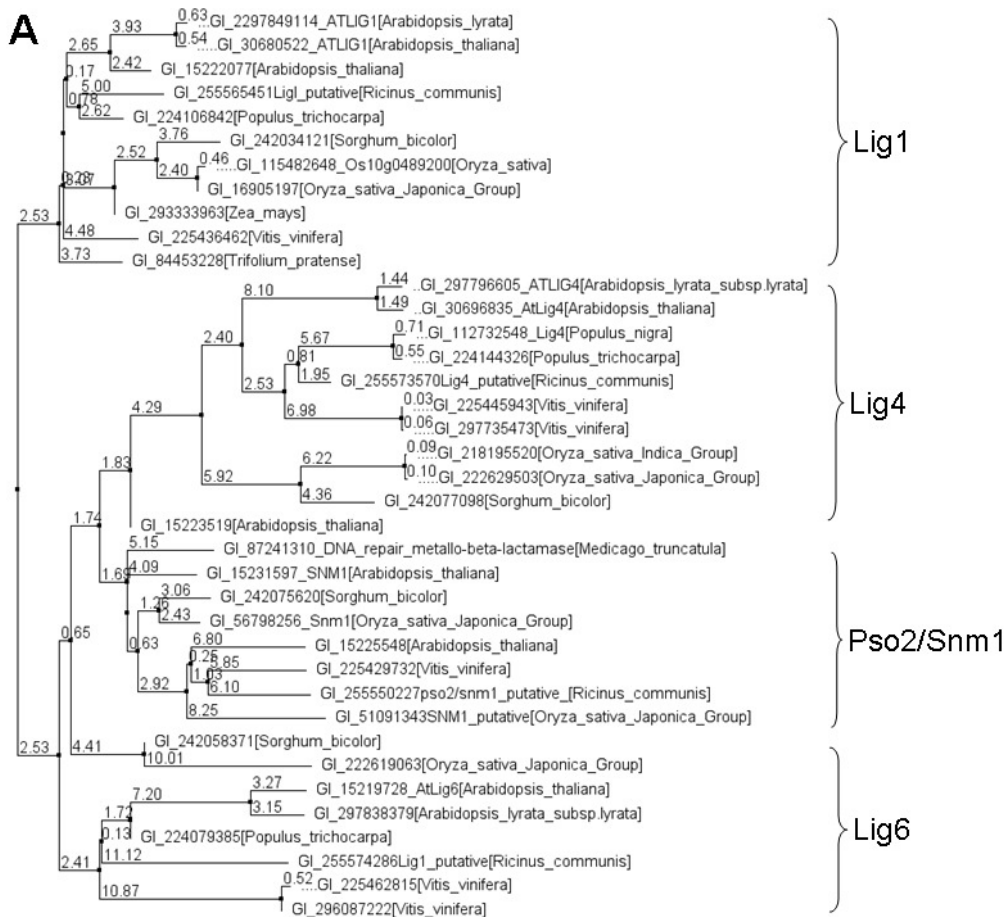
was observed in the *Atlig6* mutants. Since all DNA ligases are closely related, it could be that their function is redundant. The expression level of *AtLig6* is much lower than that of *AtLig1* and *AtLig4*, and therefore the function of *AtLig6* may be overshadowed when *AtLig1* and *AtLig4* are present. The *AtLig6* gene is most highly expressed during seed germination and flower development. Waterworth *et al.* (17) reported that *AtLig6* plays a role in seed germination and is a determinant of seed quality and longevity, probably by functioning in DNA repair at the earliest stages of seed germination to repair the DNA damage that had accumulated during seed storage. This suggests that *AtLig6* primarily functions only during certain specific stages of plant development. During the remaining parts of the life cycle, the other two DNA ligases seem to play the major role in DNA repair. The expression analysis also revealed that the expression of *AtLig6* was influenced by light and was induced by heat. Light and heat stresses can also induce DNA damage and *AtLig6* could specifically be recruited for DNA repair under such aversive growth conditions.

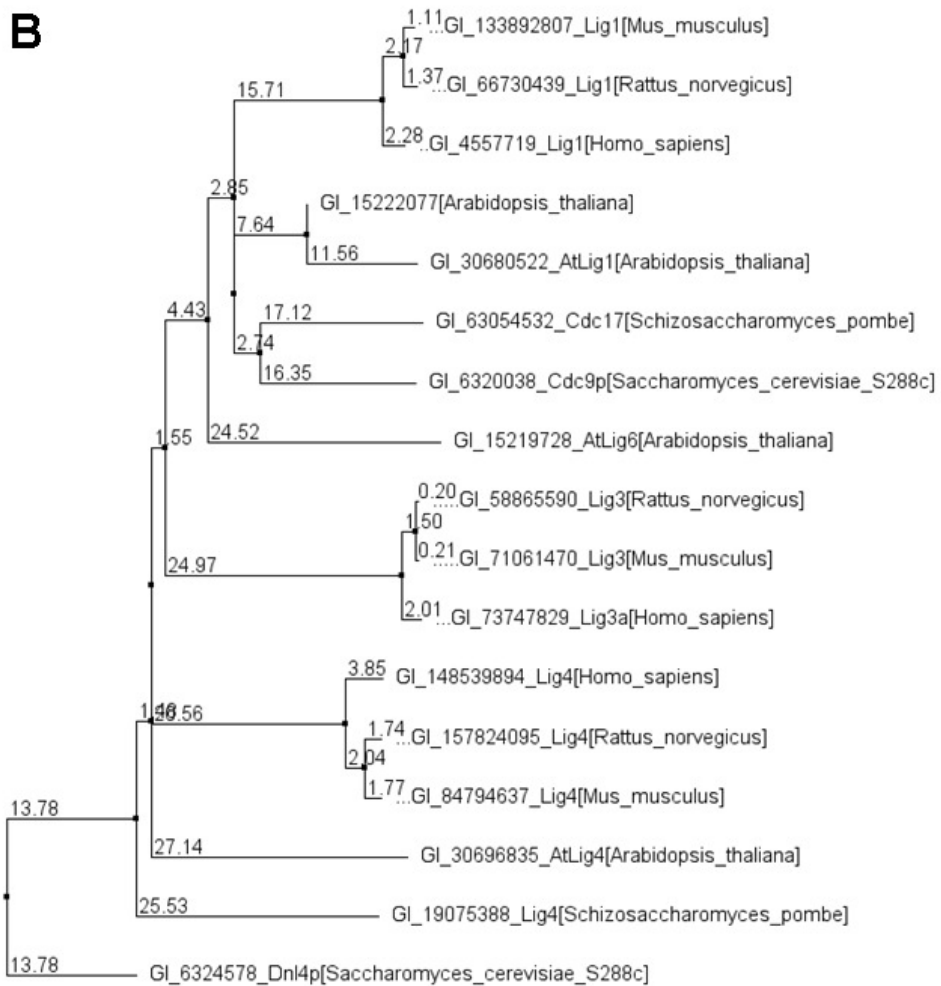
The absence of *AtLig6* did not disturb T-DNA integration neither in the background of the wild-type nor in that of the *Atlig4* mutant, indicating that *AtLig6*, like *AtLig4* (chapter 2), had no or only a minor role in T-DNA integration in germline cells. In mammalian cells, a low level of *Lig4* and *Lig3* is sufficient for efficient NHEJ (26). This could also be the case in plant cells, and all the three known ligases may collaboratively be involved in T-DNA integration. When both *AtLig4* and *AtLig6* were absent, T-DNAs were still integrated efficiently in the plant genome, suggesting that there must still be another ligase to take over that function. The frequency of gene targeting was not increased in the double *Atlig4lig6-1* mutant.

A candidate may be *AtLig1*, which is mainly involved in the ligation of Okazaki fragments during DNA replication, but may in addition also act in DNA repair (6). It is



also possible that another, so far unknown DNA ligase takes over from AtLig4 and AtLig6 in their absence. In order to find indications about the presence of other putative ligases in the *A. thaliana* genome, we retrieved sequences that shared homology and determined their relationship to the DNA ligases 1, 4 and 6 by construction of a phylogenetic tree using the neighbour joining algorithm (Figure 7A). The adenylation domain and the oligonucleotide/oligosaccharide binding-fold (OBF) domain comprise a common catalytic core unit for the ATP-dependent DNA ligase family. The conserved domains of DNA ligases from plants, mammals and yeast are shown in Figure 8. Different DNA ligases contain other specific domains. The Lig4 ligases of higher eukaryotes contain a breast cancer suppressor protein, carboxy-terminal (BRCT) domain, while the Lig3 ligases contain a poly(ADP-ribose) polymerase and DNA ligase Zn-finger (ZF-Parp) region. The Lig6 ligases contain a lactamase (Lac) domain and a DNA repair metallo-beta-lactamase (DRMBL) domain, like the proteins of the Pso/Snm1 family. The phylogenetic analysis resulted in a tree composed of four major clades (the Lig1, Lig4, Pso/Snm1 and Lig6 clades). Two putative DNA ligase-like proteins (GI\_15222077 and GI\_15223519) were found in Arabidopsis. GI\_15222077 is



**B**

**Figure 7.** Phylogenetic analysis of DNA ligases.

The trees were calculated using Jalview software and the distances were also shown. The algorithm is the neighbour joining using % identity. (A) Tree of the plant DNA ligases. (B) Tree of the conserved adenylation and OBF domains of the DNA ligases in plants, mammals and yeast.

in the clade of Lig1 and close to AtLig1. GI\_15223519 is in the clade of Pso/Snm1 (16), suggesting it could be involved in DNA crosslink repair. The GI\_15222077 protein only contains the conserved domains of the adenylation domain and the OBF domain, while the GI\_15223519 protein only contains the conserved lactamase and DRMBL domains; therefore, it is unlikely that this protein is a genuine ligase protein. Another phylogenetic tree was built with the adenylation domain and the OBF domain of DNA ligases from plants, mammals and yeast (Figure 7B). The Lig1 and Lig4 genes are present in lower eukaryotes indicating they are the oldest DNA ligases in nature. Until now Lig3 has been identified only in animals, and Lig6 has been found only in plants. The phylogenetic tree suggests that Lig3 and Lig6 were derived from Lig1 later in evolution in animals and plants, respectively.

Since the homozygous *Atlig1* mutant is lethal, the GI\_15222077 protein is not redundant with AtLig1. The expression level of the GI\_15222077 protein is even lower than AtLig6 under normal conditions according to the data of the Genevestigator data base (data not shown). But it is highly increased under hypoxia, drought, UV and light stress, and therefore may be a very good candidate for having a role in B-NHEJ.

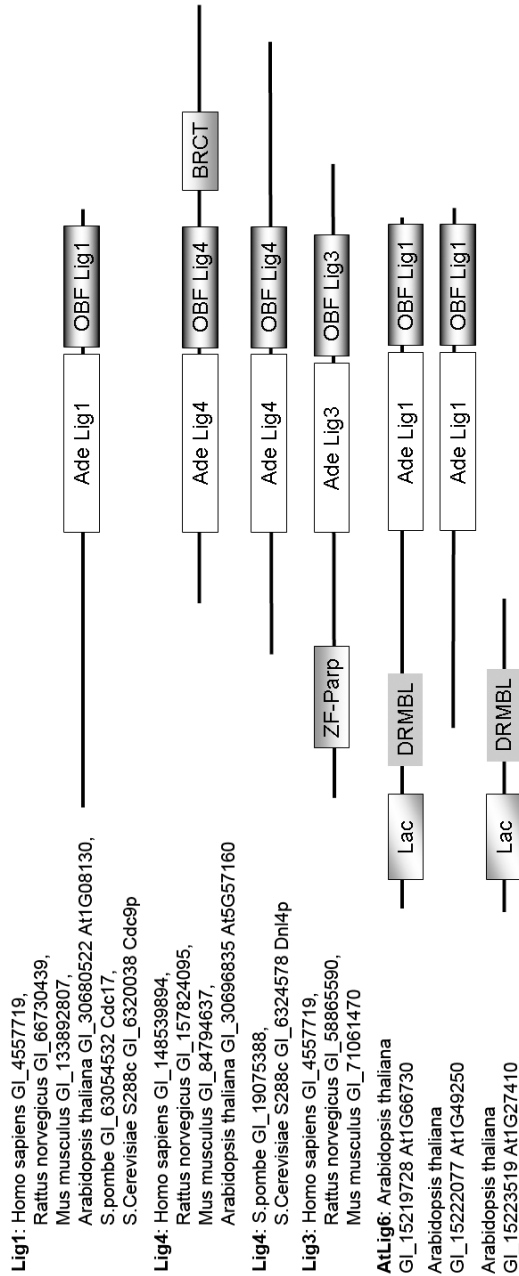


**Figure 8.** Conserved domains of the ATP-dependent DNA ligases.

The conserved domains of the DNA ligases are shown as colored rectangles and the remaining parts are shown as black lines. Ade represents the adenylation domain. OBF represents the oligonucleotide/oligosaccharide binding-fold domain. BRCT represents the breast cancer suppressor protein, carboxy-terminal domain. ZF-Parp represents the poly(ADP-ribose) polymerase and DNA ligase Zn-finger domain. Lac represents the Lactamase domain. DRMBL represents the DNA repair metallo-beta-lactamase domain.

## Acknowledgements

Amke den Dulk-Ras for the technical assistance with gene targeting project and Tiia Husso for the technical assistance with the characterization of mutants. This work was supported by the Chinese Scholarship Council (CSC) (QJ).

## Reference List

1. Timson,D.J., Singleton,M.R. and Wigley,D.B. (2000) DNA ligases in the repair and replication of DNA. *Mutat. Res.*, **460**, 301-318.
2. Pascal,J.M. (2008) DNA and RNA ligases: structural variations and shared mechanisms. *Curr. Opin. Struct. Biol.*, **18**, 96-105.
3. Shuman,S. (2009) DNA ligases: progress and prospects. *J. Biol. Chem.*, **284**, 17365-17369.
4. Martin,I.V. and MacNeill,S.A. (2002) ATP-dependent DNA ligases. *Genome Biol.*, **3**, REVIEWS3005.
5. Bonatto,D., Brendel,M. and Henriques,J.A.P. (2005) A new group of plant-specific ATP-dependent DNA ligases identified by protein phylogeny, hydrophobic cluster analysis and 3-dimensional modelling. *Functional Plant Biology*, **32**, 161-174.
6. Ellenberger,T. and Tomkinson,A.E. (2008) Eukaryotic DNA ligases: structural and functional insights. *Annu. Rev. Biochem.*, **77**, 313-338.
7. Waterworth,W.M., Kozak,J., Provost,C.M., Bray,C.M., Angelis,K.J. and West,C.E. (2009) DNA ligase 1 deficient plants display severe growth defects and delayed repair of both DNA single and double strand breaks. *BMC. Plant Biol.*, **9**, 79.
8. van Attikum,H., Bundock,P., Overmeer,R.M., Lee,L.Y., Gelvin,S.B. and Hooykaas,P.J. (2003) The Arabidopsis AtLIG4 gene is required for the repair of DNA damage, but not for the integration of *Agrobacterium* T-DNA. *Nucleic Acids Res.*, **31**, 4247-4255.
9. Critchlow,S.E., Bowater,R.P. and Jackson,S.P. (1997) Mammalian DNA double-strand break repair protein XRCC4 interacts with DNA ligase IV. *Curr. Biol.*, **7**, 588-598.
10. Mackey,Z.B., Ramos,W., Levin,D.S., Walter,C.A., McCarrey,J.R. and Tomkinson,A.E. (1997) An alternative splicing event which occurs in mouse pachytene spermatocytes generates a form of DNA ligase III with distinct biochemical properties that may function in meiotic recombination. *Mol. Cell Biol.*, **17**, 989-998.
11. Cappelli,E., Taylor,R., Cevasco,M., Abbondandolo,A., Caldecott,K. and Frosina,G. (1997) Involvement of XRCC1 and DNA ligase III gene products in DNA base excision repair. *J. Biol. Chem.*, **272**, 23970-23975.
12. Wang,H., Rosidi,B., Perrault,R., Wang,M., Zhang,L., Windhofer,F. and Iliakis,G. (2005) DNA ligase III as a candidate component of backup pathways of nonhomologous end joining. *Cancer Res.*, **65**, 4020-4030.
13. Audebert,M., Salles,B. and Calsou,P. (2004) Involvement of poly(ADP-ribose) polymerase-1 and XRCC1/DNA ligase III in an alternative route for DNA double-strand breaks rejoining. *J. Biol. Chem.*, **279**, 55117-55126.
14. McVey,M. and Lee,S.E. (2008) MMEJ repair of double-strand breaks (director's cut): deleted sequences and alternative endings. *Trends Genet.*, **24**, 529-538.
15. Liang,L., Deng,L., Nguyen,S.C., Zhao,X., Maulion,C.D., Shao,C. and Tischfield,J.A. (2008) Human DNA ligases I and III, but not ligase IV, are required for microhomology-mediated end joining of DNA double-strand breaks. *Nucleic Acids Res.*, **36**, 3297-3310.
16. Bonatto,D., Revers,L.F., Brendel,M. and Henriques,J.A. (2005) The eukaryotic Pso2/Snm1/Artemis proteins and their function as genomic and cellular caretakers. *Braz. J. Med. Biol. Res.*, **38**, 321-334.
17. Waterworth,W.M., Masnavi,G., Bhardwaj,R.M., Jiang,Q., Bray,C.M. and West,C.E.

- (2010) A plant DNA ligase is an important determinant of seed longevity. *Plant J.*, **63**, 848-860.
18. Alonso,J.M., Stepanova,A.N., Leisse,T.J., Kim,C.J., Chen,H., Shinn,P., Stevenson,D.K., Zimmerman,J., Barajas,P., Cheuk,R. *et al.* (2003) Genome-wide insertional mutagenesis of *Arabidopsis thaliana*. *Science*, **301**, 653-657.
  19. de Pater,S., Caspers,M., Kottenhagen,M., Meima,H., ter Stege,R. and de Vetten,N. (2006) Manipulation of starch granule size distribution in potato tubers by modulation of plastid division. *Plant Biotechnol. J.*, **4**, 123-134.
  20. Weijers,D., Franke-van,D.M., Vencken,R.J., Quint,A., Hooykaas,P. and Offringa,R. (2001) An *Arabidopsis* Minute-like phenotype caused by a semi-dominant mutation in a RIBOSOMAL PROTEIN S5 gene. *Development*, **128**, 4289-4299.
  21. Murashige,T. and Skoog,F. (1962) A Revised Medium for Rapid Growth and Bio Assays with Tobacco Tissue Cultures. *Physiologia Plantarum*, **15**, 473-497.
  22. Clough,S.J. and Bent,A.F. (1998) Floral dip: a simplified method for *Agrobacterium*-mediated transformation of *Arabidopsis thaliana*. *Plant J.*, **16**, 735-743.
  23. Hanin,M., Volrath,S., Bogucki,A., Briker,M., Ward,E. and Paszkowski,J. (2001) Gene targeting in *Arabidopsis*. *Plant J.*, **28**, 671-677.
  24. Masson,J. and Paszkowski,J. (1992) The Culture Response of *Arabidopsis-Thaliana* Protoplasts Is Determined by the Growth-Conditions of Donor Plants. *Plant Journal*, **2**, 829-833.
  25. van Attikum H., Bundock,P. and Hooykaas,P.J. (2001) Non-homologous end-joining proteins are required for *Agrobacterium* T-DNA integration. *EMBO J.*, **20**, 6550-6558.
  26. Windhofer,F., Wu,W. and Iliakis,G. (2007) Low levels of DNA ligases III and IV sufficient for effective NHEJ. *J. Cell Physiol*, **213**, 475-483.

## SUMMARY

DNA double-strand breaks (DSBs) are one of most dangerous forms of DNA damage for organisms. These breaks can be repaired by homologous recombination (HR) using homologous sequences or by non-homologous end joining (NHEJ). The latter mechanism is the major route for DSB repair in higher eukaryotes, such as animals and plants. Until now, evidence showed that there are several pathways for NHEJ. The first identified pathway is the classical NHEJ (C-NHEJ), which is dependent on the Ku70/Ku80 dimer, and utilizes Lig4/XRCC4/XLF to ligate the DNA ends. In mammals, DSBs still can be repaired in the absence of C-NHEJ via the so-called backup NHEJ (B-NHEJ) pathway. All these DSB repair pathways are regulated in a competitive and cooperative manner to maintain genome stability. It has been found that DSB repair is also largely responsible for the integration of exogenous DNA that is added for the purpose of obtaining genetically modified cells and organisms. If we could manipulate the balance of the DSB repair pathways towards HR on purpose, it would be possible to increase the frequency of gene targeting (GT), which would have enormous advantages in studies on gene function, and would enable the targeted modification of genes in the genome and precise genetic modification of crops. The current knowledge of cell responses to DSBs and gene targeting is reviewed in **chapter 1**. The aim of my thesis was to study DSB repair in plants and thereby identify potential factors, by which gene targeting can be increased in plants.

The studies described in **chapter 2** focused on the characterization of *Arabidopsis thaliana* mutants which were deficient in C-NHEJ, including the *Atku70*, *Atku80* and *Atlig4* mutants. The homozygous mutants were phenotypically indistinguishable from wild-type plants. However they were sensitive to DNA damaging agents such as bleomycin and MMS, indicating that AtKu70, AtKu80 and AtLig4 play an important role in DNA repair. The results from comet assays showed that these mutants had more DNA damage than the wild-type, but these mutants still have the ability to repair DSBs. This was in line with the results of *in vitro* end joining assays, which showed that the NHEJ mutants were still capable of end joining though the capacity was lower than that of the wild-type. This revealed that there exists a B-NHEJ pathway in plants. Since NHEJ may be the major route for *Agrobacterium* T-DNA integration, the frequencies of T-DNA integration and gene targeting were also tested for these NHEJ mutants and previously described *Atku70* and *Atmre11* mutants. The *Atku70*, *Atku80* and *Atmre11* mutants had decreased T-DNA integration in Arabidopsis germline cells, whereas the *Atlig4* mutant was hardly affected. It showed that most NHEJ factors were important for T-DNA integration in plants except AtLig4. Some other ligase may take over the role of DNA ligation in absence of AtLig4. Unfortunately, the frequency of gene targeting was not altered in the *Atku70*, *Atku80* and *Atlig4* mutants, although a slight increase was seen in the *Atmre11* mutant. It revealed again that there must be some B-NHEJ pathways in plants as well. In chapters 3 to 5, we investigated these putative B-NHEJ pathways.

In mammals, Poly(ADP-ribose) polymerase 1 (Parp1) and Parp2 have been reported to be involved not only in DNA single strand break (SSB) repair, but also to be a major component in B-NHEJ. The homologues of Parp1 and Parp2 have been identified in plants, and evidence showed they are involved in stress tolerance and programmed cell death. Whether they are also involved in DNA repair in plants was unclear. The study on this issue is described in **chapter 3**. Two Arabidopsis T-DNA insertion mutants (*Atparp1* and *Atparp2*) were functionally characterized. The results showed that AtParp1 is involved in DNA repair, and that it has an important role especially in SSB repair. Though the *Atparp2* mutant could tolerate the genotoxic stress equally well as the wild-type, the *Atparp1parp2* (*Atp1p2*) double mutant was more sensitive to the genotoxic stress than the *Atparp1* single mutant. The expression of *AtParp2* was increased in NHEJ mutants. All these results suggested that AtParp2 may also be involved in DNA repair, but probably has a minor role. The capacity of DNA end joining was slightly reduced in all the *Atparp* mutants. The products of *in vitro* end joining assays revealed in lower amounts of products of micro-homology mediated end joining (MMEJ) with the extract from the *Atp1p2* mutant compared with that from the *Atparp1* and *Atparp2* single mutants and the wild-type. AtParp1 and AtParp2 may thus be functionally redundant and play a role in MMEJ, which is a characteristic of B-NHEJ in mammals. The frequency of *Agrobacterium* mediated T-DNA transformation via floral dip did not change in the *Atparp* mutants probably because C-NHEJ plays the major role in that process, as was described in **chapter 2**.

**Chapter 4**, describes experiments in which the mutations in AtParp1 and AtParp2 were combined with those in the C-NHEJ pathway (Ku80) in Arabidopsis. The *Atparp1parp2ku80* (*Atp1p2k80*) triple mutant was hypersensitive as compared to the individual mutants to agents generating DSBs (and SSBs), indicating that the AtParp proteins acted in a different pathway of DSB repair than Ku and are thus involved in the alternative B-NHEJ pathway. Both the *Atp1p2* and the *Atp1p2k80* triple mutants were especially deficient in MMEJ, indicating that the Parp-mediated B-NHEJ facilitates MMEJ in plants as well as in mammals. The end joining products obtained in the *Atku80* mutant revealed that Ku protected the DNA ends from resection, suggesting that Ku and Parp proteins are involved in distinguished NHEJ pathways and probably compete with each other. Surprisingly, a deficiency of *AtParp1* and *AtParp2* rescued end joining deficiency in the *AtKu80*. The results of the comet assays showed that the triple mutant had more DNA damage than other mutants, but it still had the ability to repair it to some level. It revealed that a third NHEJ pathway must exist, which is probably suppressed by Ku and Parp proteins under normal conditions. The *Atp1p2k80* mutant had a reduced T-DNA integration efficiency via floral dip transformation. But the gene targeting frequency of the triple mutant was not significantly different from that of the wild-type. Another unknown alternative NHEJ pathway may take control of this process when both C-NHEJ and B-NHEJ are absent.

In the last step of DSB repair, the DNA ends are ligated by ATP-dependent DNA ligases. Lig3 was reported to be involved in B-NHEJ together with Parp proteins in mammals. No



ortholog of Lig3 is present in plants, but Lig6 has been identified as a novel plant-specific ATP-dependent DNA ligase. *In silico* studies indicated that Lig6 had more similarity to Pso2/Snm1, Lig4 and Lig3 than to Lig1, suggesting that it may also be involved in DNA repair. **Chapter 5** described the function of *AtLig6* and *in silico* analysis of its homologs. Two homozygous mutants of *AtLig6* were obtained and crossed with the *Atlig4* mutant to get the two double mutants (*Atlig4lig6-1* and *Atlig4lig6-2*). The two *Atlig6* single mutants could tolerate bleomycin treatment equally well as the wild-type. The *Atlig4lig6-1* and *Atlig4lig6-2* double mutants were hypersensitive to bleomycin, but this was similar to the sensitivity of the *Atlig4* single mutant. The expression pattern analyzed via Genevestigator showed that the expression level of *AtLig6* was lower than that of *AtLig1* and *AtLig4* and was especially induced at the stages of seed germination and flowering. It could be that *AtLig6* only functions in some specific developmental stages. The frequency of T-DNA integration was hardly affected by the deficiency of *AtLig6* and *AtLig4* (**chapter 2**), nor was the frequency of gene targeting different. The alignment of DNA ligase sequences pointed to one candidate, which is a putative DNA ligase possibly functioning in the B-NHEJ. Another possibility is that *AtLig1* is active in the B-NHEJ pathway.

In conclusion, plants have multiple systems for DSB DNA repair, not only the Ku-dependent C-NHEJ, but also the alternative B-NHEJ. *AtParp1* and *AtParp2* play a role in B-NHEJ which prefers to utilize areas of micro-homology. As sessile organisms, the plants need to strongly adapt to all the assaults. It may therefore be necessary for plants to have more than one alternative B-NHEJ pathway to survive. It will be interesting to study the nature of this third or fourth pathway of NHEJ in the future. With a thorough understanding of all these NHEJ pathways, methods to increase the gene targeting frequency may be developed.

## SAMENVATTING

Dubbel strengs breuken (DSB-en) in DNA vormen een van de meest ernstige vormen van DNA schade. Organismen hebben twee manieren om zulke DNA breuken te herstellen, via homologe recombinatie of "non-homologous end joining" (NHEJ). De eerste manier maakt gebruik van homologe gebieden in het DNA, die gebuikt worden om de breuk foutloos te herstellen. Bij de tweede methode worden de DNA einden direct aan elkaar gezet. In eukaryoten zoals planten en dieren wordt voornamelijk deze laatste methode gebruikt. Er zijn aanwijzingen dat er meerdere routes voor NHEJ zijn. Er is de klassieke route (C-NHEJ) die afhankelijk is van het Ku70/Ku80 eiwitcomplex en het Lig4/XRCC4/XLF eiwitcomplex. Wanneer een van deze eiwitcomplexen niet functioneel is, wordt een alternatief of back-up NHEJ herstelmechanisme (B-NHEJ) actief in zoogdieren. Alle herstelmechanismen werken samen om zo goed mogelijk het genoom intact te houden.

Herstelmechanismen voor DSB-en in het DNA zijn ook betrokken bij het inbouwen van exogeen DNA om genetisch gemodificeerde organismen te verkrijgen. Indien we de balans van de verschillende herstelmechanismen zouden kunnen manipuleren, zouden we in staat moeten zijn om de homologe recombinatie te bevorderen. Op die manier zouden we de frequentie van "gene-targeting" (GT; een methode om via homologe recombinatie een stuk endogeen DNA uit te wisselen met een ander stuk DNA) moeten kunnen verhogen, wat een enorm voordeel zou zijn voor studies naar de functie van genen en de precieze genetische modificatie van gewas planten. In planten is deze methode zeer lastig, omdat de frequentie zeer laag is.

In hoofdstuk 1 wordt de huidige kennis beschreven van de cellulaire respons op het ontstaan en herstel van DSBs en de resultaten verkregen met gene-targeting. Het doel van mijn thesis was om herstel van DSB-en in planten te bestuderen en om zo potentiële factoren te identificeren, waarmee de frequentie van GT verhoogd kan worden.

In hoofdstuk 2 worden een aantal Arabidopsis mutanten bestudeerd die gestoord zijn in genen die actief zijn in de C-NHEJ route. De mutanten zien er onder standaard condities normaal uit, maar wanneer ze blootgesteld worden aan bleomycine, dat DNA schade veroorzaakt dat voornamelijk bestaat uit DSB-en, worden de planten erg ziek. Echter met behulp van zogenaamde comet-assays is te zien dat na een herstel periode wel DNA herstel plaats vindt. Dit is een aanwijzing dat er nog een tweede NHEJ route is, die in deze mutanten actief is. Omdat NHEJ DNA herstelroutes ook tijdens Agrobacterium T-DNA transformatie zorgen voor het inbouwen van het T-DNA in het plantengenoom, hebben we ook T-DNA integratie en GT bestudeerd in deze mutanten. In de Ku70, Ku80 en Mre11 mutanten is de frequentie van T-DNA integratie slechts 10-20% ten opzichte van het wild-type. Dit betekent dat Ku en Mre11 belangrijk zijn voor T-DNA integratie. Maar er wordt nog wel, zij het met lage frequentie, T-DNA ingebouwd in deze mutanten. Dus er vindt nog NHEJ plaats. In de Lig4 mutant is de frequentie niet lager dan in het wild-type. De functie van Lig4 wordt waarschijnlijk overgenomen wordt door een van de andere ligasen in het

geval dat Lig4 inactief is. De GT frequentie in de Ku en Lig4 mutanten is niet veranderd ten opzichte van de wild-type. De Mre11 mutant geeft wel een lichte verhoging. Al deze resultaten duiden erop dat er ook in planten een alternatieve NHEJ route moet zijn. In de rest van de hoofdstukken wordt deze route nader bestudeerd.

In dierlijke cellen speelt poly(ADP-ribose) polymerase1 (Parp) niet alleen een rol bij herstel van enkelstrengs breuken, maar ook in de alternatieve NHEJ route. In planten zijn twee Parp genen geïdentificeerd, die betrokken zijn bij stress tolerantie en geprogrammeerde celdood. Hun rol bij herstel van DNA schade wordt bestudeerd in hoofdstuk 3, met behulp van planten waarin een of beide Parp genen zijn gemuteerd. Hieruit blijkt dat Parp1 een rol speelt in het herstel van DNA schade, voornamelijk van enkelstrengs breuken. Mutatie van zowel Parp 1 als ook Parp 2 zorgt voor nog grotere gevoeligheid voor chemicaliën die DNA schade veroorzaken. In vitro "end joining" laat zien dat voornamelijk "end joining" via microhomologie (MMEJ) is verstoord in deze mutanten. Er was geen meetbaar effect van deze mutaties op T-DNA integratie en GT.

In hoofdstuk 4 worden de gevolgen bestudeerd van mutaties in beide NHEJ routes tegelijk. Deze mutanten (Ku80,Parp1,Parp2) zijn nog gevoeliger voor DNA schade dan wanneer alleen de klassieke of alternatieve route is uitgeschakeld. Dit betekent dat de eiwitten inderdaad betrokken zijn bij verschillende DNA herstel routes. "End joining" studies laten zien dat Parp betrokken is bij MMEJ en dat Ku de DNA uiteinden beschermt voor afbraak. Wanneer beide routes uitgeschakeld zijn, is de in vitro "end joining" weer onverwacht hoog, op het wild-type niveau. De twee Parp genen hebben beide eenzelfde functie in MMEJ en uitschakelen van beide genen is nodig om de MMEJ te inactiveren. T-DNA integratie is sterk verlaagd in de Parp/Ku mutant, maar nog steeds aanwezig. Al deze resultaten samen laten zien dat er nog steeds "end joining" plaats vindt als beide NHEJ routes uitgeschakeld zijn en dat er dus nog een derde NHEJ route moet zijn.

In de laatste stap voor herstel van DSB-en worden de DNA uiteinden aan elkaar gezet door ATP-afhankelijke DNA ligase enzymen. In zoogdieren is Lig3 verantwoordelijke voor deze stap in de B-NHEJ route. In planten is geen Lig3 aanwezig. Daarom is het plantspecifieke Lig6 en zijn mogelijke rol in B-NHEJ bestudeerd met behulp van mutanten in het Lig6 gen. Tevens zijn planten bestudeerd die gemuteerd zijn in zowel Lig4 als ook in Lig6. Geen duidelijke functie voor herstel van DSB-en of het inbouwen van T-DNA of GT kon worden vastgesteld voor Lig6. Bestuderen van beschikbare DNA databases liet zien dat er mogelijk nog een ander ligase gen is in planten dat mogelijk de functie overneemt van Lig4 en Lig6 in het geval dat beide genen uitgeschakeld zijn.

Er kan dus worden geconcludeerd dat planten een aantal NHEJ routes hebben om DSB-en te herstellen, niet alleen de klassieke Ku-afhankelijke route, maar ook meerdere alternatieve routes. Omdat planten goed moeten kunnen omgaan met allerlei vormen van stress, omdat ze die niet uit de weg kunnen gaan, zou het noodzakelijk kunnen zijn om meerdere alternatieve NHEJ routes te hebben om te overleven. Het is een bijzonder interessante uitdaging om op te helderen welke factoren zorgen voor deze derde, tot nu

toe nog onbekende en hypothetische route. Een gedetailleerde kennis van alle in planten beschikbare NHEJ routes zal in de toekomst mogelijk wel kunnen leiden tot de ontwikkeling van methoden om de GT frequentie te verhogen.

## Curriculum Vitae

Qi Jia was born on March 25<sup>th</sup>, 1981 in Wuhu, Anhui Province, China. She attended high school at Wuhu No. 1 middle school. In 1998, she started studies at the Biotechnology Department of Shenyang Agricultural University, China. In 1999, she started her research training at the Enzyme Engineering Lab under the supervision of Dr. Hongman Chen and Dr. Guoshi Kan with the project on the usage of chitinase to protect the tomato from diseases and in 2002 she got her bachelor degree in biotechnology. After her graduation, she worked as an editor for half a year in Wuhu. From 2003 to 2006, she was a master student of biochemistry and molecular biology in Nanjing University in China, and did research in the National Key Laboratory of Pharmaceutical Biotechnology under the supervisor of Prof. Dr. Zichun Hua. During this period, she worked on the one hand on the characterization of tomato Senu3 and senescence in tomato, and on the other hand on expression, purification and analysis of the recombinant proteins thymosin beta 4 and thymosin beta 10 in *E. coli*. She obtained her MSc degree in 2006, and in the same year she started her PhD project at the Molecular and Development Genetics department, Institute of Biology, Leiden University (IBL) in the Netherlands, under the supervision of Dr. B. Sylvia de Pater and Prof. Dr. Paul J.J. Hooykaas. The topic of her project was DNA repair and gene targeting in end joining plant mutants (this thesis). During this time she was also involved in research leading to a publication about the role of Arabidopsis eIF4B2 in PCD (Gaussand, Jia, van der Graaff and et al, *Frontier in Plant Physiology*, 2011).

## ACKNOWLEDGEMENTS

Time flies. Four years went past after the cold windy and rainy day I first arrived in the Netherlands. Now I would like to express my sincere gratitude to all the warm-hearted people who fulfill all my happiness during my stay in this tiny but great country.

First of all, I would like to thank Paul, who gave me the opportunity to work in his wonderful group. I really learned a lot in his lab and spent a very happy time as well.

Sylvia, I think only “thank you” can not express my gratitude to you. Since you gave me a warm welcome when I arrived at the Clusius lab, I benefited a lot from all kind of your supervision, not only for scientific work but also for scientific life.

Amke, thank you for helping me a lot with the gene targeting project and all the troubles I met, especially the Dutch letters.

Marijn, thanks for all the help in the lab and teaching Dutch culture to me and my students. Tiia and Bego, my lovely and sweet students, thanks a lot for killing the plants with me together.

Ward, Gerda, Jan, thanks for all the professional technical help. Jeroen and Karolina, my first office mates, thanks for all the happy time we spend together. Marcel, thanks for all the useful tips for the lay-out of my thesis.

Beatrice, Johan, Maartje, Martijn, Philippe, Paulo, Patrick, Eri, Xiaolei Niu, Xiaorong Zhang, Li Wang, Xiong Yang, Fang Huang, Myckel, Yuanwei Fan, Shuxin Zhang, Yi Chen, Jingxia Shao, Yu Zhang, Aijun Sun, Xiaoyu Guo, and all the colleagues, thanks for all the help in the lab and the weekly work discussion. Hongtao Zhang, Fang Yu, Meiliang Zhou, Qifang Pan, Yanxia Zhang, Chao Cui, Shuning He, Yuntao Dai and all the Chinese colleges in IBL, thanks for the feeling of home.

Yu Qin and Feng Wang, we applied together for the scholarship, we came to the Netherlands in the same year, and we shared all the feeling about happiness and worries when we came to this far-away place. Thanks for your company in the four years. 秦宇, 同窗八载, 情深意重. Fang Wang and Heer Zhao, thanks for you to let me know that vinegar or no vinegar is a problem. Chunxiu Hu, Xin Leng, Ting Chen, Ling Xu, Yan Zhang, my honey sisters, thanks for your sweetness. Maya Feng, Ying Zhao, Jun Wang, Peici Wang, Zhi Ding, Wenjie Liao, Lu Feng, Lan Song, Guiling Chen, Chao Zhu, Wen Zhang, thanks for your friendship.

Last, but not least, I would like to thank my family. 亲爱的妈妈和爸爸, 感谢你们的对我的热情洋溢的爱, 人生苦短, 你们让我感受到幸福和快乐. 坚强和顽固的羊多, 懒惰和苛求的胖胖, 我也爱你们. 还有在妈妈最艰难的时候的各位家人们, 无论是贴身的照顾, 还是远方的问候, 都深深感动并极大的鼓励了我们, 也使远在大陆另一边的我能放心的坚强的走下去. 贾坤志, 也感谢你的一贯鼓励和支持.

Qi Jia  
Leiden, 2011

A